UNIVERSIDADE DE LISBOA

FACULDADE DE CIÊNCIAS

DEPARTAMENTO DE BIOLOGIA VEGETAL

Optimization of a Bioassay to Evaluate *Escherichia coli* Stress Responses

Ana Lúcia Evaristo Russo

Mestrado em Microbiologia Aplicada

Dissertação orientada por:

Cecília R.C. Calado

Ana Tenreiro

2017

Acknowledgments

First of all, I would like to express my sincere gratitude to my advisors, Professor Cecília Calado for giving me the opportunity to work in a totally different area from mine and with a very innovative technique, the infrared spectroscopy. Thank you as well for all the support, availability and advise given during this project. To *the Instituto Superior de Engenharia de Lisboa* (ISEL) for having received me in the second year of the master's degree.

I also appreciate to DrugsPlatf-2017 and GenTox-2017 projects, financed by Instituto Politécnico de Lisboa, for supporting this work.

To Bernardo Cunha for all the patience to guide me in the first practical tests, for all the advices and also for having done all the data processing, which was crucial for the analysis of my results.

I also want to thank to all my post-graduation professors for all the knowledge they passed to me, which have been very useful during my master thesis and to *Faculdade de Ciências da Universidade de Lisboa* for having accepted my candidature in the Master of Microbiology.

A hearthfelt thank to my colleagues that shared this academic journey with me, who supported me and gave me the strength to continue. We started this journey together but, unfortunately, we had to finish it apart. However, I am very grateful for meeting you. To all of my friends for supporting me.

To my beloved boyfriend, Miguel Mataloto, the greatest thanks for all the patience and unconditionally support during this last year and for having accompanied me in all the stages of this journey. I am truly sure that I could not made it without you.

Last but not least, an enormous thank to my family, especially my mother, father, sister, grandmother and grandfathers, who had support me more than anyone at all stages of my life. To my parent’s thank you for allowing me to have an education, this would be completely impossible without you.

Abstract

In the last decade, Fourier Transform Infrared Spectroscopy (FTIR) has been applied in several areas, being an increasingly used technique in microbiology, especially for whole cell metabolomics fingerprint. However, the reproducibility of this technique is influenced by a large number of factors such as the physiological state of cells, sample manipulation and growth conditions. In order to solve this problem, the present work intends to optimize a bioassay for evaluating the response of microorganisms to stress conditions, using *Escherichia coli* as a model, as its metabolic pathways share pronounced similarities to mainstream pathways across other microorganisms.

The bioassay was optimized in terms of nutrient medium concentration, *E.coli* growth phase and exposed time to the stress agents. The stress agents used were: ethanol, bleach, sodium chloride, hydrochloric acid and sodium hydroxide. These agents were chosen for having different mechanisms of action in microorganism's cells. A bioassay which allows to evaluate the metabolic response of the microorganism cell when exposed to stress conditions is important to increase knowledge about microbial metabolism and for example for the development of new drugs. After the bioassay optimization, it was decided to test the assay exposing the *E. coli* cells to six antibiotics, whose mechanism of action is known. This allows to observe if the optimization of the bioassay meets the objective of differentiating samples exposed to different substances. It was observed that the conditions that allow higher reproducibility and sensitivity of the bioassay are different for each type of stress agent, but as a general rule exposing the cells to stress agents for 24 hrs, use the nutrient medium 1.25x concentrate and the cells in the stationary growth phase were the global optimal conditions to distinguish the various mechanisms of action on the metabolism of *E. coli* cells.

The approach described allowed to identify the impact of each parameter on the metabolic resolution of the biomolecular fingerprint acquired by FTIR spectroscopy, and therefore, the adapted bioassay maximizes the metabolic fingerprinting ability of the method, namely to characterize different metabolic stress responses.

KEYWORDS: Stress Response, *Escherichia coli*, Fourier transform Infra-red Spectroscopy, Bioassay, Metabolic Fingerprinting

Resumo

Na última década, a espectroscopia por transformada de Fourier (FTIR) tem vindo a ser aplicada às mais diversificadas áreas, sendo uma técnica cada vez mais utilizada em microbiologia, por permitir obter resultados num curto espaço de tempo e por ter um baixo custo por análise. No entanto, a reprodutibilidade desta técnica é influenciada por um grande número de fatores, entre os quais, o estado fisiológico das células, o método de manipulação da amostra e as condições de crescimento. Para tentar solucionar este problema, o presente trabalho pretende otimizar um bioensaio, baseado em espectroscopia de infravermelho, para avaliar a resposta metabólica dos microrganismos quando expostos a condições de stress, utilizando a bactéria *Escherichia coli* como modelo, uma vez que as suas vias metabólicas são muito semelhantes com as de outros microrganismos.

O bioensaio foi otimizado em termos da concentração de nutriente do meio de cultura, (tendo sido testadas as concentrações 1.25, 2.5 e 5x), fase de crescimento da bactéria *E. coli* (onde foram utilizadas células na fase exponencial, no início da fase estacionária e na fase estacionária) e o tempo de exposição das células aos agentes de stress (1, 8 e 24 h). Os agentes de stress utilizados foram: álcool, lixívia, cloreto de sódio, ácido clorídrico e hidróxido de sódio. Estes agentes foram escolhidos por teres diferentes mecanismos de ação nas células dos microrganismos. É de extrema importância o desenvolvimento e otimização de bioensaios que permitam avaliar a resposta metabólica das células dos microrganismos quando expostos a condições adversas, para aumentar o conhecimento sobre o metabolismo microbiano e, por exemplo, para o desenvolvimento de novos antibióticos. Após a otimização do bioensaio, foi decidido testar o ensaio expondo as células de *E. coli* a seis antibióticos diferentes, cujos mecanismos de ação são conhecidos. Desta maneira, é possível observar se a otimização do bioensaio cumpre o objetivo de diferenciar amostras expostas a diferentes substâncias.

Observou-se que as condições que permitem obter uma maior reprodutibilidade e sensibilidade do bioensaio são diferentes para cada tipo de agente de stress, mas regra geral, expor as células aos agentes de stress durante 24 horas, usar o meio 1.25x concentrado e as células na fase de crescimento estacionária permite distinguir os vários mecanismos de ação no metabolismo das células de *E. coli*.

A metodologia descrita permitiu identificar o impacto de cada parâmetro na resolução metabólica da impressão digital biomolécula adquirida pela espectroscopia FTIR e, portanto, o bioensaio otimizado maximiza a capacidade metabólica de impressão digital do método, nomeadamente ao caracterizar diferentes respostas metabólico ao stress.

Palavras-Chave: Resposta ao stress, *Escherichia coli*, Espectroscopia de infravermelho por transformada de Frourier, Bioensaio, Impressão metabólica

Table of contents

List of figures V
List of Abbreviations X
1. Thesis overview 1
1.1 Objectives 1
1.2 Thesis Outline 1
2. Introduction 2
2.1 Infrared spectroscopy 2
2.1.1 Instrumentation 4
2.1.2 Acquisition Modes 6
2.1.3 Applications to Microbiology 6
2.1.4 Chemometrics and Spectral pre-processing techniques 8
2.2 Bioassay optimization 11
2.2.1 *Escherichia coli* bacteria and stress responses 12
2.2.2 Application of the bioassay 14
3. Materials and methods 16
3.1 Culture growth conditions and Bioassay 16
3.2. Preparation of solutions of stress agents 17
3.3 Preparation of antibiotic solutions 18
3.4 FTIR spectra acquisition, preprocessing and analysis 19
4. Results and Discussion 20
4.1 Bioassay optimization 20
4.1.1 Effect of nutrient media concentration 21
4.1.2 Effect of *E. coli* growth phase 31
4.1.3 Incubation time 38
4.1.4 Global analysis of the bioassay 48
4.2 Application of the bioassay 50
5. Conclusions and prospects 59
6. References 60

List of figures

Figure 2.1 - Electromagnetic spectrum (Adapted from: KHANACADEMY, 2017) 2
Figure 2.2 - Regions of the infrared spectrum (Adapted from: Edmund Scientific, 2017) 3
Figure 2.3 - MIR absorption spectrum with bands associated to molecular bounds of biomolecules highlighted (Graça *et al*., 2013) 8
Figure 2.4 - Spectral derivatives (Adapted from: ASD_{Inc}, 2017) 10
Figure 2.5 – PCA of different *E. coli* isolates to see if the unidentified isolates correspond to the known isolate. The different colours represent the different isolates of *E.coli*, the black ones are identified as ST131 isolates, while other colours indicate groups of unknown sequence types (Adapted from: Harrison and Hanson, 2007) 11
Figure 4.1 - FTIR spectra obtained from quintuplicates of assays of *E. coli* cells incubated for 1 hour (T1) with ethanol concentrations of 0 (C0), 2 (C1) and 10% (C2) (v/v) a) without preprocessing, b) preprocessed by baseline correction, normalization and MSC, c) preprocessing by second derivative. 20
Figure 4.2 - PCA score plot of FTIR spectra of *E.coli* submitted to different ethanol concentrations (C0 = 0; C1 = 2; C2 = 10% (V/V)) and incubated with different nutrient media concentration (M 1.25x, 2.5x and 5x). a) without preprocessing b) preprocessed by base line correction and normalization Amide I. PC1, PC2 and PC3 represents 95%, 4% and 1% of data variance, respectively 22
Figure 4.3 - PCA score plot of FTIR spectra of *E. coli* submitted to different bleach concentrations (C0 = 0; C1 = 10; C2 = 80 ppm) and incubated with different nutrient media concentration (M 1.25x, 2.5x and 5x) a) preprocessed by base line correction and Min Max normalization b) preprocessed second derivative. PC1, PC2 and PC3 represent 98%, 1% and 1% of data variance, respectively..... 23
Figure 4.4 – PCA score plot of FTIR spectra of *E. coli* submitted to different sodium chloride concentrations (C0 = 0; C1 = 4; C2 = 8% (W/V)) and incubated with different nutrient media concentration (M 1.25x, 2.5x and 5x) a) preprocessed by base line correction, Min Amide I normalization and MSC b) preprocessed by base line correction, MinMax normalization and MSC. PC1, PC2 and PC3 represent 98%, 1% and 1% of data variance, respectively..... 25
Figure 4.5 - PCA score plot of FTIR spectra of *E. coli* submitted to different hydrochloric acid concentrations (C0 = 0; C1 = 250; C2 = 500 μL) and incubated with different nutrient media concentration (M 1.25x, 2.5x and 5x) a) preprocessed by base line correction, Min Amide I normalization and MSC b) preprocessed by second derivative. PC1, PC2 and PC3 represent 95%, 4% and 1% of data variance, respectively 27
Figure 4.6 - PCA score plot of FTIR spectra of *E. coli* submitted to different sodium hydroxide concentrations (C0 = 0; C1 = 250; C2 = 500 μL) and incubated with different nutrient media concentration (M 1.25x, 2.5x and 5x) a) preprocessed by base line correction b) preprocessed by MinMax normalization and MSC. PC1, PC2 and PC3 represent 95%, 4% and 1% of data variance, respectively..... 29
Figure 4.7 - PCA score plot of FTIR spectra of *E. coli* submitted to different concentrations (C) of the stress agents ethanol (A1), bleach (A2), sodium chloride (A3), hydrochloric acid (A4) and sodium hydroxide (A5) and different nutrient media concentration (M 1.25x, 2.5x and 5x) a) medium 1.25x, with spectra preprocessed by second derivative, b) medium 2.5x, with spectra preprocessed by base line correction, MinMax normalization and MSC c) medium 5x, with spectra preprocessed by Min

Amide I normalization and MSC. PC1, PC2 and PC3 represent 96%, 3% and 1% of data variance, respectively..... 30
Figure 4.8 - PCA score plot of FTIR spectra of *E. coli* submitted to different ethanol concentrations (C0 = 0; C1 = 2; C2 = 10% (V/V)) and in different growth phase (8, 16 and 24 hrs), preprocessed by base line correction and Min Amide I normalization. PC1, PC2 and PC3 represent 98%, 1% and 1% of data variance, respectively 31
Figure 4.9 - PCA score plot of FTIR spectra of *E. coli* submitted to different bleach concentrations (C0 = 0; C1 = 10; C2 = 80 ppm) and in different growth phase (8, 16 and 24 hrs), preprocessed by base line correction, MinMax normalization and MSC. PC1, PC2 and PC3 represent 98%, 1% and 1% of data variance, respectively 32
Figure 4.10 - PCA score plot of FTIR spectra of *E. coli* submitted to different sodium chloride concentrations (C0 = 0; C1 = 4; C2 = 8% (W/V)) and in different growth phase (8, 16 and 24 hrs), preprocessed by base line correction. PC1, PC2 and PC3 represent 95%, 4% and 1% of data variance, respectively..... 33
Figure 4.11 - PCA score plot of FTIR spectra of *E. coli* submitted to different hydrochloric acid concentrations (C0 = 0; C1 = 250; C2 = 500 µL) and in different growth phase (8, 16 and 24 hrs), a) preprocessed by second derivative. PC1, PC2 and PC3 represent 94%, 5% and 1% of data variance, respectively..... 34
Figure 4.12 - PCA score plot of FTIR spectra of *E. coli* submitted to different sodium hydroxide concentrations (C0 = 0; C1 = 250; C2 = 500 µL) and in different growth phase (8, 16 and 24 hrs), preprocessed by second derivative. PC1, PC2 and PC3 represent 91%, 6% and 3% of data variance, respectively..... 35
Figure 4.13 - PCA score plot of FTIR spectra of *E. coli* submitted to different concentrations (C) of the stress agents ethanol (A1), bleach (A2), sodium chloride (A3), hydrochloric acid (A4) and sodium hydroxide (A5) and different in different growth phase (8, 16 and 24 hrs) a) after eight hrs of growth, preprocessed by second derivative b) after sixteen hrs of growth, preprocessed by base line correction, Min Amide I normalization and MSC c) after twenty-four hrs of growth, preprocessed by second derivative. PC1, PC2 and PC3 represent 98%, 1% and 1% of data variance, respectively..... 37
Figure 4.14 - PCA score plot of FTIR spectra of *E. coli* submitted to different ethanol concentrations (C0 = 0; C1 = 2; C2 = 10%) and with different incubation times (1, 8 and 24 hrs) a) preprocessed by base line correction and MinMax normalization b) preprocessed by second derivative. PC1, PC2 and PC3 represent 98%, 1% and 1% of data variance, respectively 38
Figure 4.15 - PCA score plot of FTIR spectra of *E. coli* submitted to different bleach concentrations (C0 = 0; C1 = 10; C2 = 80 ppm) and with different incubation times (1, 8 and 24 hrs) a) preprocessed by second derivative b) preprocessed by Min Amide I normalization and MSC. PC1, PC2 and PC3 represent 98%, 1% and 1% of data variance, respectively 40
Figure 4.16 - PCA score plot of FTIR spectra of *E. coli* submitted to different sodium chloride concentrations (C0 = 0; C1 = 4; C2 = 8% (W/V)) and with different incubation times (1, 8 and 24 hrs) a) without preprocessing b) preprocessed by MinMax normalization and MSC. PC1, PC2 and PC3 represent 98%, 1% and 1% of data variance, respectively 42
Figure 4.17 - PCA score plot of FTIR spectra of *E. coli* submitted to different hydrochloric acid concentrations (C0 = 0; C1 = 250; C2 = 500 µL) and with different incubation times (1, 8 and 24 hrs) a) without preprocessing b) preprocessed by second derivative. PC1, PC2 and PC3 represent 95%, 4% and 1% of data variance, respectively. 44
Figure 4.18 - PCA score plot of FTIR spectra of *E. coli* submitted to different sodium hydroxide concentrations (C0 = 0; C1 = 250; C2 = 500 µL) and with different incubation times (1, 8 and 24 hrs)

a) preprocessed by base line correction, Min Amide I normalization and MSC b) preprocessed by second derivative. PC1, PC2 and PC3 represent 88%, 8% and 4% of data variance, respectively..... 45
Figure 4.19 - PCA score plot of FTIR spectra of *E. coli* submitted to different concentrations (C) of the stress agents ethanol (A1), bleach (A2), sodium chloride (A3), hydrochloric acid (A4) and sodium hydroxide (A5) and with different incubation times (1, 8 and 24 hrs) a) after one hr of incubation, preprocessed by second derivative b) after eight hrs of incubation, preprocessed by second derivative c) after twenty four hrs of incubation, preprocessed by second derivative. PC1, PC2 and PC3 represent 95%, 4% and 1% of data variance, respectively. 47
Figure 4.20 - PCA score plot of FTIR spectra of *E. coli* submitted to different concentrations of the antibiotic amoxicillin (C0 = 0; C1 = 0.01; C2 = 0.04; C3 = 0.2; C4 = 5; C5 = 25; C6 = 62.5; C7 = 125 mg/μL) a) preprocessed by second derivative b) preprocessed by second derivative. PC1, PC2 and PC3 represent 98%, 1% and 1% of data variance, respectively. 51
Figure 4.21 - PCA score plot of FTIR spectra of *E. coli* submitted to different concentrations of the antibiotic ampicillin (C0 = 0; C1 = 0.01; C2 = 0.04; C3 = 0.2; C4 = 5; C5 = 25; C6 = 62.5; C7 = 125 mg/μL) a) without preprocessing b) preprocessed by second derivative. PC1, PC2 and PC3 represent 98%, 1% and 1% of data variance, respectively. 52
Figure 4.22 - PCA sore plot of FTIR spectra of *E. coli* submitted to different concentrations of the antibiotic ciprofloxacin (C0 = 0; C1 = 0.01; C2 = 0.04; C3 = 0.2; C4 = 5; C5 = 25; C6 = 62.5; C7 = 125 mg/μL) a) preprocessed by base line correction and Min Amide I normalization b) preprocessed by Min Amide I normalization. PC1, PC2 and PC3 represent 98%, 1% and 1% of data variance, respectively..... 53
Figure 4.23 - PCA sore plot of FTIR spectra of *E. coli* submitted to different concentrations of the antibiotic erythromycin (C0 = 0; C1 = 0.01; C2 = 0.04; C3 = 0.2; C4 = 5; C5 = 25; C6 = 62.5; C7 = 125 mg/μL) a) preprocessed by base line correction and Min Amide I normalization b) preprocessed by second derivative. PC1, PC2 and PC3 represent 98%, 1% and 1% of data variance, respectively.. 54
Figure 4.24 - PCA sore plot FTIR spectra of *E. coli* submitted to different concentrations of the antibiotic metronidazole (C0 = 0; C1 = 0.01; C2 = 0.04; C3 = 0.2; C4 = 5; C5 = 25; C6 = 62.5; C7 = 125 mg/ μL) a) preprocessed by base line correction, Min Amide I normalization and MSC b) preprocessed by Min Max normalization. PC1, PC2 and PC3 represent 98%, 1% and 1% of data variance, respectively 55
Figure 4.25 - PCA sore plot FTIR spectra of *E. coli* submitted to different concentrations of the antibiotic neomycin (C0 = 0; C1 = 0.01; C2 = 0.04; C3 = 0.2; C4 = 5; C5 = 25; C6 = 62.5; C7 = 125 mg/μL) a) preprocessed by base line correction, Min Amide I normalization and MSC b) preprocessed by Min Max normalization. PC1, PC2 and PC3 represent 98%, 1% and 1% of data variance, respectively..... 56
Figure 4.26 - PCA sore plot FTIR spectra of *E. coli* submitted to different concentrations of the all antibiotics tested (amoxicillin, ampicillin, ciprofloxacin, erythromycin, metronidazole and neomycin) a) preprocessed by base line correction and Min Amide I normalization b) pre-processed by base line correction and Min Amide I normalization. PC1, PC2 and PC3 represent 98%, 1% and 1% of data variance, respectively 58

List of Tables

Table 2.1 - Spectra bands and its associated absorbing chemical groups and corresponding biomolecules (Adapted from: Naumann, 2001) 7
Table 2.2 - Sigma factors of *E. coli* (Adapted from: Abee and Wouters, 1999) 12
Table 3.1 - Stock solutions of the stress agents and quantities in the assays……17
Table 0.2 - Summary of assays conditions……17
Table 3.3 - Reaction mixtures of the solution 250 mg/L 18
Table 3.4 - Reaction mixtures of the solution 1 mg/L 18
Table 4.1 - p-values of the spectral ratios obtained from the quintuplicates of the assay with *E. coli* with different concentrations of ethanol (C0 = 0; C1 = 2; C2 = 10% (V/V)) and incubated with different nutrient media concentration (M 1.25x, 2.5x and 5x). The statistically significant p-values ($p<0.05$) are highlighted in green 22
Table 4.2 - p-values of the spectral ratios obtained from the quintuplicates of the assay with *E. coli* with different concentrations of bleach (C0 = 0; C1 = 10; C2 = 80 ppm) and incubated with different nutrient media concentration (M 1.25x, 2.5x and 5x). The statistically significant p-values ($p<0.05$) are highlighted in green 24
Table 4.3 - p-values of the spectral ratios obtained from the quintuplicates of the assay with *E. coli* with different concentrations of sodium chloride (C0 = 0; C1 = 4; C2 = 8% (W/V)) and incubated with different nutrient media concentration (M 1.25x, 2.5x and 5x). The statistically significant p-values ($p<0.05$) are highlighted in green the statistically significant p-values are highlighted in green..... 26
Table 4.4 - p-values of the spectral ratios obtained from the quintuplicates of the assay with *E. coli* with different concentrations of hydrochloric acid (C0 = 0; C1 = 250; C2 = 500 μL) and incubated with different nutrient media concentration (M 1.25x, 2.5x and 5x). The statistically significant p-values ($p<0.05$) are highlighted in green 28
Table 4.5 - p-values of the spectral ratios obtained from the quintuplicates of the assay with *E. coli* with different concentrations of sodium hydroxide (C0 = 0; C1 = 250; C2 = 500 μL) and incubated with different nutrient media concentration (M 1.25x, 2.5x and 5x). The statistically significant p-values ($p<0.05$) are highlighted in green 29
Table 4.6 - p-values of the spectral ratios obtained from the quintuplicates of the assay with *E. coli* with different ethanol concentrations (C0 = 0; C1 = 2; C2 = 10% (V/V)) and in different growth phase (8, 16 and 24 hrs). The statistically significant p-values ($p<0.05$) are highlighted in green 32
Table 4.7 - p-values of the spectral ratios obtained from the quintuplicates of the assay with *E. coli* with different bleach concentrations (C0 = 0; C1 = 10; C2 = 80 ppm) and in different growth phase (8, 16 and 24 hrs). The statistically significant p-values ($p<0.05$) are highlighted in green 33
Table 4.8 - p-values of the spectral ratios obtained from the quintuplicates of the assay with *E. coli* with different sodium chloride concentrations (C0 = 0; C1 = 4; C2 = 8% (W/V)) and in different growth phase (8, 16 and 24 hrs). The statistically significant p-values ($p<0.05$) are highlighted in green 34
Table 4.9 - p-values of the spectral ratios obtained from the quintuplicates of the assay with *E. coli* with different hydrochloric acid concentrations (C0 = 0; C1 = 250; C2 = 500 μL) and in different growth phase (8, 16 and 24 hrs). The statistically significant p-values ($p<0.05$) are highlighted in green 35
Table 4.10 - p-values of the spectral ratios obtained from the quintuplicates of the assay with *E. coli* with different sodium hydroxide concentrations (C0 = 0; C1 = 250; C2 = 500 μL) and in different

growth phase (8, 16 and 24 hrs). The statistically significant p-values (p<0.05) are highlighted in green 36
Table 4.11 - p-values of the spectral ratios obtained from the quintuplicates of the assay with *E. coli* with different ethanol concentrations (C0 = 0; C1 = 2; C2 = 10%) and with different incubation times (1, 8 and 24 hrs). The statistically significant p-values (p<0.05) are highlighted in green 39
Table 4.12 - p-values of the spectral ratios obtained from the quintuplicates of the assay with *E. coli* with different bleach concentrations (C0 = 0; C1 = 10; C2 = 80 ppm) and with different incubation times (1, 8 and 24 hrs). The statistically significant p-values (p<0.05) are highlighted in green the statistically significant p-values are highlighted in green 41
Table 4.13 - p-values of the spectral ratios obtained from the quintuplicates of the assay with *E. coli* with different sodium chloride concentrations (C0 = 0; C1 = 4; C2 = 8% (W/V)) and with different incubation times (1, 8 and 24 hrs). The statistically significant p-values (p<0.05) are highlighted in green 43
Table 4.14 - p-values of the spectral ratios obtained from the quintuplicates of the assay with *E. coli* with different acid hydrochloric concentrations (C0 = 0; C1 = 250; C2 = 500 μL) and with different incubation times (1, 8 and 24 hrs). The statistically significant p-values (p<0.05) are highlighted in green 44
Table 4.15 - p-values of the spectral ratios obtained from the quintuplicates of the assay with *E. coli* with different sodium hydroxide concentrations (C0 = 0; C1 = 250; C2 = 500 μL) and with different incubation times (1, 8 and 24 hrs). The statistically significant p-values (p<0.05) are highlighted in green 46
Table 4.16 - Optimal conditions for the bioassay for each stress agent taking into account nutrient concentration, *E. coli* growth phase and incubation time 48
Table 4.17 - Main spectral ratios that reflected the effect of each stress agents on the cell metabolism 50
Table 4.18 - p-values of the spectral ratios obtained from the quintuplicates of the assay with *E. coli* with different amoxicillin concentrations (C0 = 0; C1 = 0.01; C2 = 0.04; C3 = 0.2; C4 = 5; C5 = 25; C6 = 62.5; C7 = 125 mg/μL). The statistically significant p-values (p<0.05) are highlighted in green. 51
Table 4.19 - p-values of the spectral ratios obtained from the quintuplicates of the assay with *E. coli* with different ampicillin concentrations (C0 = 0; C1 = 0.01; C2 = 0.04; C3 = 0.2; C4 = 5; C5 = 25; C6 = 62.5; C7 = 125 mg/μL). The statistically significant p-values (p<0.05) are highlighted in green 53
Table 4.20 - p-values of the spectral ratios obtained from the quintuplicates of the assay with *E. coli* with different ciprofloxacin concentrations (C0 = 0; C1 = 0.01; C2 = 0.04; C3 = 0.2; C4 = 5; C5 = 25; C6 = 62.5; C7 = 125 mg/μL). The statistically significant p-values (p<0.05) are highlighted in green 54
Table 4.21 - p-values of the spectral ratios obtained from the quintuplicates of the assay with *E. coli* with different erythromycin concentrations (C0 = 0; C1 = 0.01; C2 = 0.04; C3 = 0.2; C4 = 5; C5 = 25; C6 = 62.5; C7 = 125 mg/μL). The statistically significant p-values (p<0.05) are highlighted in green 55
Table 4.22 - p-values of the spectral ratios obtained from the quintuplicates of the assay with *E. coli* with different metronidazole concentrations (C0 = 0; C1 = 0.01; C2 = 0.04; C3 = 0.2; C4 = 5; C5 = 25; C6 = 62.5; C7 = 125 mg/μL). The statistically significant p-values (p<0.05) are highlighted in green. 56
Table 4.23 - p-values of the spectral ratios obtained from the quintuplicates of the assay with *E. coli* with different neomycin concentrations (C0 = 0; C1 = 0.01; C2 = 0.04; C3 = 0.2; C4 = 5; C5 = 25; C6 = 62.5; C7 = 125 mg/μL). The statistically significant p-values (p<0.05) are highlighted in green 57

List of Abbreviations

ATR: Attenuated total reflection

BT: Bacto tryptone

DPT: Data point table

Far-IR: Far infrared

FTIR: Fourier Transform Infrared

IR: Infrared

MIR: Mid-Infrared

MSC: Multiple scattering correction

NIR: Near-Infrared

OD: Optical density

PC: Principal component

PCA: Principal component analysis

RNAP: RNA polymerase

ROS: Reactive oxygen species

SNR: Signal-to-noise ratio

YE: Yeast extract

1. Thesis overview

1.1 Objectives

The main goal of the present study was to optimize a bioassay to evaluate the biochemical and metabolic profile of *Escherichia coli* (*E. coli*) bacteria, when exposed to diverse environmental conditions as stress agents as: ethanol, bleach, sodium chloride, hydrochloric acid, sodium hydroxide and antibiotics. The bioassay is based on Fourier Transform Infrared (FTIR) spectroscopy analysis of micro volume of an incubation mixture of *E. coli* cells with a nutrient medium and the stress agents. The FTIR spectra are acquired in a simple, rapid, economic, sensitive and high-throughput mode. In order to reach a high sensitivity in the evaluation the effect of environmental conditions in the bacteria metabolism, it is intended to optimise the following conditions related to the incubation mixture of the bacteria with the stress agents: nutrient medium concentration, *E. coli* growth phase and incubation time. Another goal was to find spectral biomarkers for the changes that occur in the metabolism of bacteria when exposed to stress conditions.

1.2 Thesis Outline

The present work is divided into three parts: general introduction, optimization of a bioassay based on Fourier Transform Infrared spectroscopy and bioassay testing through exposure of *E. coli* to different antibiotics. The first part includes a description of IR spectroscopy, where some theoretical explanations about the technique and the description of the analysis methods are presented. The last two sections of this work are related to the experimental work carried out. For the bioassay optimization, the following parameters of the bacteria incubation mixture with the stress agents were evaluated: the growth phase of the bacteria, incubation time of the reaction mixture with the stress agents and the composition of the nutrient medium used on the incubation mixture. Finally, the optimized bioassay was used to evaluate the effect of six different antibiotics on the bacteria metabolism that affects the bacteria metabolism by different mechanisms as by inhibiting the cell membrane synthesis, the protein synthesis and DNA synthesis.

2. Introduction

2.1 Infrared spectroscopy

Spectroscopy consists in the study of electromagnetic radiation emitted or absorbed by a body. The term began to be used at the end of the XIX century, after Bunsen and Kirchhoff, in 1860, found that absorption and emission spectra made it possible to determine the presence of certain chemical elements in a sample, which allowed the discovery of cesium, rubidium and thallium (Thomas, 1991). Nowadays, a spectrum is understood as the representation of a given magnitude referring to a study object as a function of the frequency, energy or wavelength of the absorbed or emitted radiation. Absorption occurs when the emitted radiation is attenuated by the sample and emission takes place when radiation is produced by the sample due to excitation by a light source (Thomas, 1991). The set of electromagnetic radiation constitutes the electromagnetic spectrum, which is dividing into several regions: gamma rays, x-rays, ultraviolet, visible, infrared, microwave, radio (figure 2.1).

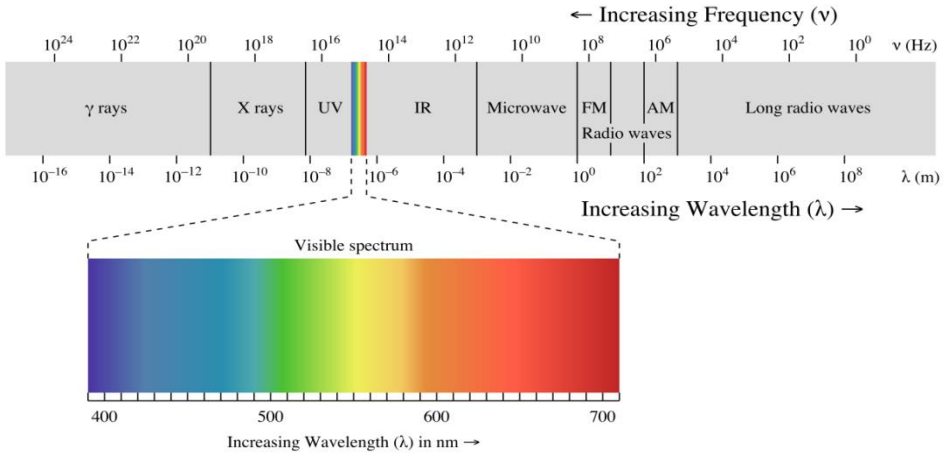

Figure 2.1 - Electromagnetic spectrum (Adapted from: KHANACADEMY, 2017)

In this work was intended to use infrared (IR) radiation to study the metabolic changes in *E. coli* bacteria when exposed to adverse conditions. In 1800, William Herschel discovered that IR is a non-ionizing radiation in the invisible portion of the electromagnetic spectrum that is adjacent to the long wavelengths. Herschel placed a mercury thermometer on the spectrum obtained by a crystal prism with the purpose of measuring the heat emitted by each colour. He found that the heat was stronger closer to the red light of the spectrum. This was the first experiment that observed that heat can be captured in the image form, as with visible light (Oliveira and Silva, 2014). The IR region can be subdivided into three distinct zones, according to the wavelength: near infrared (NIR), medium infrared (MIR) and far infrared (far-IR). Far-IR ranges from 400 to 4 cm^{-1} in the IR spectrum, MIR represents the region between 4000 and 400 cm^{-1} and NIR the region between 14000 and 4000 cm^{-1} (Figure 2.2) (Smith, 2011). In this work, was used the MIR radiation, which will be discussed later.

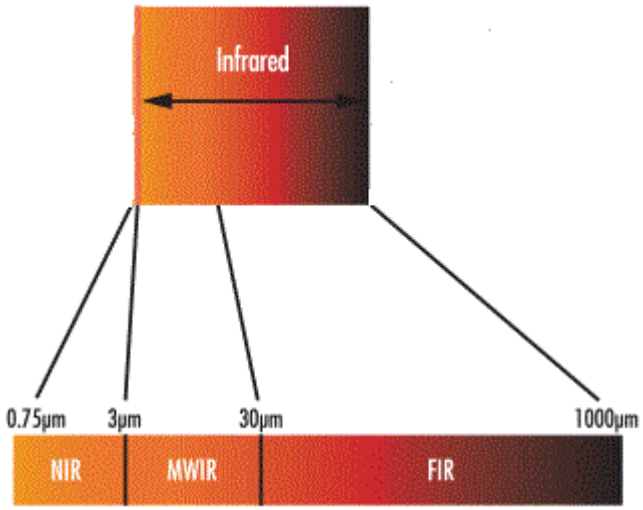

Figure 2.2 - Regions of the infrared spectrum (Adapted from: Edmund Scientific, 2017)

The IR absorbed by the molecules in the sample, stimulates its molecular vibration. At temperatures above absolute zero the molecule atoms are in continuous vibration with respect to each other. When a molecule is exposed to IR radiation it only absorbs the frequencies corresponding to its own vibration frequency. These changes in the vibration mode of molecules produce the bands in the IR spectrum. Each band is characterized by a frequency and amplitude (Duygu, 2009). Almost any molecule that possesses covalent bounds absorbs IR radiation, excepting monoatomic molecules (He or Ne) and homopolar diatomic molecules ($H2$, O2 …). Since monoatomic molecules have only one atom, it does not have dipolar moment. Homopolar diatomic molecules are formed by only one type of atoms, having the same electronic filed, so it does not have a dipolar moment as well. All the other type of molecules has dipolar moment absorbing IR radiation which allow it's quantitative or qualitative analysis by IR spectroscopy (Griffiths, 2002). Considering the changes in the vibrational modes of the molecules, there are essentially two types of vibrations, which can be classified depending on changes on the bond length or angle: stretching and bending vibrations (Figure 2.3). The stretching is a symmetric or antisymmetric rhythmical movement along the bond length. The bending vibration occurs when there is a change of the angle between two atoms or a group of atoms (Babrah, 2009).

MIR spectroscopy is an extremely reliable and widely recognized fingerprinting technique. As previously mentioned mid-infrared represents the region between 4000 and 400 cm^{-1}. It includes fundamental vibration signatures of major molecules that compose the tissues and biological fluids. Therefore, the absorption spectrum in mid-infrared of a biologic element is representative of its composition because it accurately reflects the structure of the molecules constituting the sample, which makes this technique more sensitive and more complete in terms of spectra information, comparing to NIR spectroscopy because most bands in NIR region are consequence of overtones and combinations of vibrations from different chemical elements and functional group. Another advantage is that the calibration data in the mid-infrared is much more generic than in the NIR and thus it is more likely transferable from instrument to instrument (Smith, 2011). On the other hand, water absorbs much more radiation in the MIR region than in NIR region, which can be a problem when we are analysing aqueous samples, being usually necessary an extra step of sample dehydration before

spectral acquisition. Furthermore, MIR radiation has a shorter wavelength than NIR radiation and consequently less energy, so the ability of this kind of radiation to penetrate the sample is reduced (Landgrebe *et al.*, 2010). Therefore, deciding which technique will be the measurement of choice depends on the sample format, the required sample environment, the available database and which process provides the most relevant information to answer the required question.

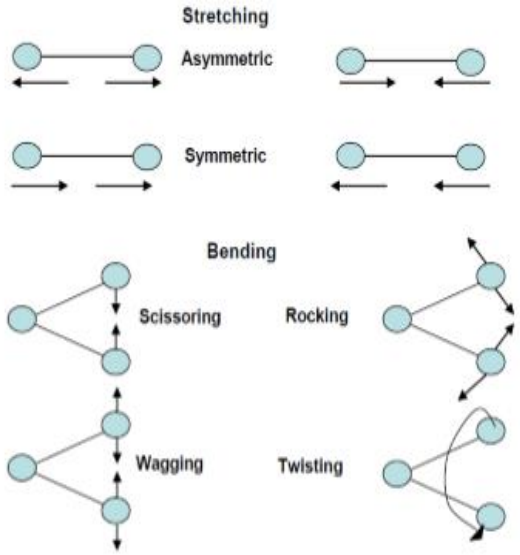

Figure 2.3 - Molecular vibrational modes (Babrah, 2009)

2.1.1 Instrumentation

Infrared (IR) spectroscopy is a technique that is being increasingly used in biology, especially for whole cell metabolomics fingerprint. The instrument used in IR spectroscopy is called infrared spectrometer or spectrophotometer and consists mainly in a beam source, a monochromator or an interferometer (depending on the type of spectrometer), a sample holder or sample presentation interface and a detector that will detect the radiation that is transmitted or reflect by the sample (Reich, 2005). The beam source may consist on an inert solid thermally heated or in an incandescent filament like tungsten or quartz/halogen lamps, for NIR region, and carbon-silicon bars, for MIR radiation (Christian, 1994).

The interferometer consists of a beam splitter, a fixed mirror, and a mirror that translates back and forth, very precisely. The beam splitter is made of a special material that transmits half of the radiation striking it and reflects the other half. Radiation from the source strikes the beam splitter and separates into two beams. One beam is transmitted through the beam splitter to the fixed mirror and the second is reflected by the beam splitter to the moving mirror. The fixed and moving mirrors reflect the radiation back to the beam splitter (figure 2.4). Again, half of the reflected radiation is transmitted and half is reflected at the beam splitter, resulting in one beam passing to the detector and the second back to the source (Martin, 2002). The Michelson interferometer is still used today in most Fourier Transformed Infra-Red (FTIR) spectrometers. The first FTIR equipment to be marketed was

manufactured by Digilab, subsidized by Block Engeneering in Massachusetts in the late 1960's. This first FTIR incorporated an interferometer developed by Albert Abraham Michelson in 1880 (Thermo Scientific, 2008).

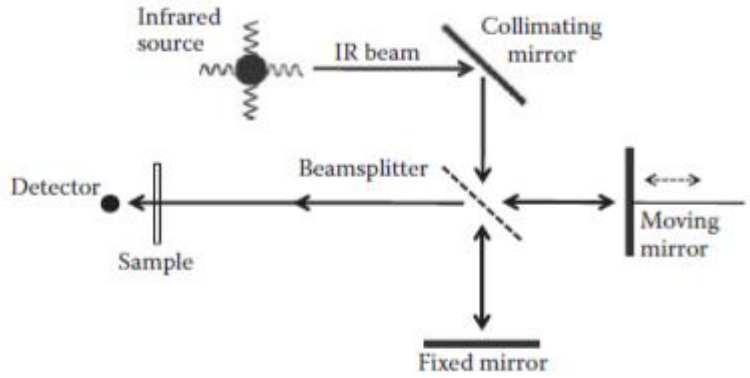

Figure 2.4 - Scheme of the Michelson interferometer (Smith, 2011)

FTIR spectroscopy uses a composite beam of light with varying wavelengths. Once the absorbance measurement is performed, the light beam is modified to a combination of wavelengths different from the previous beam, which forms a second set of data. This process is repeated several times. The resulting spectrum is called an interferogram (a spectrum consisting on intensity versus acquisition time) that is later traduce to the final IR spectrum (intensity versus frequency or wavelengths) by the mathematical operation called Fourier-Transform (Stuart, 2004). The IR spectrum is characteristic of each type of molecule, since it depends mainly of the atoms mass, their geometric arrangement and the bound forces between them. Since there are no two different molecules that possess these three same characteristics, each molecule will have, in theory, a distinct spectrum. Extending that concept, two different samples, with distinct molecular composition will also have different spectra. This principle is the foundation of IR spectroscopy and it makes possible to virtually distinguish, qualify or quantify any type of sample (Smith, 2011).

FTIR spectroscopy has advantages over classical molecular biology techniques, such as speed and simplicity of execution, need for few consumables and reduced cost per analysis, in the same time has advantages over the dispersive spectrometer since the FTIR spectrometer simultaneously collects data from a wide spectral range (Thermo Scientific, 2008).

2.1.2 Acquisition Modes

Depending on the sample properties, FTIR spectra can be acquired mainly in three different experimental configurations: transmission, reflection-absorption (transflection) or attenuated total reflection (ATR). The first one operates by transmitting IR radiation through sample-substrate, whereas in transflection the radiation interacts with sample and is most reflected back but a part is also absorbed by the substrate. Finally, on the ATR mode, the sample is placed on a crystal with a higher refractive index than the sample, inducing total internal reflection of incident radiation, which is attenuated and penetrates into the sample as an evanescent wave (Lima, 2015).

In transflection, the low-emissivity slides, commonly used as reflector substrates, contribute to the formation of a standing wave perpendicular to sample surface that leads to spectral changes not related with the sample biochemical properties (Greenler, 1966). In transmission mode, spectra collected are submitted to a variety of physical effects occurring at the same time with absorption, and requires corrections for phenomena, such as light scattering, refraction, dispersion and other optical effects specifically related to measuring thin films, which may also induce spectral distortions (Chan, 2013). The ATR sampling mode presents usually a high SNR (signal-to-noise ratio) compared to those obtained by transfection and transmission configurations (Lima, 2015), however for diluted samples the SRN signal can also be low. In this work the transmission mode was used because it is the most suitable for the type of samples used (liquid/aqueous samples), also due to its capacity to be measured in high-throughput mode.

2.1.3 Applications to Microbiology

Stair and Coblentz in 1935 were perhaps the first to record the spectra of biological materials such as onion skins, the membrane of fish bladder, bat's wings, egg albumin, egg membranes (Norris, 1959) and Randall *et al*. (1951) were the first to record the spectra of whole cells of bacteria. In 1959 was published an article stating that bacteria have a characteristic infrared spectrum, unique to each strain. However, at that time it was considered a very time consuming process. Naumann and his collaborators highly contributed for the descriptions of the FTIR spectroscopy applications to microbiology as presented today. Through their studies they were able to elaborate a table where the various functional groups that can be present in the microbial cells are described. The regions of MIR spectrum corresponding to each group of biomolecules are nowadays well characterized, namely regions associated with proteins, lipids, amino acids and even lactate, urea or glucose absorption (Bellisola, 2012) (figure 2.5). Generally, the study of a particular strain characteristic uses one or more spectral zones and not just a single functional group. An adaptation of the table described by Naumann can be seen in the table 2.1.

Table 2.1 - Spectra bands and its associated absorbing chemical groups and corresponding biomolecules (Adapted from: Naumann, 2001)

Wave number	Designation
~3500	O-H stretching movements of hydroxyl groups
~3200	N-H stretches of proteins
~2955	Asymmetric C-H stretching movements of -CH3 in fatty acids
~2930	Asymmetric C-H distances of > CH_2
~2918	Asymmetric C-H stretching movements of > CH_2 in fatty acids
~2898	C-H stretching movements in methyl groups
~2870	Symmetrical C-H distending movements of -CH_3
~2850	Symmetrical C-H distances of > CH_2 in fatty acids
~1740	Stretching movements > C=O of the esters
~1715	Stretching movements > C=O of carbonic acids
~1680	Stretching movements > C=O of nucleic acids
~1695	Components of the amide I band
~1685	Resulting from beta-antiparallel sheets
~1675	Beta configuration of proteins
~1655	Alpha helical structures of amide I
~1637	Structures of the beta sheets of amide I
~1550 – 1520	Amide II
~1515	Tyrosine band
~1468	C-H deformation of > CH_2
~1400	Symmetric distending movements C=O of COO^-
~1310 - 1240	Protein amide III band
~1250 – 1220	Asymmetric distending movements P=O of > PO^-_2 of phosphodiesters
~1200 – 900	C-O and C-C distension movements and C-O-C deformation of carbohydrates
~1090 – 1085	Symmetrical distending movements P=O of > PO_2^-
~720	Rotation of the C-H bond of > CH_2
~900 - 600	Fingerprint region of the microorganism

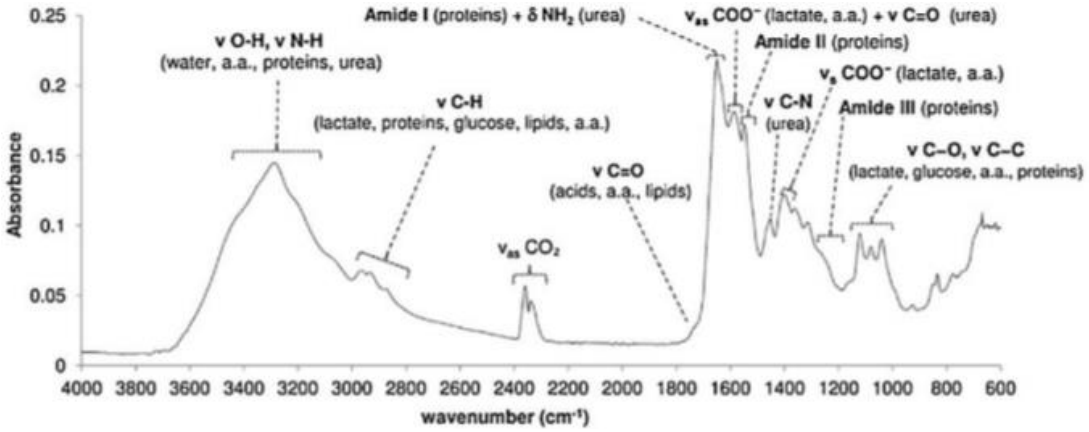

Figure 2.3 - MIR absorption spectrum with bands associated to molecular bounds of biomolecules highlighted (Graça *et al*., 2013)

Since then, spectroscopic methods have been applied for diverse biological applications, such as monitoring microbial and mammalian cell cultures. This allows to estimate, from a single spectrum, several variables such as cell growth, nutrients consumption (*e.g*., glucose and glycerol), metabolic by-products (*e.g*., ethanol and acetate) production and consumption and plasmids and recombinant proteins production (Arnold, *et al*., 2003; Sellick, *et al*., 2010). The high sensitivity of MIR spectroscopy also enabled bacteria typing and subtyping (Amiali, *et al*., 2007; Davis , *et al*., 2012), the detection of cell cycle events and mechanism discrimination of cell death between apoptosis and necrosis (Jamin, *et al*., 2003; Hammiche, *et al*., 2005), monitoring of stem cells differentiation (Aksoy and Severcan, 2012), cancer-related research and diagnosis (Bogomolny, *et al*., 2007), other diseases diagnosis (*e.g*., renal failure (Khanmohammadi, *et al*., 2013), and metabolic fingerprinting of amniotic fluid for early prenatal disorders (Graça, *et al*., 2013). In most of the works described, whole microorganism cells were analysed and presented very complex spectra since the resulting spectrum depends on the total chemical composition of cells (intracellular material, membrane and wall). Due to the complexity of the resulting spectrum, an evaluation of the spectra through multivariate analysis is indispensable (Chemometrics) (Lavine, 1998).

2.1.4 Chemometrics and Spectral pre-processing techniques

Chemometrics is the use of mathematical and statistical methods to improve the understanding of chemical information and to correlate quality parameters or physical properties to analytical instrument data (Roggo *et al*., 2007). Chemometrics was first introduced in the chemical field, being nowadays a widely used tool in several other areas such as spectroscopy (Geladi, 2003). The science of chemometrics gives spectroscopists many efficient ways to solve the calibration problem for analysis of spectral data. Chemometrics can be used to enhance methods development and make routine use of statistical models for data analysis (Bu, 2007). The application of pre-processing techniques is a very important step in the analysis of spectral data, since it enables the elimination of physical phenomena due to undesired variations, such as noise, differences along the sample thickness, and differences in the number cells across the sample and scattering events. This procedure has the goal of minimizing the irrelevant information present in the final spectra (Bu, 2007). In the present work some pre-processing techniques are reviewed, namely those used along the work: baseline correction, normalization, multiplicative scatter correction and spectral derivatives.

Not always the obtained spectra are grounded at zero. The type of algorithm used depends on the baseline correction needed. Those spectra which are dislocated from zero by a constant value are the simpler cases, since subtracting the value in question from the spectrum is usually enough. Though there are more difficult cases, for instance cases in which the baseline presents a slope, or even spectra with curvatures. In these cases an algorithm generating a function, a linear or polynomial function, can bring the spectrum to zero (Otto, 1999; Smith, 2011). There are probably two main disadvantages of using baseline correction algorithms. First, it is difficult to find a function that adjusts properly to the spectrum curvature, although there are already some good algorithms. Besides, the curvature along the spectrum is not always equal, so a unique function will hardly adjust correctly to the entire spectrum. Therefore, sometimes it is preferred to apply derivatives for offset correction. The problem of applied derivatives is that the resulting spectra will be noisier than the raw one (Smith, 2011).

The goal of normalization is pre-processing the data in order to minimize differences between the samples that are related with factors, such as differences in cell concentration. A careful design of the experience is still a critical factor that must be always taken into account before pre-processing the data. There are several methods for normalizing spectral data (Randolph, 2006). In the present work, all spectra were normalized using the Amide I band, at 1650 cm^{-1}. Basically, all spectra were divided by a previously determined constant, so all the spectra ended up having the same intensity at 1650 $^{-1}$.

The multiplicative scatter correction (MSC) has been proposed as method in NIR spectroscopy to correct signals for noise. Light scattering or change in path length for each sample is estimated relative to that of an ideal sample. For this method a reference spectrum is necessary, which is usually the mean spectrum of all available spectra. MSC works by fitting each spectrum to the average spectrum, which is thought to be the ideal, performing a transformation where the spectral data ($x1$, $x2$, …, xp) is converted into new values ($z1$, $z2$, …, zp), where p corresponds to wavelengths (Fearn *et al*., 2009). The following equation describes the transformation from x to z

$$zi = \frac{xi-a}{b}$$, (Equation 2.1)

where a represents the intercept and b the slope of a least-squares regression of $x1$, $x2$, …, xp on the values $r1$, $r2$, …, rp coming from the reference spectra.

Spectral derivatives are normally employed to remove baseline offsets and for highlighting spectral information, through the resolution of overlapping bands (figure 2.6). Applying the first derivate is extremely useful in cases where the offset is constant, since de first derivate of a constant is zero. The second derivative can also be applied and the result will be not only the removal of the baseline offset but also the resolution of overlapping bands (Otto, 1999). First and second derivatives can also be useful to highlight subtle differences between spectra, allowing to extract more information from spectral data. However, before applying derivatives, it is important to have in mind that the derivative spectra will have more noise than the initial one, so first and second derivatives must be applied in spectral data with high SNR, or using filters as polynomial fitting do decrease noise before application of derivatives (Lourenço *et al*., 2012; Scholz *et al*., 2012).

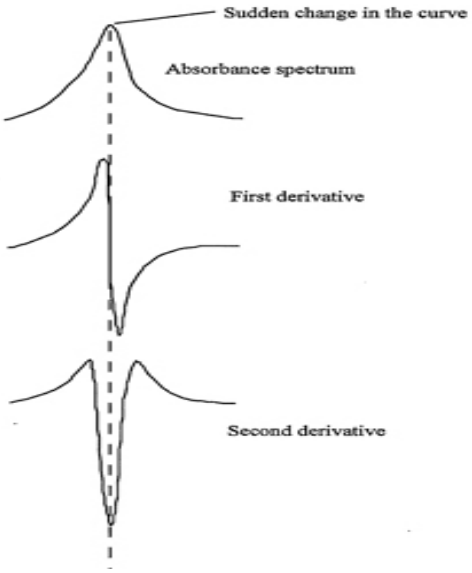

Figure 2.6 - Spectral derivatives (Adapted from: ASD_{inc}, 2017)

Principal component analysis (PCA) is a probably the most used processing technique to emphasize variation on data and bring out strong patterns in a dataset. It is often used to make data easy to explore and visualize when we are dealing with high dimensional data as spectral data (Jollife, 2002). It is a mathematical procedure that uses an orthogonal transformation to convert a set of observations of possibly correlated variables into a set of values of linearly uncorrelated variables called principal components. The number of major components is less than or equal to the number of original variables. PCs are ordered in terms of variance in the data set explained, with the first PCs representing the major variance in the data (Jollife, 2002).

The initial data matrix is decomposed as following:

$$X = TP^T + E, \text{ (Equation 2.2)}$$

where n is the number of samples in X, p is the number of variables in X, g is the number of chosen factors, X $(n \times p)$ is the descriptor data matrix, T $(n \times g)$ is the score matrix, P $(p \times g)$ represents the loading matrix and E $(n \times p)$ is the error matrix for the X-data matrix. Thus, a PC is described as a combination of loadings and scores, where loadings represent the contribution of each wavenumber to the PC and scores results from linear combinations of the initial data in X. Therefore each spectrum can be described as a combination of principle components (Naes *et al*., 2002).

Since the variance fraction can be covered by one, two or three PCs, it is possible to visualize almost the entire data by plotting these PCs against each other. In theory the samples with closer scores will be more similar to each other (figure 2.7) (Otto, 1999).

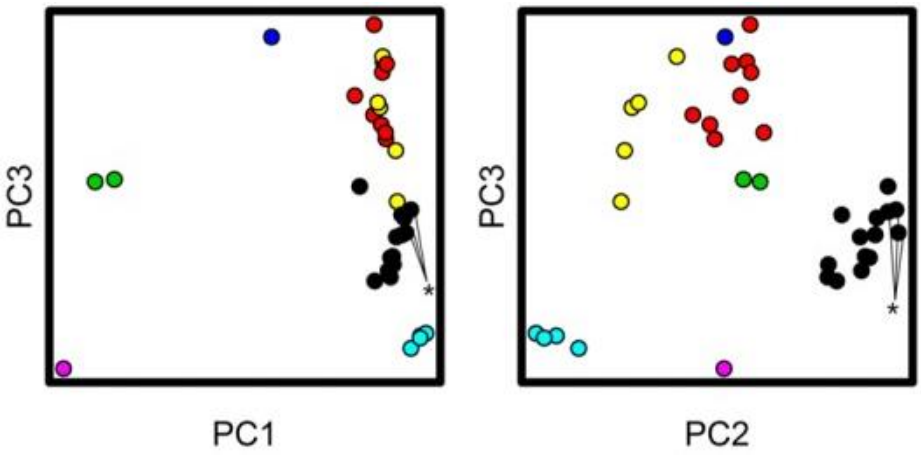

Figure 2.7 – PCA of different *E. coli* isolates to see if the unidentified isolates correspond to the known isolate. The different colours represent the different isolates of *E.coli*, the black ones are identified as ST131 isolates, while other colours indicate groups of unknown sequence types (Adapted from: Harrison and Hanson, 2007)

2.2 Bioassay optimization

Bioassays are an important tool to determine the biological effect caused by chemical, physical or biological agents on specific cells in environmental sciences in which complex mixtures of toxic compounds are present. In general, a bioassay could serve to detect metabolic perturbations, quantify the extent of the metabolic changes and classify the type of alterations observed. The uncovering of a metabolic modification is the basic of every bioassay, but not many tests are designed to quantify and classify the changes detected, though these two additional pieces of information are instrumental to understand not only that, for instance, there is a toxic agent in the sample, but also which type of action exerts and the strength of its activity (Corte, 2010).

Infrared spectroscopy was introduced as a tool to provide fingerprints of microorganisms, in the early nineties, demonstrating that the spectrum describes the metabolic state of the cells, bringing the Fourier transform infrared spectroscopy technique in the group of the metabolomics procedures (Helm, 1991). The metabolic alterations caused by different types of stress in microorganisms were studied with FTIR in a number of cases such as the bacterial response to antibiotics, the effect of starvation or different types of environmental stress (Corte, 2010).

This work intends to improve a bioassay that allows the study of the metabolic alterations in bacteria when exposed to stress conditions, taking into account three variables: growth phase of the culture, time of exposure to the stress agent and nutrient medium concentration. For this study was chose to use five substances that cause different types of stress, which will be explained later, but first it will make a small introduction of the bacterium chosen for this study: *Escherichia coli*.

2.2.1 *Escherichia coli* bacteria and stress responses

Escherichia coli is a widespread bacteria that can survive and adapt to growth under a wide range of conditions (Moen *et al*., 2009). *E. coli* is in the family *Enterobacteriaceae*. The bacteria is gram negative, rod shaped, non-spore forming and motile with peritrichous flagella or nonmotile. They can grow under aerobic and anaerobic conditions and have an optimum temperature of growth between 35 and 40°C (CDC, 2015). Together with *Staphylococcus aureus* it is the most common and one of the oldest symbiotic bacteria in mankind. It was discovered by the German-Austrian Theodor Escherich, in 1885 (Kyriakides, 1998). *E. coli* bacteria usually live in the intestines of people and animals. Most of the strains are harmless and actually are an important part of a healthy human intestinal tract. However, some *E. coli* are pathogenic being associated with intestinal and extra intestinal infections in humans and many animals (CDC, 2015). It is the most thoroughly studied bacterium, and is often a preferred model organism, as it uses mainstream metabolic pathways that are similar to the corresponding metabolic functions in other bacteria (Liang *et al*., 2002).

Escherichia coli encounter numerous different stresses during their growth, survival, and infection. Many bacterial species exhibit a general stress response that can be induced by different stress conditions and, phenotypically, renders the cells broadly stress resistant (Chung *et al*., 2006). A basic knowledge of how different adverse conditions affect *E. coli* is important when exploring the response potential, understanding how bacteria adapt and minimize the risk of illness (Chung *et al*., 2006).

Microorganisms have developed signal transduction systems to sense environmental stresses and to control the coordinated expression of genes involved in cellular defence mechanisms. These evolved protective or adaptive networks assist microorganisms to modify their environments and/or to survive the stress condition. A common regulatory mechanism involves sigma factors. Sigma factors are small proteins that bind to RNA polymerase (RNAP). The presence of the sigma factor allows the RNAP enzyme to bind at specific promoter sequences on the chromosome, and initiate transcription of particular genes, depending on the sigma factor. This way, genetic expression is controlled at the transcription level. In *E. coli*, the housekeeping σ factor, σ^{70}, is responsible for transcription from many of the gene promoters under normal nonstress conditions (Chung *et al*., 2006; Hengge-Aronis, 2002).

Table 2.2 - Sigma factors of *E. coli* (Adapted from: Chung *et al*., 2006)

Sigma factor	Gene	Function
σ^{70}	*rpoD*	Housekeeping functions
$\sigma^{54}(\sigma^{N})$	*glnF, nrtA, rpoN*	Nitrogen-regulated genes
σ^{32}	*htpT, rpoH*	Heat-shock genes
$\sigma^{24}(\sigma^{E})$	*rpoE*	Heat-shock genes
σ^{28}	*flbB+flaI, rpoF*	Flagella synthesis/chemotaxis
$\sigma^{38}(\sigma^{S})$	*rpoS, katF*	Starvation/general stress response

Under stress conditions, alternative σ factors to σ70 with different promoter specificities are induced, resulting in the expression of specialized regulons, in response to a variety of stresses. In this manner, gene expression is modified by different sigma factors. In *E. coli* and other enteric bacteria, σS (*RpoS*) is the master regulator of the general stress response. The sigma factors of *E. coli* are listed in Table 2.2 (Hengge-Aronis, 2002).

Five well known stressing chemicals, at different concentrations, were used to the bioassay optimization: ethanol (EtOH), sodium hypochlorite (commercially known as bleach), sodium chloride (NaCl), hydrochloric acid (HCl) and sodium hydroxide (NaOH). These chemicals are characterized by different cytotoxic mechanisms as briefly outlined below.

Ethanol damages cell wall and membrane integrity, causing increased stress, particularly reactive oxygen species (ROS), which damages DNA and reduces the O_2 level. Decreased cross-membrane proton gradient from membrane damage, coupled with hypoxia, leads to reduced ATP production by aerobic respiration, driving cells to rely more on fatty acid oxidation, anaerobic respiration and fermentation for ATP production. The reduced ATP generation results in substantially decreased synthesis of macromolecules (Cao, *et al*., 2017). Ethanol can directly bind to 213 proteins including transcription factors, altering their function. All these changes together induce multiple stress responses, reduced biosynthesis, cell viability and growth. The main target of ethanol activity appears to be the cell membrane (Canetta, 2006). Ethanol-adapted *E. coli* cells restore the majority of these reduced activities through selection of specific genomic mutations and alteration of stress responses, ultimately restoring normal ATP production, macromolecule biosynthesis, and growth (Cao, *et al*., 2017).

Bleach, mainly constituent by sodium hypochlorite, oxidizes the microorganisms and attacks essential cell components including lipids, proteins and DNA (Ho-Hyuk *et al*., 2008).

The antimicrobial activity of sodium induces loss of the membrane integrity and cell disruption at high concentrations, enzymatic inhibition and problems in the lipids and phospholipids metabolism. The aminoacids undergo a chloramination reaction forming chloramines (Estrela, 2003). Salt causes slow and poor growth and induces glycerol accumulation. The effect to which salt concentration causes changes in bacterial growth depends on the osmotic balance required for such growth. Some bacteria require a high salt concentration to initiate growth, whereas other bacteria would not survive under these conditions. Although *E. coli* may have optimal growth in the absence of salt, it is still growing in its presence but in a slower rate (Corte, 2010).

E. coli is a neutrophile bacterium, which means that the optimum pH of growth is close to pH 7. Stress induced by acids and bases, such as HCl and NaOH, causes changes in intracellular pH, which impairs cell viability (Salmond *et al*., 1984). The antimicrobial activity of organic acids, such as acetic acid, is thought to be due to the ability of the undissociated acid to freely cross the cell membrane and release protons inside the cell. The lowering of pH is opposed in the cell by removal of excess protons at the expense of ATP, which depletes ATP reserves, resulting in death (Hosein, *et al*., 2011). An alternative explanation for the toxicity of organic acids is that acid anions become trapped in the cell cytoplasm and accumulate inside the cell, raising ionic strength and potentially disrupting metabolism. Decreasing intracellular pH results in a low transmembrane pH gradient and may reduce anion levels inside the cell. This may result in reduced metabolic activity, because enzymes in the cytoplasm may not function well below neutral pH (Hosein, *et al*., 2011).

Exposure of gram-negative bacteria to high pH destroys cell membranes and causes leakage of the internal cell content. Cell membranes may be disrupted by saponification of lipids or solubilisation of proteins. Gram negative cells are also susceptible to alkaline pH, in part because the thin peptidoglycan layer loses structural integrity and ruptures (Sharma and Beuchat, 2004).

2.2.2 Application of the bioassay

The bioassay that is intended to be optimized in this work may be applied to different types of studies such as monitoring the effect of various substances on the metabolism of microorganisms, development of new drugs, evaluate the efficiency of treatments. In this case it was chosen to evaluate the mechanism of action of six antibiotics. From 1940, the use of antibiotics was generalized, which revolutionized the treatment of infectious diseases, contributing significantly to the reduction of mortality. However, its excessive and often inappropriate use has promoted the emergence and proliferation of resistant bacteria (INSA, 2010). This fact makes extremely important the development of new techniques that allow the in-depth study of the effect of each antibiotic on the metabolism of bacteria.

The selected antibiotics were: ampicillin, amoxicillin, neomycin, ciprofloxacin, metronidazole and erythromycin. These antibiotics were chosen for having different mechanisms of action. Ampicillin and amoxicillin act by inhibiting cell wall synthesis. On the other hand, neomycin and erythromycin inhibits protein synthesis. Finally, ciprofloxacin and metronidazole act by interfering with DNA synthesis.

Ampicillin is a semi-synthetic derivative of penicillin that functions as an orally active broad-spectrum antibiotic. Is a penicillin beta-lactam antibiotic. Ampicillin has *in vitro* activity against gram-positive and gram-negative aerobic and anaerobic bacteria (Williamson, *et al*., 1980).

Amoxicillin is a broad spectrum semisynthetic antibiotic similar to ampicillin, except that its resistance to gastric acid allows higher serum levels with oral administration. It is a moderate-spectrum antibiotic active against a wide range of gram-positive, and a limited range of gram-negative organisms. The incidence of β-lactamase-producing resistant organisms, including *E. coli*, appears to be increasing. Amoxicillin is sometimes combined with clavulanic acid, a β-lactamase inhibitor, to increase the spectrum of action against gram-negative organisms, and to overcome bacterial antibiotic resistance mediated through β-lactamase production (Okamoto, *et al*., 2002)

The mechanism of action of ampicillin and amoxicillin consists in binding to specific penicillin binding proteins (PBPs) located within the bacterial cell wall. It inhibits the third and last stage of bacterial cell wall synthesis. Cell lysis is then mediated by bacterial cell wall autolytic enzymes such as autolysins. These two antibiotics are indicated for the treatment of ear, nose and throat, genitourinary tract and skin infections, and lower respiratory tract structure due to susceptible (b-lactamase-negative) strains of *Streptococcus spp.* (only a and b-hemolytic strains), *S. pneumoniae*, Staphylococcus spp., *H. influenzae*, *E. coli*, *P. mirabilis* or *E. faecalis* (Okamoto, *et al*., 2002).

Neomycin is an aminoglycoside antibiotic. Aminoglycosides work by binding to the bacterial 30S ribosomal subunit, causing misreading of t-RNA, leaving the bacterium unable to synthesize proteins vital to its growth. Aminoglycosides are useful primarily in infections involving aerobic,

gram-negative bacteria, such as Pseudomonas, Acinetobacter, and Enterobacter. In addition, some mycobacteria, including the bacteria that cause tuberculosis, are susceptible to aminoglycosides. Infections caused by gram-positive bacteria can also be treated with aminoglycosides, but other types of antibiotics are more potent and less damaging to the host. In the past the aminoglycosides have been used in conjunction with penicillin-related antibiotics in streptococcal infections for their synergistic effects, particularly in endocarditis. Aminoglycosides are mostly ineffective against anaerobic bacteria, fungi and viruses (Gill and Amyes, 2004).

Erythromycin is a macrolide antibiotic produced by *Saccharopolyspora erythraea*. It inhibits bacterial protein synthesis by binding to the bacterial 50S ribosomal subunits. Binding inhibits peptidyl transferase activity and interferes with translocation of amino acids during translation and assembly of proteins. Erythromycin may be bacteriostatic or bactericidal depending on the organism and drug concentration. Is indicated for treatment of infections caused by susceptible strains of microorganisms in the following diseases: respiratory tract infections (upper and lower), in the treatment of infections due to *Corynebacterium minutissimum*, intestinal amebiasis caused by *Entamoeba histolytica*, skin and soft tissue infections caused by *Streptococcus pyogenes* and *Staphylococcus aureus*, primary syphilis caused by *Treponema pallidum*, infections caused by *Chlamydia trachomatis*, nongonococcal urethritis caused by *Ureaplasma urealyticum*, and Legionnaires disease caused by *Legionella pneumophila* (Douthwaite and Aagaard, 1993).

Ciprofloxacin is a broad-spectrum anti-infective agent of the fluoroquinolone class and it has *in vitro* activity against a wide range of gram-negative and gram-positive microorganisms. There is no known cross-resistance between ciprofloxacin and other classes of antimicrobials. The bactericidal action of ciprofloxacin results from the inhibition of enzymes topoisomerase II (DNA gyrase) and topoisomerase IV, which are required for bacterial DNA replication, transcription, repair, strand supercoiling repair, and recombination (Leavis, *et al*., 2006). Ciprofloxacin is indicated for the treatment of the following infections caused by susceptible organisms: urinary tract infections, acute uncomplicated cystitis, chronic bacterial prostatitis, lower respiratory tract infections, acute sinusitis, skin and skin structure infections, bone and joint infections, complicated intra-abdominal infections, infectious diarrhea, typhoid fever, uncomplicated cervical and urethral gonorrhoea (Leavis, *et al*., 2006).

Metronidazole, a synthetic antibacterial and antiprotozoal agent of the nitroimidazole class, is used against protozoa such as *Trichomonas vaginalis*, amebiasis, and giardiasis. It is extremely effective against anaerobic bacterial infections and is also used to treat Crohn's disease, antibiotic-associated diarrhea, and rosacea. Metronidazole is a prodrug. Unionized metronidazole is selective for anaerobic bacteria due to their ability to intracellularly reduce metronidazole to its active form. The reduced metronidazole covalently binds to DNA, disrupt its helical structure, inhibiting bacterial nucleic acid synthesis and resulting in bacterial cell death (Li, *et al*., 2007).

3. Materials and methods

3.1 Culture growth conditions and Bioassay

The bacteria *Escherichia coli* strain JM 101 (ATCC 33876) was chosen as a model organism for its ease of manipulation, non-pathogenic nature (biosafety class 1) as well as lack of resistance mechanisms in its genome: supE thi- 1 Δ(lac-proAB) [F´ traD36 proAB lacIqZΔM15].

The bioassay consisted of a reaction mixture of 1000 µL with 100 µL of *E.coli*, with an OD600nm of 50, 400 µL of nutrient medium 2.5x and 500 µL of water and/or stress agent. The nutrient medium used in the bioassay was prepared by the following mode: 3.75 mL of the stock solution (10% of Yeast extract + 20% Bacto tryptone + 5x phosphate buffer 0.2 M) and the volume was complete with buffer to a final volume of 15 mL. The bioassay with a nutrient medium concentration consisted, therefore, in a final concentration of *E. coli* with an OD600nm of 5, YE of 1%, BT of 2% and phosphate buffer of 0.02 M. The bioassay incubation mixture was incubated for 1 hr at 37^{o}C. In the bioassay, were tested for stress agents, three different concentrations of it: zero concentration (corresponding to control experiment) and two different concentrations as presented in table 3.1. Each assay was conducted in quintuplicate.

The *E. coli* cells used in the bioassay were prepared from the following procedure: 1 mL of *E. coli* cells (-80^{o}C aliquots) were grown for 8, 16 or 24 hrs (corresponding to mid-exponential, early stationary and stationary growth phase, respectively) on a 250 mL erlenmeyer with 60 mL of working volume (containing 6 mL of YE (10%) and BT (20%) plus 12 mL of phosphate buffer of 0.2 M and the volume was complete with water), in an orbital incubator (TH30 and SM30, Edmund Buhler GmbH) (at 37^{o}C, 250 rpm).

After *E. coli* growth, and due to small variabilities in the growth curve, the absorbance of the inoculum biomass was measured and re-suspend till an OD600nm of 50. For that, the culture medium was centrifuged for 15 min at 4000 rpm (Rotanta 460R, Hettich Zentrifugen).

An overall procedure was established to optimize the following bioassay conditions: nutrient media concentration, *E. coli* growth phase and incubation time, as resumed in table 3.2. In summary, in the first assay *E. coli* cells grown till stationary growth phase (*i.e*. 24 hrs) were used, and the bioassay mixture was incubated for 1 hr, and the following medium concentrations were evaluated: 1.25, 2.5 and 5x. On the second study, and to evaluate the effect of the *E. coli* growth phase, it was used an incubation time of 1 hr, and incubation mixture containing 2.5x medium, and *E. coli* cells growth till the mid-exponential, early-stationary and stationary growth phase were used. In the final assay, it was evaluated the effect of incubating the mixture for 1, 8 and 24 hrs, using a medium at 2.5x and *E. coli* cells grown till stationary growth phase.

Table 3.1 - Stock solutions of the stress agents and quantities in the assays

Stress agent	Stock Solution	Concentration in biological assay			Stock Solution Volume (µL)			Water volume (µL)		
		C0	C1	C2	C0	C1	C2	C0	C1	C2
Ethanol	20%	0%	2%	10%	0	100	500	500	400	0
Bleach	263 ppm	0 ppm	10 ppm	80 ppm	0	38	305	500	462	195
NaCl	16% (p/V)	0%	4%	8%	0	250	500	500	250	0
HCl	4 M	0 M	0,2 M	2 M	0	50	500	500	450	0
NaOH	1 M	0 M	0,05 M	0,5 M	0	50	500	500	450	0

Table 3.2 - Summary of assays conditions

Parameter to be optimised	Tested conditions	Fixed conditions
Nutrient medium concentration	Nutrient medium concentration: 1.25x, 2.5x or 5x	Inoculum grown for 24 hrs and bioassay mixture maintained by 1 hr
***E. coli* growth phase**	Inoculum growth phase: 8, 16 or 24 hrs	Nutrient medium concentration 2.5x and bioassay mixture maintained by 1 hr
Incubation time	Incubation time: 1, 8 or 24 hrs	Inoculum grown for 24 hrs and nutrient medium concentration 2.5x

3.2. Preparation of solutions of stress agents

The following concentrations of stress agents were used: 20% ethanol, 263 ppm bleach, 16% (ρ/V) NaCl, 4 M HCl and 1 M NaOH. The preparation of these stock solutions aimed to obtain certain final concentrations or pH of each stress agent in the assays, as summarized in the table 3.1.

For the preparation of 20% ethanol solution, 20 mL of ethanol 96% plus 80 mL of water was used for a final volume of 100 mL. In the case of the 263 ppm bleach preparation, a 525 ppm solution (100 µL bleach plus 10 mL water) was first prepared and then 5 mL of the above solution was withdrawn where 5 mL of water was added to obtain the concentration of bleach 263 ppm. The 16% NaCl solution was prepared by joining 16 g of NaCl with water to a final volume of 100 mL.

The 4 M HCl and1 M NaOH solutions were prepared using the following equation:

$$M = \frac{m}{(MM \times V)}, \text{ (equation 3.1)}$$

where M represents molarity, m is the mass, V is the volume and MM is the molar mass.

In the case of HCl, in addition to applying the equation (which resulted in 14.585 g of HCl to 100 mL of solution), its density (1.19 g/cm³) must be taken into account. However, has the HCl solution is at 36% (v/v), a total of 34.04 mL was taken in account to prepare a final solution of 100 mL.

Applying equation 3.1, 3.99 g of NaOH was used in a final volume of 100 mL. The pH of the HCl and NaOH mixture assays was measured. The mixture with the highest concentration (C2) of HCl had pH 2 and the lowest concentration (C1) pH 3.39. In the case of NaOH, the mixture with the highest concentration (C2) was pH 10.66 and the lowest concentration (C1) 8.47.

3.3 Preparation of antibiotic solutions

For the application of the bioassay, eight concentrations of each antibiotic were tested. The only difference in this assay is that the final volume of the reaction mixture was halved, that resulted in the used of 200 µL of nutrient medium, 250 µL of the antibiotic and/or water and 50 µL of inoculum. The antibiotic concentrations chosen are in accordance with those tested in previous studies for the bacterium *E. coli*. To obtain the eight final concentrations required, two solutions of each antibiotic were prepared, one more concentrated (250 mg/L) and one less concentrated (1 mg/L).

To prepare the solution 250 mg/L, 0.00125g of antibiotic was weighed into a 5 mL flask and the volume was filled with 0.2 M buffer. The 1 mg/L solution was prepared by adding 10 µL of the 250 mg/L solution to 2.5 mL of buffer. All solutions were sterilized by filtration. Reaction mixtures (antibiotic plus buffer) were prepared according to tables 3.3 and 3.4.

Table 3.3 - Reaction mixtures of the solution 250 mg/L

Concentrations	C7	C6	C5	C4
Volume of the solution 250 mg/L (µL)	250	125	50	10
0.2 M Buffer Volume (µL)	0	125	200	240
Final concentration of antibiotic (mg/L)	125	62.5	25	5

Table 3.4 - Reaction mixtures of the solution 1 mg/L

Concentrations	C3	C2	C1	C0
Volume of the solution 1 mg/L (µL)	100	20	5	0
0.2 M Buffer Volume (µL)	150	230	245	250
Final concentration of antibiotic (mg/L)	0.2	0.04	0.01	0

3.4 FTIR spectra acquisition, preprocessing and analysis

At the end of all bioassays with *E. coli*, the 1 mL of incubation mixture was centrifuged for 3 min at 4000 rpm, then the supernatant was discarded and the remaining pellet was re-suspended in 200 μL of water to obtain an OD600nm of 5.

On a FTIR 96 wells plate, 20 μL of washed cells was placed in each well and 5 replicates were performed. At the end, the ZnSe plates were dehydrated in a vacuum desiccator with silica gel inside, for approximately two hrs. FTIR measurements were performed in transmission mode resourcing to a HTS-XT module coupled to a Vertex-70 spectrometer (Bruker Optics®, Germany). All spectra were recorded in the range between 4000 and 400 cm^{-1}. Spectral resolution was set at 4 cm^{-1}, sampling 64 scans per sample.

Using the spectrometer software OPUS® and OPUS LAB® spectra were exported to Data point table (DPT) files and handled in Matlab R2012b (Matworks, Natick, MA, USA). Spectra preprocessing combinations evaluated included offset correction, to reduce baseline and slope distortions, Multiplicative scatter correction (MSC), to counteract scattering phenomena with additive and multiplicative effects, and normalization at the Amide I band (1690-1620 cm^{-1}) to compensate intensity variations by forcing spectra maximum to 1, highlighting patterns in the data. Additionally, the Savitzky-Golay method was chosen to determine the first and second derivative of spectra, using a 15-point window and a 2nd degree.

4. Results and Discussion

4.1 Bioassay optimization

The effect on the molecular fingerprint of *E. coli* exposed to the following five types of stress agents was evaluated: ethanol, sodium hypochlorite, sodium chloride, hydrochloric acid and sodium hydroxide. These agents were chosen due to its low price and since its exposure results in highly different *E. coli* metabolic responses. The objective was to determine if the following parameters of the bioassay affect the capacity of the bioassay to discriminate the effect of different stress agents and the stress agent's concentration: nutrient media concentration, *E. coli* growth phase and incubation time. To do this, the spectra obtained from *E. coli* pellets obtained along bioassays were first preprocessed, with baseline correction, normalization, MSC and using the second derivative (figure 4.1).

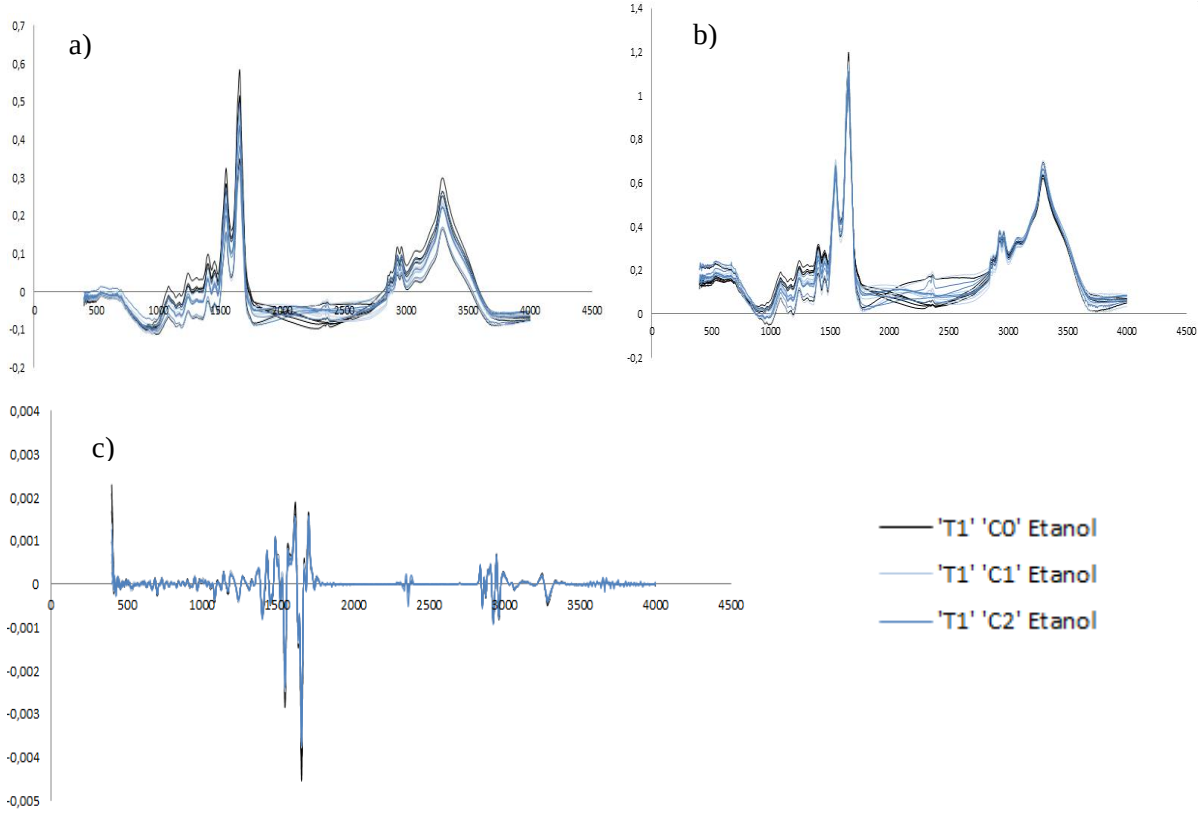

Figure 4.1 - FTIR spectra obtained from quintuplicates of assays of *E. coli* cells incubated for 1 hr (T1) with ethanol concentrations of 0 (C0), 2 (C1) and 10% (C2) (v/v) a) without preprocessing, b) preprocessed by baseline correction, normalization and MSC, c) preprocessing by second derivative

The PCA of spectra was also evaluated to better explore and visualize the high-dimensionality spectral data. The bioassay condition that results in a score plot with replicas of the concentration of stress agent grouped together and apart from other concentrations should be selected.

The different components of a FTIR spectrum can also be associated by univariate analysis to individual components, *e.g*., to determine spectral biomarkers, as done, *e.g*., for identifying the mechanism of cell death and stem cells differentiation (Jamin, *et al*., 2003), and even biochemical and metabolic information, as conducted during diseases research and diagnosis (Bogomolny, *et al*., 2007; Ahmed, *et al*., 2010). In the present study, the spectral ratios instead of a single peak were considered to minimise the effect of different biomass concentrations. The wavelengths to study were chosen according to the analysis of the second derivative peaks of the spectra while considering its biomolecular significance. The following spectral ratios were evaluated: 2960/2920, 2960/2850, 1655/1550, 1080/1240, 1450/1470, 1550/1240, 1650/1240, 1170/1550, 1170/1650, 1655/1690 and 1655/1630. The differences in the bands' ratios between groups of experiments were considered statistically significant in a student's t test when a p-value lower than 0.05 is achieved.

4.1.1 Effect of nutrient media concentration

The nutrient mediums at concentrations of 1.25x, 2x, and 5x on the incubation mixture were evaluate.

In the case of the first agent tested (ethanol), it was observed in the PCA score plots (figure 4.2) that the lowest nutrient concentration (*i.e*. 1.25x) resulted in best separation of the control samples (*i.e*. with zero concentration of ethanol) from the samples with ethanol.

The spectral ratios that presented more statistically significant p-values when comparing the assay without ethanol and samples with ethanol were: A2960/2920 and A2960/2850 (table 4.1). These wavelengths represent asymmetric C-H stretching movements of –CH3 and of –CH2 in fatty acids, respectively, reflecting this way the cytoplasmic membrane status. Interestingly, when using a nutrient concentration of 5x the spectral ratio A2960/2850 enable to discriminate the effect of all ethanol concentrations. It was also observed significant statistically p-values with the spectral ratio A1170/1550. The wavelength 1550 cm^{-1} represents the Amide II band that is due to C-N stretching vibrations in combination with N-H bending and the wavelength 1170 cm^{-1} represents the C-O and C-C distension movements and C-O-C deformation of carbohydrates.

a)

b)

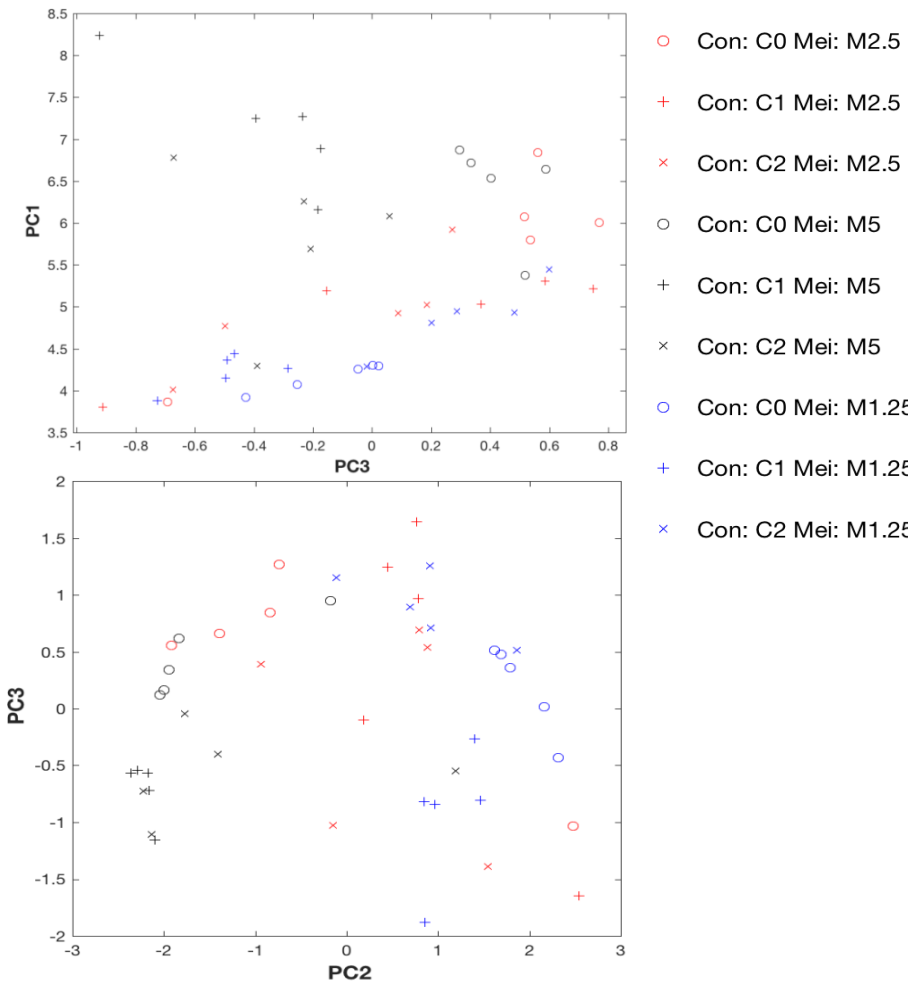

Figure 4.2 - PCA score plot of FTIR spectra of *E.coli* submitted to different ethanol concentrations (C0 = 0; C1 = 2; C2 = 10% (V/V)) and incubated with different nutrient media concentration (M 1.25x, 2.5x and 5x). a) without preprocessing b) preprocessed by base line correction and normalization Amide I. PC1, PC2 and PC3 represents 95%, 4% and 1% of data variance, respectively

Table 4.1 - p-values of the spectral ratios obtained from the quintuplicates of the assay with *E. coli* with different concentrations of ethanol (C0 = 0; C1 = 2; C2 = 10% (V/V)) and incubated with different nutrient media concentration (M 1.25x, 2.5x and 5x). The statistically significant p-values (p<0.05) are highlighted in green

Spectral ratio	**Media concentration**	**C0 *versus* C1**	**C0 *versus* C2**	**C1 *versus* C2**	**C0 *versus* C1 and C2**
A2960/2920	M2.5x	0.089	0.007	0.421	0.002
	M5x	0.011	0.008	0.152	5.81E-04
	M1.25x	0.109	1.31E-05	4.21E-04	0.233
A2960/2850	M2.5x	0.029	5.63E-04	0.081	2.8E-04
	M5x	0.045	0.001	0.029	0.001
	M1.25x	0.158	4.76E-04	4.76E-04	0.324
A1170/1550	M2.5x	0.012	0.855	0.035	0.239
	M5x	0.831	0.021	0.029	0.253
	M1.25x	0.038	0.526	0.016	0.055

In the score plots obtained from the assay with bleach (figure 4.3), the best separation of samples with bleach from the ones without bleach was reached with a medium contained a nutrient concentration of 5x. In the score plots of PC2 vs PC3, it was even observed a higher effect of the nutrient medium concentration than the effect of bleach itself in the *E. coli* metabolism, as independent sample clusters in function of the nutrient medium concentration were observed. This indicates that a higher bleach concentration should be used.

With bleach, the spectral rations with more p-values statistically significant were also: A2960/2920 and A2960/2850 (table 4.2). It was observed that when the nutrient concentration of 2.5x is used it is possible to discriminate the effect of bleach concentration on the *E. coli* lipids. Statistically significant p-values were also found in the spectral ratio A1655/1240. The wavelength 1655 cm^{-1} represents the alpha helical structures of Amide I and the wavelength 1240 cm^{-1} represents the phosphate groups present in molecules such as DNA and RNA. Therefore, this spectral ratio allows to evaluate the effect on the proteins and on the genetic material of the cells.

When comparing the PCA analysis with the analysis of the spectral ratios it is possible to observe that these analyses were not in agreement, being according to the PCA 5x medium the best nutrient medium to detect the action of the bleach on the *E. coli* metabolism but according to the spectral ratios the 2.5x was the best nutrient medium.

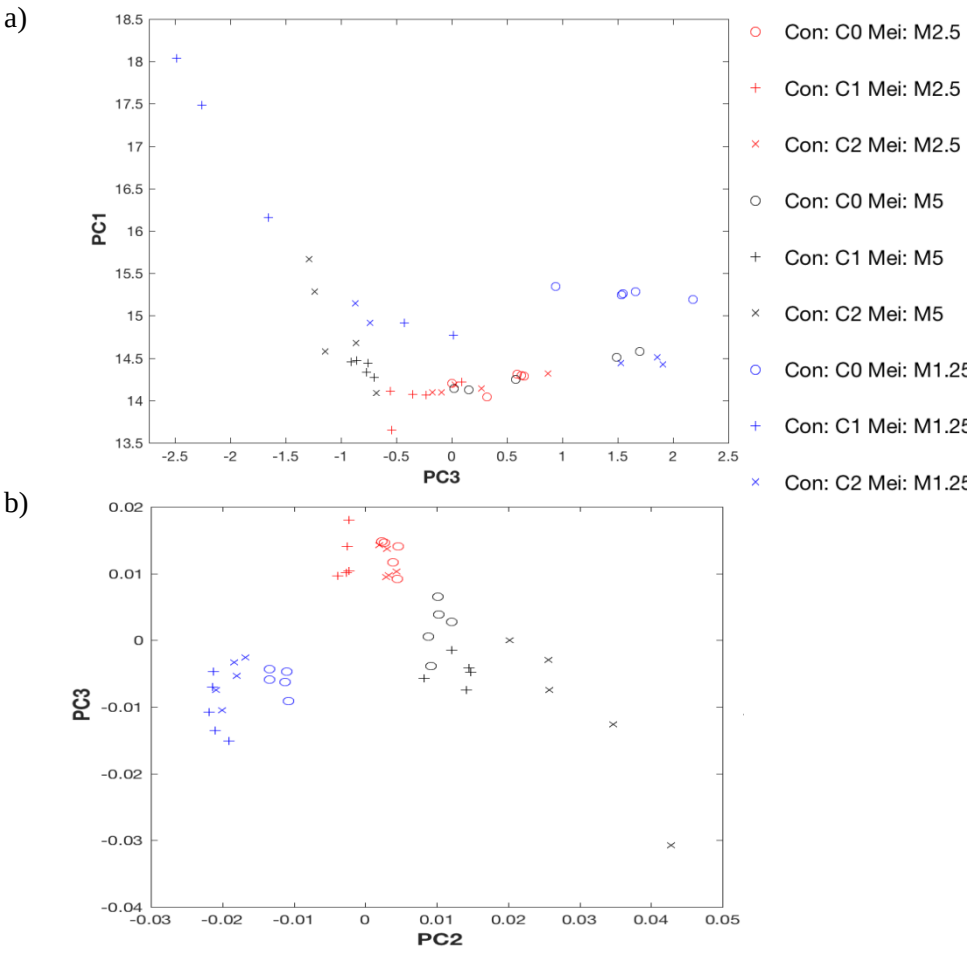

Figure 4.3 - PCA score plot of FTIR spectra of *E. coli* submitted to different bleach concentrations (C0 = 0; C1 = 10; C2 = 80 ppm) and incubated with different nutrient media concentration (M 1.25x, 2.5x and 5x) a) preprocessed by base line correction and Min Max normalization b) preprocessed second derivative. PC1, PC2 and PC3 represent 98%, 1% and 1% of data variance, respectively

Table 4.2 - p-values of the spectral ratios obtained from the quintuplicates of the assay with *E. coli* with different concentrations of bleach (C0 = 0; C1 = 10; C2 = 80 ppm) and incubated with different nutrient media concentration (M 1.25x, 2.5x and 5x). The statistically significant p-values ($p<0.05$) are highlighted in green

Spectral ratio	**Media concentration**	**C0 *versus* C1**	**C0 *versus* C2**	**C1 *versus* C2**	**C0 *versus* C1 and C2**
A2960/2920	M2.5x	0.012	0.011	0.018	0.003
	M5x	0.179	0.247	0.057	0.893
	M1.25x	8.63E-05	0.002	0.275	2.41E-05
A2960/2850	M2.5x	4.95E-04	0.001	0.035	3.58E-07
	M5x	0.145	0.192	0.029	0.815
	M1.25x	0.001	0.005	0.623	1.19E-04
A1655/1240	M2.5x	0.001	0.028	0.027	0.005
	M5x	0.615	0.154	0.029	0.493
	M1.25x	0.460	0.280	0.960	0.413

Unlike the PCA of the two previous agents, in the score plots of the assay with salt (figure 4.4) it was possible to obtain all the controls (without salt) separated from the other sample (with salt), independently of the nutrient concentration used, highlighting the strong effect of sault in the *E. coli* metabolism in relation to the previous conditions evaluated. Interestingly, for a specific nutrient concentration it was possible to discriminate the effect of the three sault concentrations on the cell metabolism. This was observed for the three nutrient concentrations.

The more statistically significant p-values were found in the spectral ratios: A2960/2920, A2960/2850 and A1550/1240 (table 4.3). The analyses of the PCA and the p-values of the spectral ratios allows to conclude that the best medium to distinguish the controls from the samples that have been exposed to the salt is the 1.25x medium, although it is possible to distinguish the effect of sault independently of the content in nutrient concentration evaluated.

a)

b)

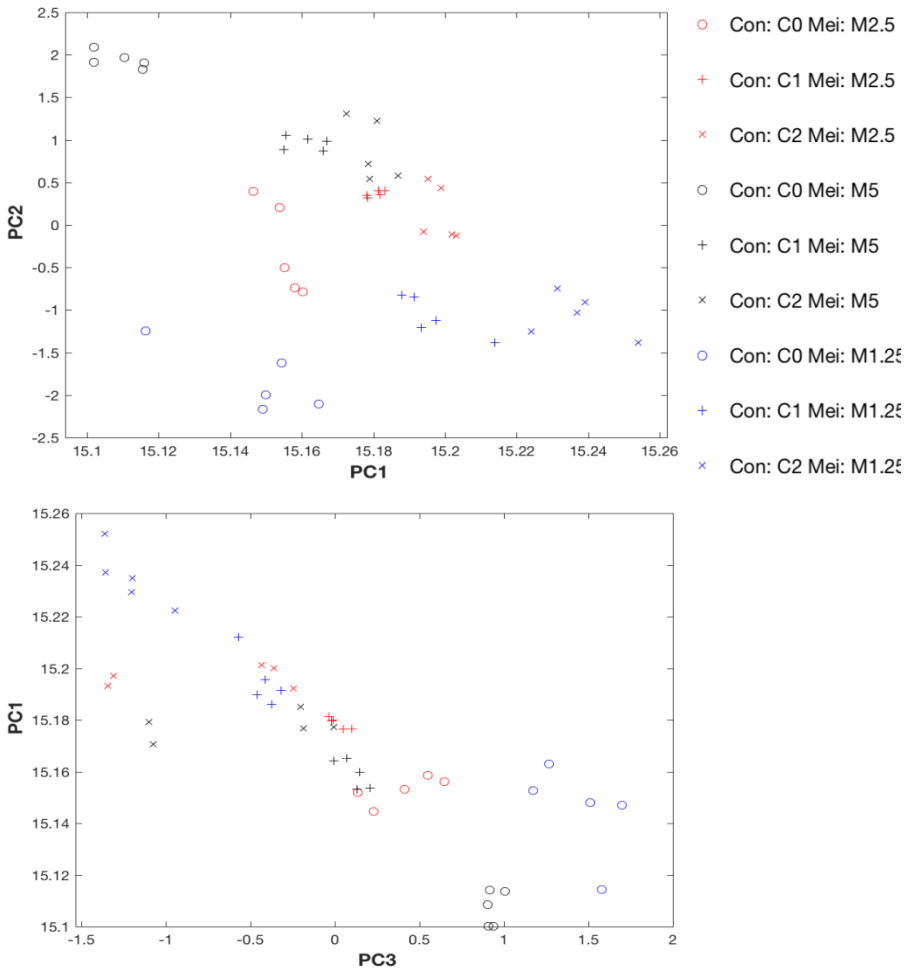

Figure 4.4 – PCA score plot of FTIR spectra of *E. coli* submitted to different sodium chloride concentrations (C0 = 0; C1 = 4; C2 = 8% (W/V)) and incubated with different nutrient media concentration (M 1.25x, 2.5x and 5x) a) preprocessed by base line correction, Min Amide I normalization and MSC b) preprocessed by base line correction, MinMax normalization and MSC. PC1, PC2 and PC3 represent 98%, 1% and 1% of data variance, respectively

Table 4.3 - p-values of the spectral ratios obtained from the quintuplicates of the assay with *E. coli* with different concentrations of sodium chloride (C0 = 0; C1 = 4; C2 = 8% (W/V)) and incubated with different nutrient media concentration (M 1.25x, 2.5x and 5x). The statistically significant p-values ($p<0.05$) are highlighted in green the statistically significant p-values are highlighted in green

Spectral ratio	**Media concentration**	**C0 *versus* C1**	**C0 *versus* C2**	**C1 *versus* C2**	**C0 *versus* C1 and C2**
A2960/2920	M2.5x	0.002	0.005	0.883	2.56E-05
	M5x	0.423	0.042	0.066	0.081
	M1.25	0.05	0.012	0.062	0.006
A2960/2850	M2.5x	0.016	0.006	0.681	5.68E-04
	M5x	0.048	0.013	0.106	0.002
	M1.25	0.079	6.27E-04	0.007	0.006
A1550/1240	M2.5x	0.027	0.092	0.024	0.638
	M5x	5.55E-04	0.008	0.799	2.67E-06
	M1.25	6.51E-04	8.57E-04	0.129	2.99E-06

In the PCA score plots of the assay with hydrochloric acid (figure 4.5) the samples in acidic medium were separated from those incubated in a neutral medium, independently of the nutrient concentration of the medium. It was also observed that the samples exposed to different acidic media were also in separated groups.

The p-values of the spectral ratios that enable to discriminate the HCl effect was according to the results observed in the PCA, being in the medium 1.25x that lead to more statistically significant results. The spectral ratios more statistically significant were: A1080/1240, A1550/1240 and A1655/1240 (table 4.4). The wavelength 1080 cm^{-1} represents phosphates in the cell. Therefore, these spectral ratios allow to observe the effect on cell proteins and at the global level of cell phosphates.

After this analyse, it was concluded that in the assays where the samples were exposed to hydrochloric acid all mediums concentrations tested allowed to distinguish between the controls and samples that were exposed to this agent, but only in the 1.25x medium was it possible to clearly distinguish the acidic pH effect.

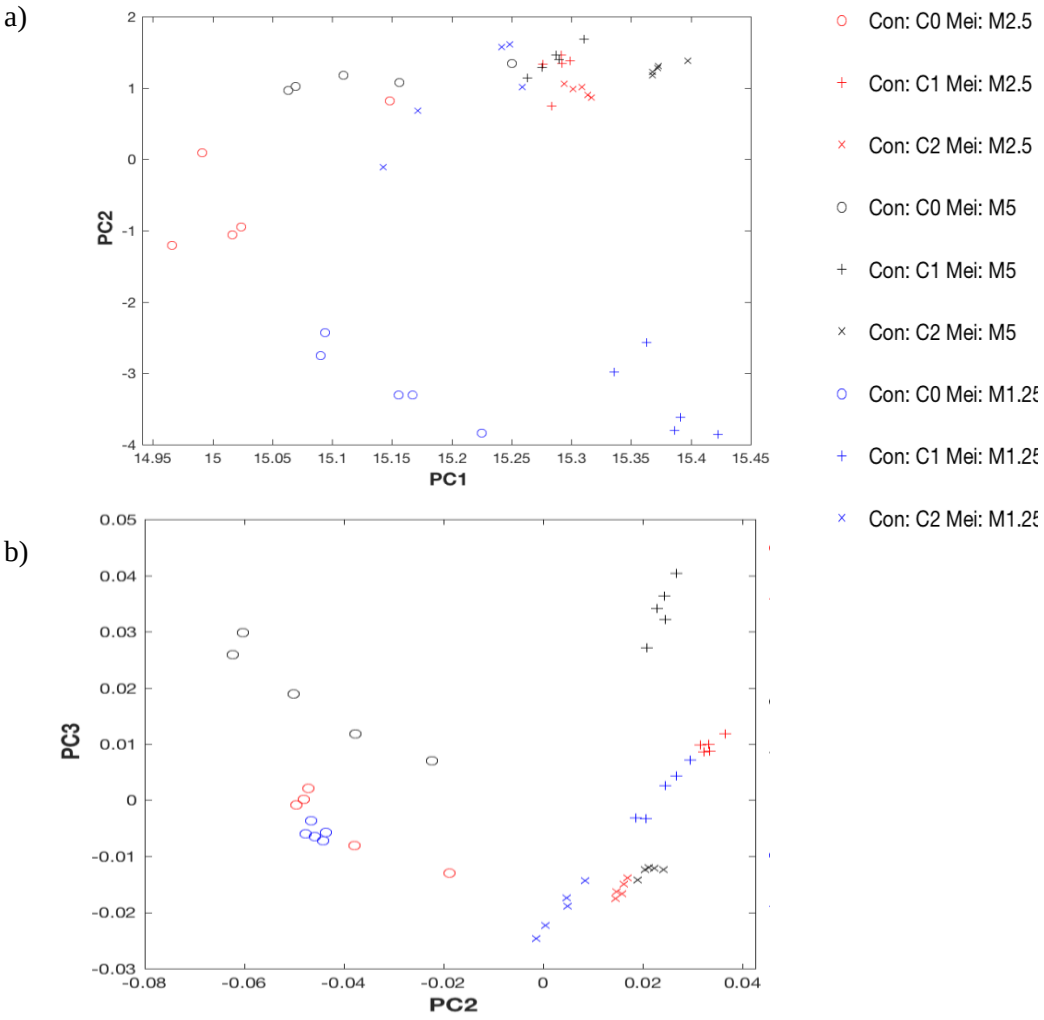

Figure 4.5 - PCA score plot of FTIR spectra of *E. coli* submitted to different hydrochloric acid concentrations (C0 = 0; C1 = 250; C2 = 500 µL) and incubated with different nutrient media concentration (M 1.25x, 2.5x and 5x) a) preprocessed by base line correction, Min Amide I normalization and MSC b) preprocessed by second derivative. PC1, PC2 and PC3 represent 95%, 4% and 1% of data variance, respectively

Table 4.4 - p-values of the spectral ratios obtained from the quintuplicates of the assay with *E. coli* with different concentrations of hydrochloric acid (C0 = 0; C1 = 250; C2 = 500 µL) and incubated with different nutrient media concentration (M 1.25x, 2.5x and 5x). The statistically significant p-values ($p<0.05$) are highlighted in green

Spectral ratio	**Media concentration**	**C0 *versus* C1**	**C0 *versus* C2**	**C1 *versus* C2**	**C0 *versus* C1 and C2**
A1080/1240	M2.5x	0.011	0.032	0.598	0.004
	M5x	0.128	0.052	0.089	0.012
	M1.25	0.019	0.013	0.166	2.10E-04
A1550/1240	M2.5x	0.016	0.011	0.654	4.47E-04
	M5x	0.248	8.96E-04	3.92E-04	0.022
	M1.25	0.001	0.002	0.080	4.46E-04
A1655/1240	M2.5x	0.027	0.011	0.259	0.001
	M5x	0.068	0.003	6.19E-04	0.403
	M1.25	0.003	0.002	0.027	0.001

The PCA score plots resulting from the assay with sodium hydroxide (figure 4.6), show that when the 5x nutrient mediums culture were used in the reaction mixture, the samples exposed to 250 µL of NaOH were in the same group that the samples that were not exposed to this agent. With the 1.25x and 2.5x nutrient mediums was possible to observe the controls separated from da samples exposed to any tested concentration of this agent.

The more statistically significant p-values were observed in the spectral ratios: A2960/2850, A1655/1240 and A1550/1240 (table 4.5). The p-values were in general more statistically significant when we used the 2.5x culture medium. After this analyse it was concluded that the 2.5x culture medium should be used to detect the action of NaOH on *E. coli* metabolism.

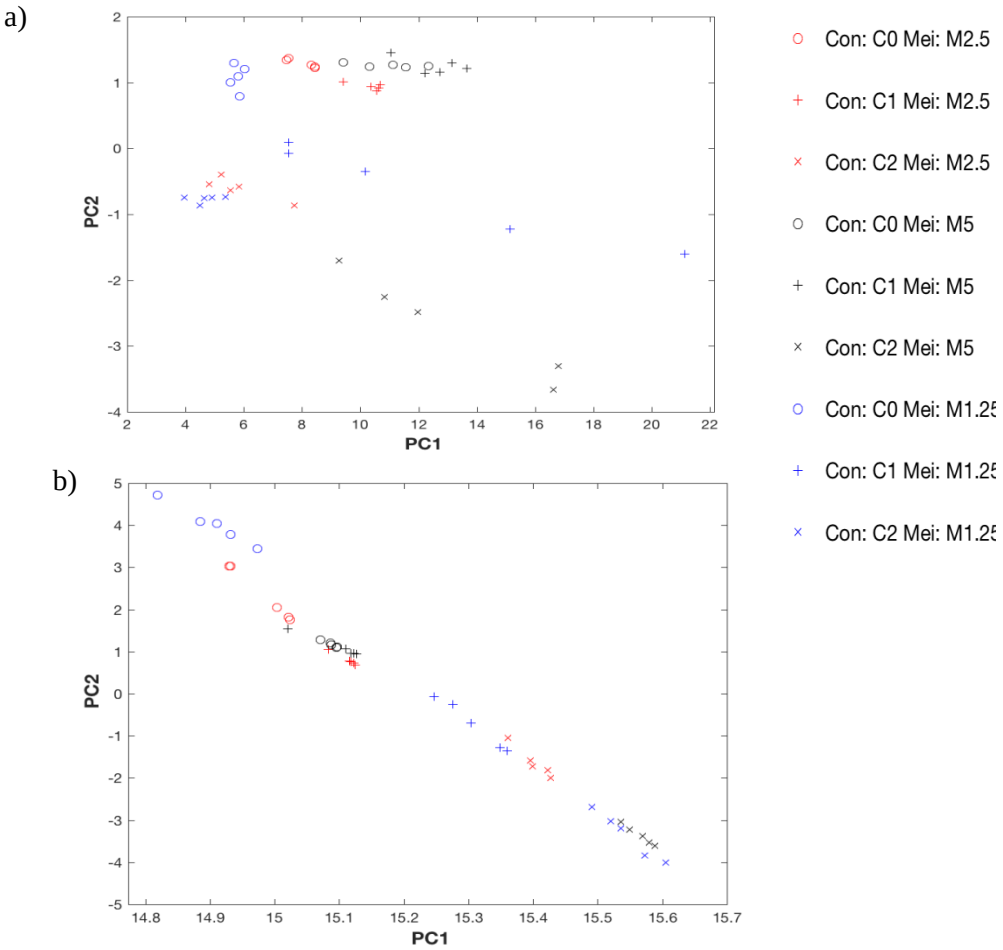

Figure 4.6 - PCA score plot of FTIR spectra of *E. coli* submitted to different sodium hydroxide concentrations (C0 = 0; C1 = 250; C2 = 500 µL) and incubated with different nutrient media concentration (M 1.25x, 2.5x and 5x) a) preprocessed by base line correction b) preprocessed by MinMax normalization and MSC. PC1, PC2 and PC3 represent 95%, 4% and 1% of data variance, respectively

Table 4.5 - p-values of the spectral ratios obtained from the quintuplicates of the assay with *E. coli* with different concentrations of sodium hydroxide (C0 = 0; C1 = 250; C2 = 500 µL) and incubated with different nutrient media concentration (M 1.25x, 2.5x and 5x). The statistically significant p-values (p<0.05) are highlighted in green

Spectral ratio	**Media concentration**	**C0 *versus* C1**	**C0 *versus* C2**	**C1 *versus* C2**	**C0 *versus* C1 and C2**
A2960/2850	M2.5x	4.90E-04	0.021	0.004	0.538
	M5x	0.029	4.18E-05	3.53E-06	0.158
	M1.25	0.223	0.002	0.011	0.600
A1550/1240	M2.5x	0.003	0.012	0.002	0.561
	M5x	0.451	1.84E-04	0.015	0.042
	M1.25	6.94E-04	0.003	0.164	7.09E-06
A1655/1240	M2.5x	0.002	0.277	0.037	0.918
	M5x	0.686	0.012	0.021	0.206
	M1.25	0.018	0.226	0.003	0.028

After the analyses per agent, were evaluated the PCA with the stress agents all together (figure 4.7). It is worth to mention that figure 4.7 represents the optimum preprocessing and the combination of PC1, PC2 and PC3 that resulted in the best separation among experiments that can be different from the PCA score plots presented before. In the analysis of all agents together, the control experiments, with zero concentration of stress agent, and conducted with the same nutrient medium concentration, should give similar FTIR spectra. In the present analysis, it was observed that as the nutrient medium concentration decreases, it becomes easier to discriminate the action of the stress agents separate the action of each stress agent. A higher nutrient concentration resulted in an apparent protection of *E. coli* from stress conditions. For example, at the highest nutrient concentration (*i.e.* of 5x) it was not possible to discriminate the effect of bleach or alcohol from the controls. It was also observed that from the conditions evaluated, the ones that most affected the *E. coli* metabolism were when using acidic or basic conditions and high salt concentrations.

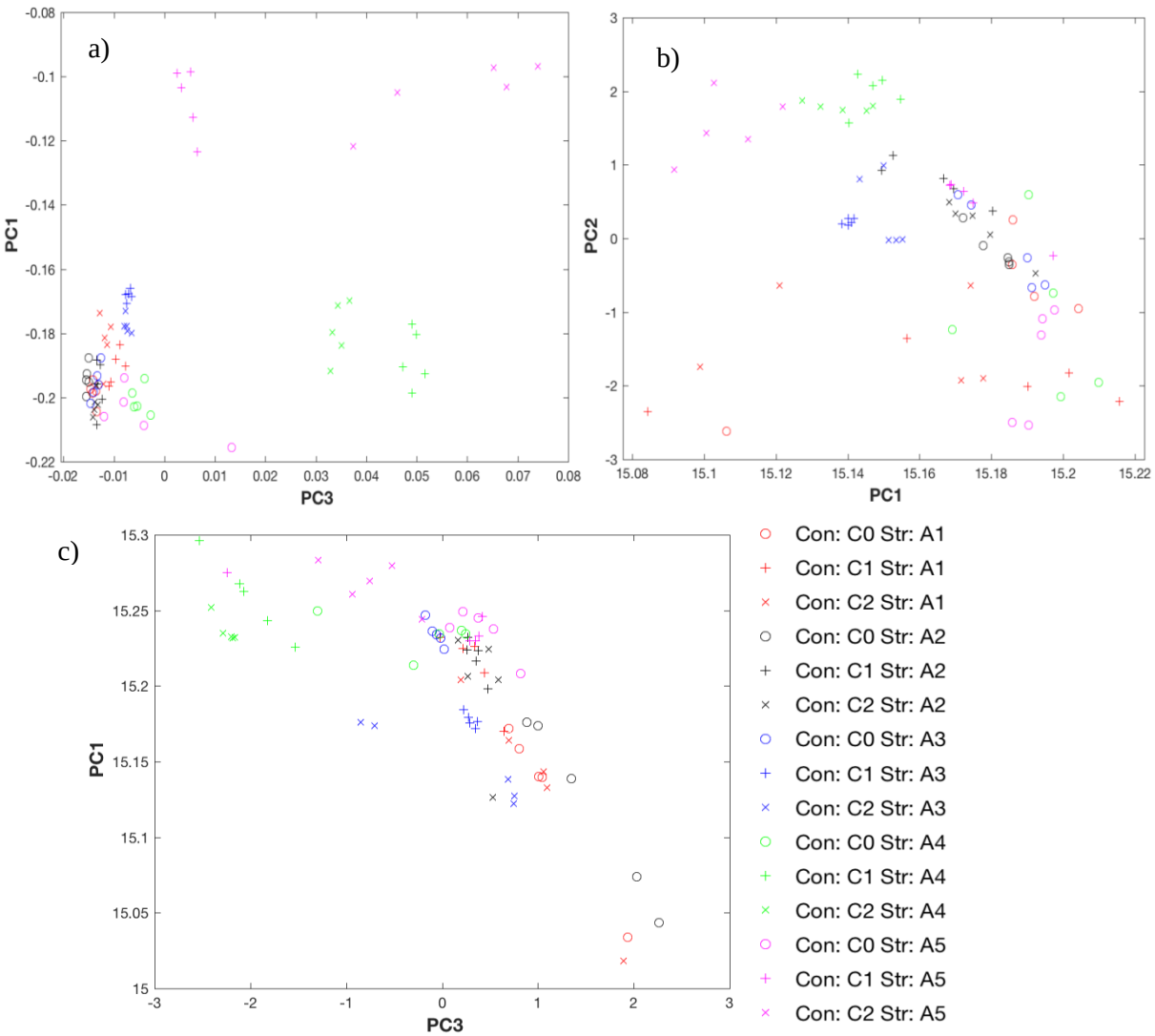

Figure 4.7 - PCA score plot of FTIR spectra of *E. coli* submitted to different concentrations (C) of the stress agents ethanol (A1), bleach (A2), sodium chloride (A3), hydrochloric acid (A4) and sodium hydroxide (A5) and different nutrient media concentration (M 1.25x, 2.5x and 5x) a) medium 1.25x, with spectra preprocessed by second derivative, b) medium 2.5x, with spectra preprocessed by base line correction, MinMax normalization and MSC c) medium 5x, with spectra preprocessed by Min Amide I normalization and MSC. PC1, PC2 and PC3 represent 96%, 3% and 1% of data variance, respectively

4.1.2 Effect of *E. coli* growth phase

The metabolic status of *E. coli* cells along the growth phases may also influence the sensitivity of the bioassay to stress agents. To evaluate this effect and optimize it, *E. coli* growth till mid-exponential, early stationary and stationary growth phases were used. Cells were exposed to stress agents for one hour and the 2.5x culture medium was used.

In the PCA score plot of the assay with ethanol (figure 4.8), was observed that when cells in stationary growth phase were used it was possible to discriminate the effect of ethanol. It was noted that as the growth time of the used *E. coli* cells increases, it becomes easier to distinguish the action of ethanol on the *E. coli* metabolism. It was also by using *E. coli* cells grown for 24 hrs that more statistically significant spectral ratios were obtained (table 4.6). The spectral ratios with more statistically significant p-values were: A2960/2920, A2960/2850 and A1550/1240.

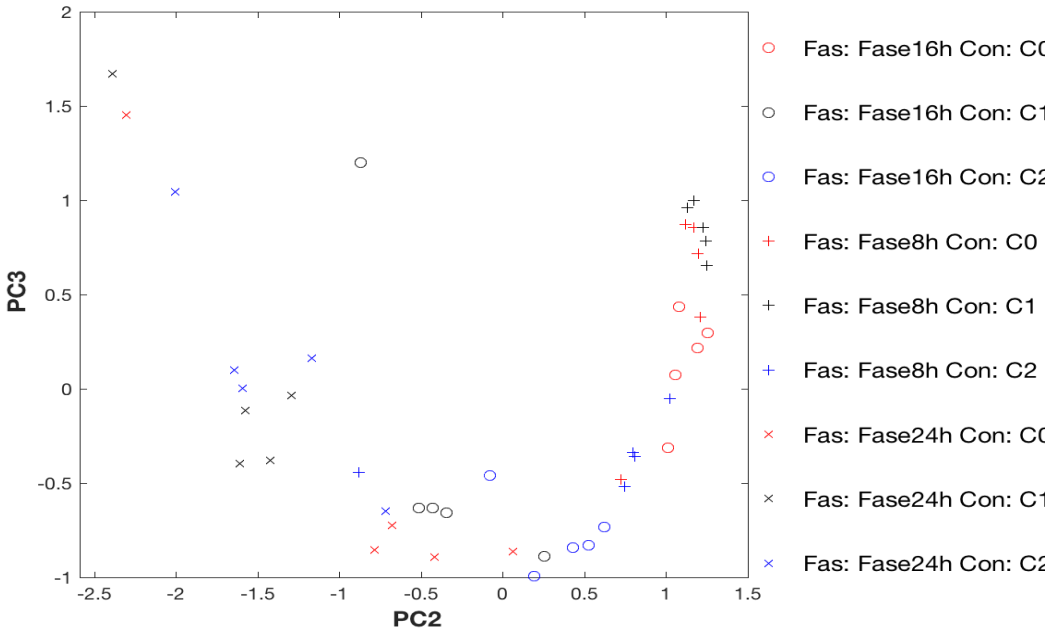

Figure 4.8 - PCA score plot of FTIR spectra of *E. coli* submitted to different ethanol concentrations (C0 = 0; C1 = 2; C2 = 10% (V/V)) and in different growth phase (8, 16 and 24 hrs), preprocessed by base line correction and Min Amide I normalization. PC1, PC2 and PC3 represent 98%, 1% and 1% of data variance, respectively

Table 4.6 - p-values of the spectral ratios obtained from the quintuplicates of the assay with *E. coli* with different ethanol concentrations (C0 = 0; C1 = 2; C2 = 10% (V/V)) and in different growth phase (8, 16 and 24 hrs). The statistically significant p-values (p<0.05) are highlighted in green

Spectral ratio	Growth phase	C0 *versus* C1	C0 *versus* C2	C1 *versus* C2	C0 *versus* C1 and C2
A2960/2920	16 hrs	0.073	0.002	7.86E-04	0.024
	8 hrs	0.182	0.344	0.017	0.769
	24 hrs	9.49E-04	7.52E-04	0.173	2.56E-06
A2960/2850	16 hrs	0.027	9.21E-04	0.004	0.012
	8 hrs	0.376	0.461	0.025	0.925
	24 hrs	5.84E-04	1.76E-04	0.045	1.63E-05
A1550/1240	16 hrs	0.005	0.005	0.509	5.61E-07
	8 hrs	1.46E-04	0.472	0.005	0.035
	24 hrs	0.002	0.035	0.011	2.26E-04

The analysis of the PCA score plots of the *E. coli* cells in several stages of growth exposed to the bleach does not allow to draw conclusions about which is the best growth phase to distinguish the action of this stress agent because all the samples were packed together (figure 4.9). The analysis of the spectral ratios points that a stationary growth phase leads to a best discrimination of bleach effect. The spectral ratios more significant statistically were: A2960/2920, A2960/2850 and A1550/1240 (table 4.7).

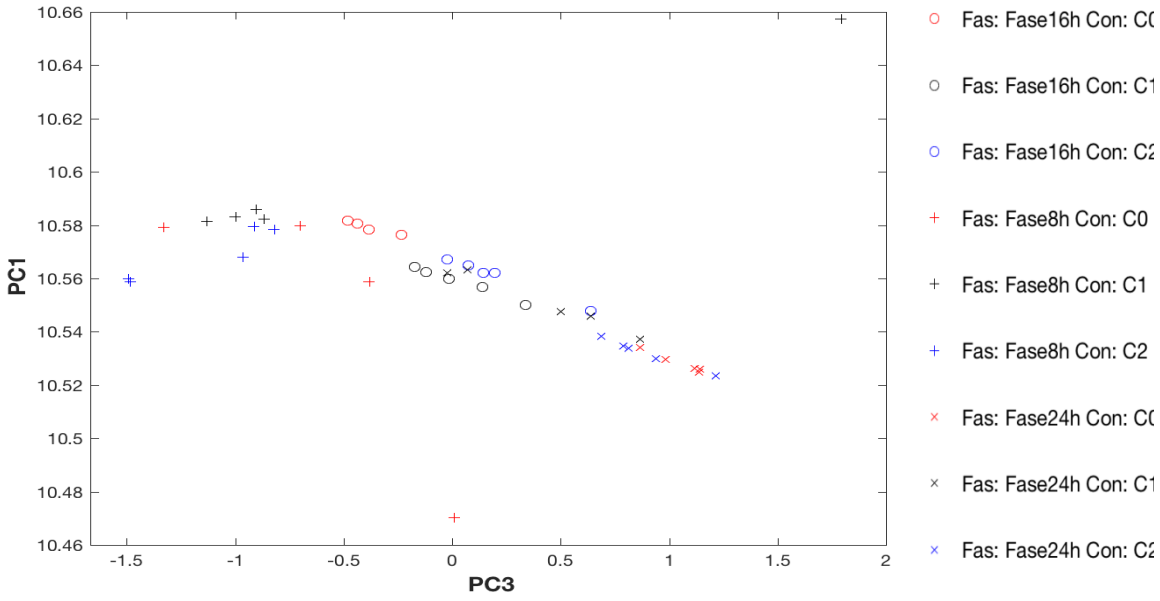

Figure 4.9 - PCA score plot of FTIR spectra of *E. coli* submitted to different bleach concentrations (C0 = 0; C1 = 10; C2 = 80 ppm) and in different growth phase (8, 16 and 24 hrs), preprocessed by base line correction, MinMax normalization and MSC. PC1, PC2 and PC3 represent 98%, 1% and 1% of data variance, respectively

Table 4.7 - p-values of the spectral ratios obtained from the quintuplicates of the assay with *E. coli* with different bleach concentrations (C0 = 0; C1 = 10; C2 = 80 ppm) and in different growth phase (8, 16 and 24 hrs). The statistically significant p-values ($p<0.05$) are highlighted in green

Spectral ratio	Growth phase	C0 *versus* C1	C0 *versus* C2	C1 *versus* C2	C0 *versus* C1 and C2
A2960/2920	16 hrs	0.007	0.002	0.890	1.31E-04
	8 hrs	0.475	0.073	0.058	0.661
	24 hrs	1.58E-04	0.033	0.036	8.29E-04
A2960/2850	16 hrs	0.032	0.004	0.727	0.001
	8 hrs	0.309	0.062	0.015	0.696
	24 hrs	1.24E-06	0.011	0.022	3.25E-05
A1550/1240	16 hrs	0.006	0.038	0.058	0.005
	8 hrs	0.135	0.659	0.204	0.534
	24 hrs	0.001	0.019	0.019	1.61E-04

In the PCA score plot of the assay with salt (figure 4.10) it was always possible to discriminate the effect of all sault concentrations on the *E. coli* metabolism, independently of the growth phase of *E. coli*. Analysing the p-values of the spectral ratios for the three growth phases tested (table 4.8), it was concluded that there were more statistically significant spectral ratios if *E. coli* grown for 16 hrs. The spectral ratios with more statistically significant were: A2960/2920, A2960/2850 and A1080/1240.

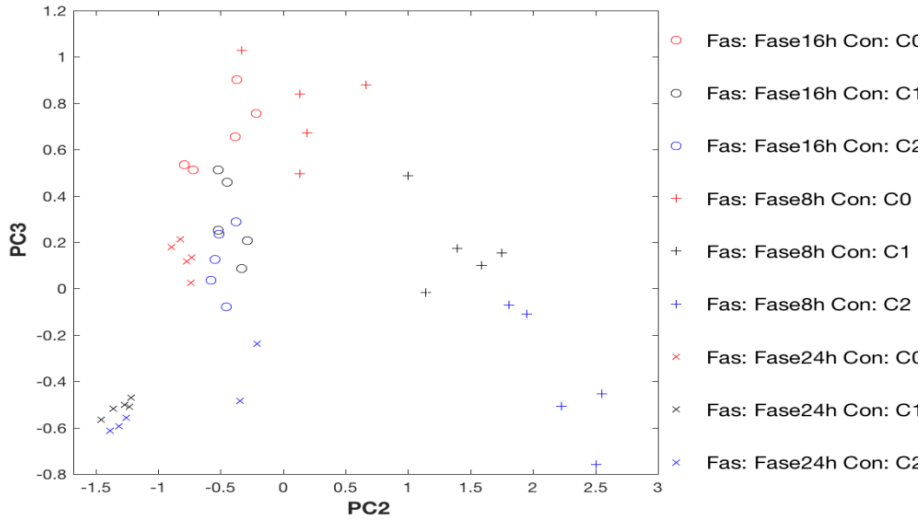

Figure 4.10 - PCA score plot of FTIR spectra of *E. coli* submitted to different sodium chloride concentrations (C0 = 0; C1 = 4; C2 = 8% (W/V)) and in different growth phase (8, 16 and 24 hrs), pre-processed by base line correction. PC1, PC2 and PC3 represent 95%, 4% and 1% of data variance, respectively

Table 4.8 - p-values of the spectral ratios obtained from the quintuplicates of the assay with *E. coli* with different sodium chloride concentrations (C0 = 0; C1 = 4; C2 = 8% (W/V)) and in different growth phase (8, 16 and 24 hrs). The statistically significant p-values ($p<0.05$) are highlighted in green

Spectral ratio	Growth phase	C0 *versus* C1	C0 *versus* C2	C1 *versus* C2	C0 *versus* C1 and C2
A2960/2920	16 hrs	5.89E-04	0.008	0.036	1.23E-05
	8 hrs	0.868	0.104	0.045	0.266
	24 hrs	8.50E-05	0.010	0.372	3.85E-06
A2960/2850	16 hrs	0.002	0.014	0.001	4.72E-05
	8 hrs	0.041	0.789	0.114	0.475
	24 hrs	4.93E-05	0.013	0.448	2.44E-05
A1080/1240	16 hrs	0.031	4.19E-04	0.148	8.59E-05
	8 hrs	0.444	0.047	0.004	0.050
	24 hrs	3.87E-05	0.012	0.068	0.003

In the case of exposure to hydrochloric acid it was easier to observe in the PCA score plots (figure 4.11) the effect of the pH medium with cells in early stationary or stationary growth phase. These results are in according to the spectral ratios: A2960/2920, A1655/1550 and A1080/1240 (table 4.9).

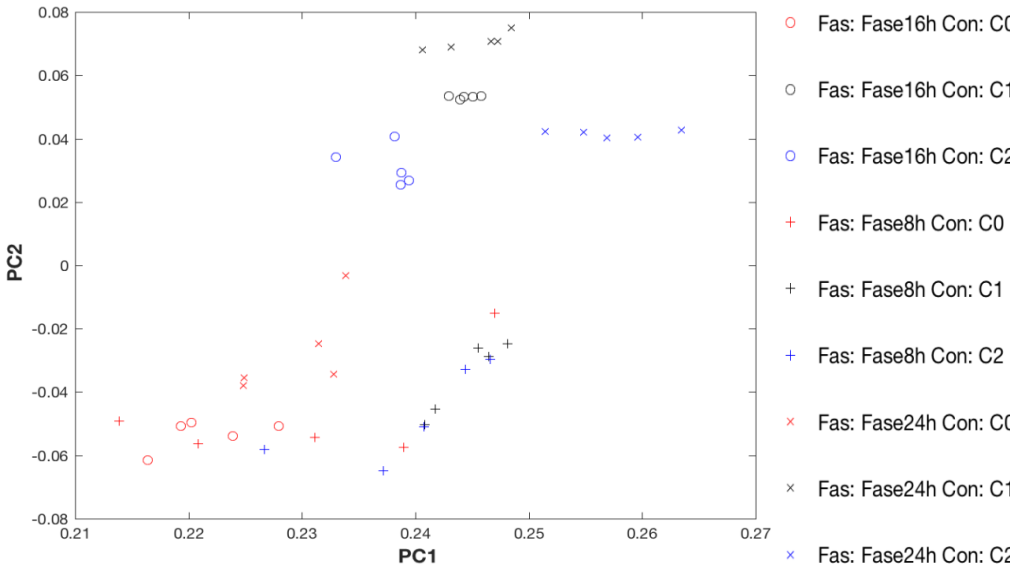

Figure 4.11 - PCA score plot of FTIR spectra of *E. coli* submitted to different hydrochloric acid concentrations (C0 = 0; C1 = 250; C2 = 500 µL) and in different growth phase (8, 16 and 24 hrs), a) preprocessed by second derivative. PC1, PC2 and PC3 represent 94%, 5% and 1% of data variance, respectively

Table 4.9 - p-values of the spectral ratios obtained from the quintuplicates of the assay with *E. coli* with different hydrochloric acid concentrations (C0 = 0; C1 = 250; C2 = 500 µL) and in different growth phase (8, 16 and 24 hrs). The statistically significant p-values (p<0.05) are highlighted in green

Spectral ratio	Growth phase	C0 *versus* C1	C0 *versus* C2	C1 *versus* C2	C0 *versus* C1 and C2
A2960/2920	16 hrs	0.001	0.031	0.046	1.03E-04
	8 hrs	0.166	0.001	0.002	0.307
	24 hrs	0.032	7.05E-04	0.096	9.55E-04
A1655/1550	16 hrs	1.26E-04	0.004	4.66E-05	0.001
	8 hrs	0.236	0.224	0.443	0.095
	24 hrs	0.003	0.008	0.005	0.002
A1080/1240	16 hrs	2.31E-05	2.68E-05	0.792	1.19E-12
	8 hrs	0.128	0.138	0.172	0.023
	24 hrs	4.90E-06	9.46E-06	0.349	2.08E-14

Finally, it was observed in PCA score plot that it is possible to discriminate the effect of basic conditions from more neutral environments, independently of the *E. coli* growth phase (figure 4.12). According to his, it was possible to define spectral ratio that statistically discriminates the effect of the basic pH on the *E. coli* metabolism and independently of the *E. coli* growth phase (table 4.10). The spectral ratios with more significant were: A2960/2850, A1080/1240 and A1170/1655.

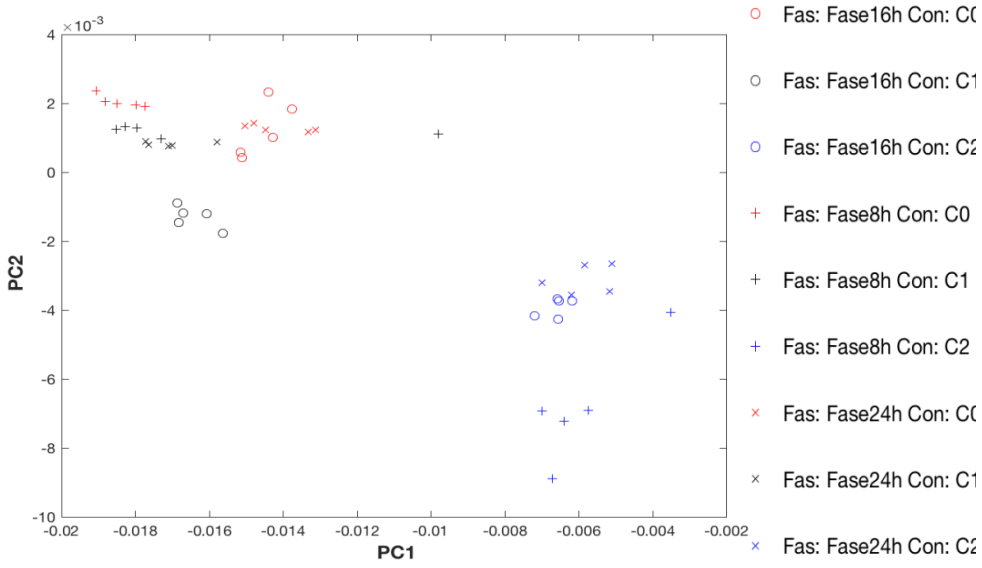

Figure 4.12 - PCA score plot of FTIR spectra of *E. coli* submitted to different sodium hydroxide concentrations (C0 = 0; C1 = 250; C2 = 500 µL) and in different growth phase (8, 16 and 24 hrs), preprocessed by second derivative. PC1, PC2 and PC3 represent 91%, 6% and 3% of data variance, respectively

Table 4.10 - p-values of the spectral ratios obtained from the quintuplicates of the assay with *E. coli* with different sodium hydroxide concentrations (C0 = 0; C1 = 250; C2 = 500 µL) and in different growth phase (8, 16 and 24 hrs). The statistically significant p-values ($p<0.05$) are highlighted in green

Spectral ratio	**Growth phase**	**C0 *versus* C1**	**C0 *versus* C2**	**C1 *versus* C2**	**C0 *versus* C1 and C2**
A2960/2850	16 hrs	3.21E-04	0.014	7.29E-04	0.679
	8 hrs	0.001	0.292	0.020	0.739
	24 hrs	4.41E-04	0.007	9.33E-04	0.621
A1080/1240	16 hrs	0.545	0.002	1.49E-05	0.041
	8 hrs	1.06E-04	3.43E-04	7.15E-04	0.023
	24 hrs	0.039	1.91E-05	1.78E-05	0.033
A1170/1655	16 hrs	0.006	2.23E-05	3.85E-04	3.79E-04
	8 hrs	0.071	0.004	0.003	0.043
	24 hrs	2.76E-04	6.25E-04	0.004	0.005

The PCA of all stress agents was conducted. It was observed that with cells that only grow for eight hrs, it was only possible to distinguish the action of high concentrations of sodium chloride and basic pH. Using *E. coli* grow of sixteen hrs it was already possible to distinguish also the action of acidic pH but, with *E. coli* grown for twenty four hrs it was possible to distinguish the action of four of the five stress agents tested (figure 4.13). As in the previous assay (nutrient concentration) in this assay it was also not possible to discriminate the action on the cell metabolism of bleach, probably due to the low concentrations used of this stress agent.

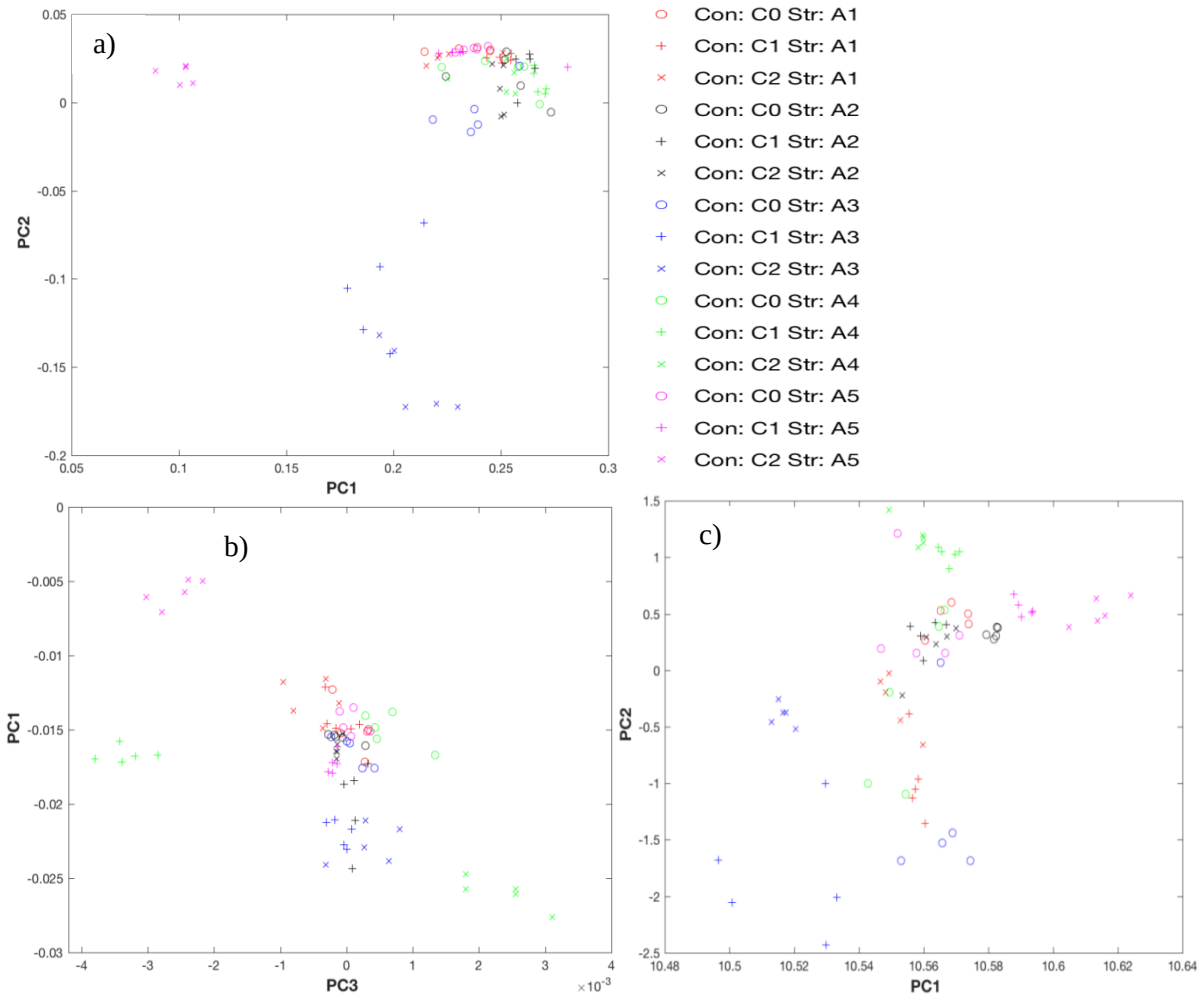

Figure 4.13 - PCA score plot of FTIR spectra of *E. coli* submitted to different concentrations (C) of the stress agents ethanol (A1), bleach (A2), sodium chloride (A3), hydrochloric acid (A4) and sodium hydroxide (A5) and in different growth phase (8, 16 and 24 hrs) a) after eight hrs of growth, pre-processed by second derivative b) after sixteen hrs of growth, preprocessed by base line correction, Min Amide I normalization and MSC c) after twenty-four hrs of growth, preprocessed by second derivative. PC1, PC2 and PC3 represent 98%, 1% and 1% of data variance, respectively

4.1.3 Incubation time

It is expected that the exposure time to the stress agent will affect the *E. coli* metabolism, and therefore the bioassay's sensitivity and reproducibility. To test this, *E. coli* was exposed to stress agents for one, eight and twenty-four hrs. An exposition time of 1 hr, would theoretically result in a more rapid assay, relevant *e.g.* when screening for potential antimicrobial agents, while an increase exposure time would increase the method reproducibility and/or sensitivity as theoretically the environment impact on the cell metabolism will be higher.

In the PCA score plots of the assay with ethanol (figure 4.14), it was possible to discriminate the effect of ethanol concentration by using any incubation time. This result was in agreement with the diverse spectral ratios that enable to discriminate this stress agent effect along the three incubation periods: A2960/2920, A2960/2850 and A1550/1240. There are spectral ratios that enable to discriminate all the experiments with ethanol using 1 or 24 hrs incubation period.

a)

b)

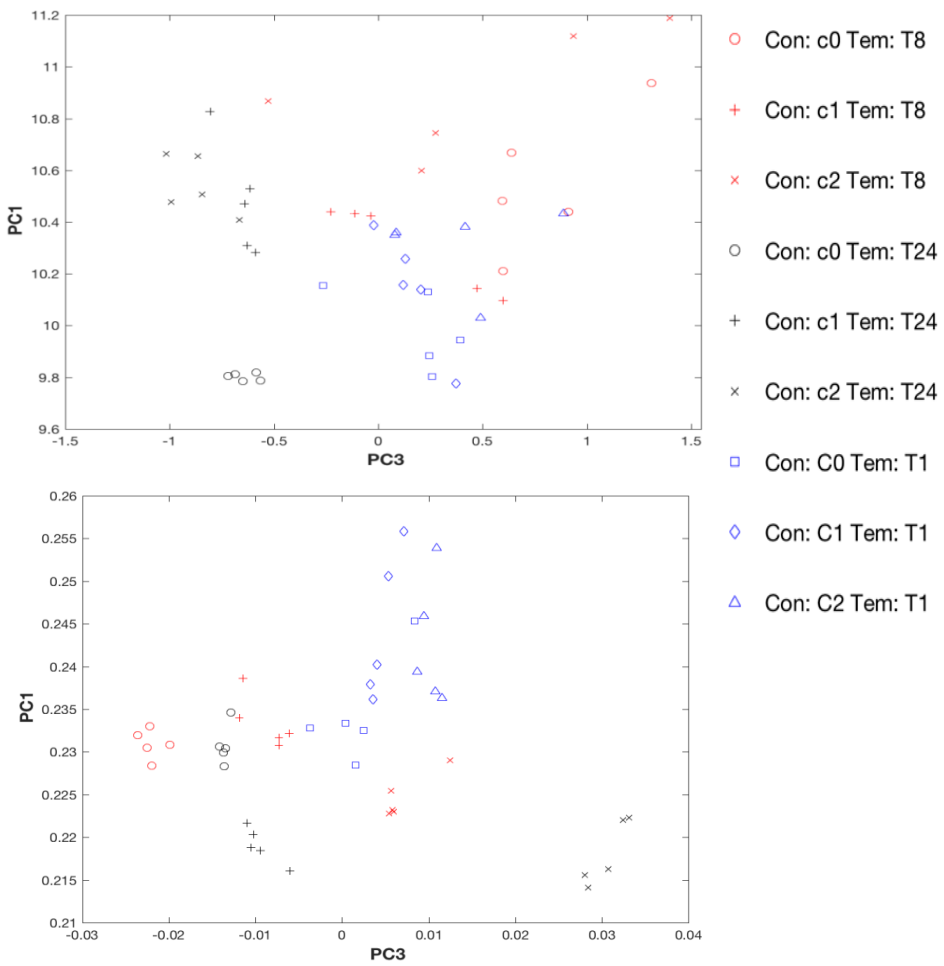

Figure 4.14 - PCA score plot of FTIR spectra of *E. coli* submitted to different ethanol concentrations (C0 = 0; C1 = 2; C2 = 10%) and with different incubation times (1, 8 and 24 hrs) a) preprocessed by base line correction and MinMax normalization b) preprocessed by second derivative. PC1, PC2 and PC3 represent 98%, 1% and 1% of data variance, respectively

Table 4.11 - p-values of the spectral ratios obtained from the quintuplicates of the assay with *E. coli* with different ethanol concentrations (C0 = 0; C1 = 2; C2 = 10%) and with different incubation times (1, 8 and 24 hrs). The statistically significant p-values ($p<0.05$) are highlighted in green

Spectral ratio	**Incubation time**	**C0 *versus* C1**	**C0 *versus* C2**	**C1 *versus* C2**	**C0 *versus* C1 and C2**
A2960/2920	8 hrs	0.061	2.50E-04	0.001	0.033
	24 hrs	0.001	2.58E-05	8.30E-05	1.95E-04
	1 hr	9.49E-04	7.52E-04	0.173	2.538E-06
A2960/2850	8 hrs	0.098	7.47E-04	0.002	0.043
	24 hrs	0.002	0.010	0.059	0.001
	1 hr	5.84E-04	1.76E-04	0.045	1.63E-05
A1550/1240	8 hrs	0.031	8.89E-04	0.014	0.005
	24 hrs	0.007	0.023	1.88E-04	0.662
	1 hr	0.002	0.035	0.011	2.26E-04

In the assay with bleach the PCA score plots (figure 4.15), highlight that it is only possible to discriminate the effect of bleach when using an incubation period equal or higher than 8 hrs. The score plots of cells exposed to the stress agent for 24 hrs were more separated from the controls in relation to an incubation period of 8 hrs. The spectral ratios (table 4.12) more significant to discriminate the effect of this stress agent were: A2960/2920, A2960/2850 and A1655/1240. These entire spectral ratios enable to discriminate all experiments conducted with this stress agent when using an incubation period of 1 hr.

a)

b)

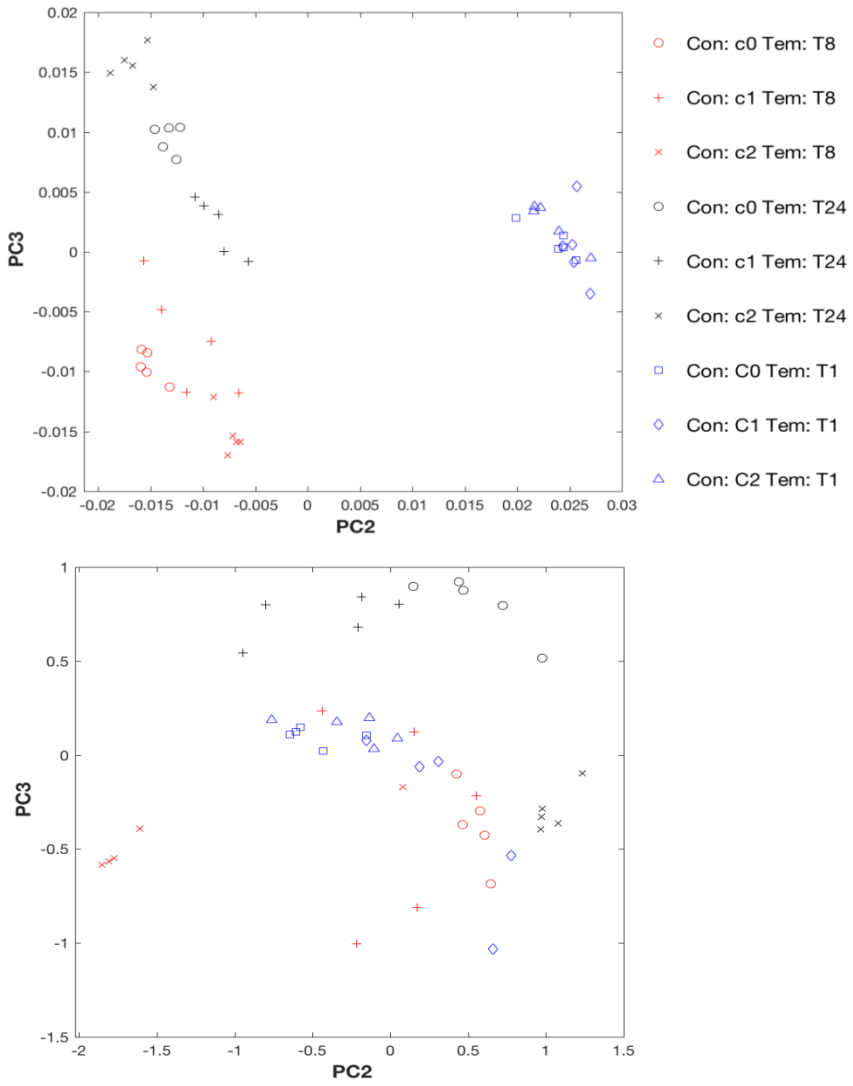

Figure 4.15 - PCA score plot of FTIR spectra of *E. coli* submitted to different bleach concentrations (C0 = 0; C1 = 10; C2 = 80 ppm) and with different incubation times (1, 8 and 24 hrs) a) preprocessed by second derivative b) preprocessed by Min Amide I normalization and MSC. PC1, PC2 and PC3 represent 98%, 1% and 1% of data variance, respectively

Table 4.12 - p-values of the spectral ratios obtained from the quintuplicates of the assay with *E. coli* with different bleach concentrations (C0 = 0; C1 = 10; C2 = 80 ppm) and with different incubation times (1, 8 and 24 hrs). The statistically significant p-values (p<0.05) are highlighted in green the statistically significant p-values are highlighted in green

Spectral ratio	**Incubation time**	**C0 *versus* C1**	**C0 *versus* C2**	**C1 *versus* C2**	**C0 *versus* C1 and C2**
A2960/2920	8 hrs	0.006	3.50E-05	0.584	6.04E-05
	24 hrs	0.025	0.024	0.008	0.765
	1 hr	1.58E-04	0.037	0.036	8.29E-04
A2960/2850	8 hrs	0.004	3.36E-06	0.983	5.14E-06
	24 hrs	0.011	0.019	0.005	0.674
	1 hr	1.24E-06	0.011	0.022	3.25E-05
A1655/1240	8 hrs	0.621	0.031	0.044	0.285
	24 hrs	0.007	0.008	0.419	0.002
	1 hr	0.001	0.019	0.019	1.61E-04

In the PCA score plots of the assay with sodium chloride (4.16 figure) the controls were all separate of the samples that were exposed to this stress agent, independently of the incubation period. The spectral ratios (table 4.13) that enable to discriminate the effect of salt were: A2960/2920, A1550/1240 and A1655/1630.

a)

b)

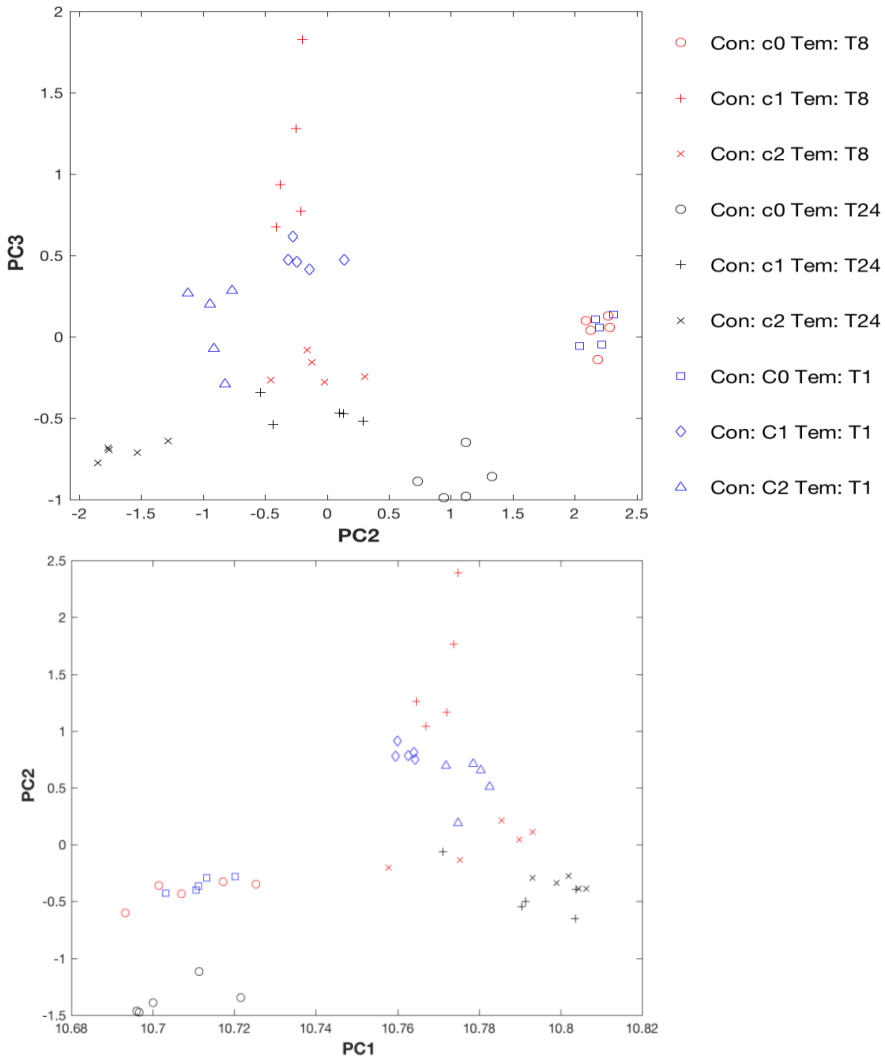

Figure 4.16 - PCA score plot of FTIR spectra of *E. coli* submitted to different sodium chloride concentrations (C0 = 0; C1 = 4; C2 = 8% (W/V)) and with different incubation times (1, 8 and 24 hrs) a) without preprocessing b) preprocessed by MinMax normalization and MSC. PC1, PC2 and PC3 represent 98%, 1% and 1% of data variance, respectively

Table 4.13 - p-values of the spectral ratios obtained from the quintuplicates of the assay with *E. coli* with different sodium chloride concentrations (C0 = 0; C1 = 4; C2 = 8% (W/V)) and with different incubation times (1, 8 and 24 hrs). The statistically significant p-values ($p<0.05$) are highlighted in green

Spectral ratio	**Incubation time**	**C0 *versus* C1**	**C0 *versus* C2**	**C1 *versus* C2**	**C0 *versus* C1 and C2**
A2960/2920	8 hrs	0.003	6.54E-04	8.25E-04	5.81E-05
	24 hrs	0.005	6.77E-06	3.53E-06	0.009
	1 hr	0.032	7.05E-04	0.096	9.55E-04
A1550/1240	8 hrs	0.122	0.002	0.013	0.006
	24 hrs	4.36E-04	8.88E-04	0.013	1.84E-04
	1 hr	0.002	0.002	0.694	2.39E-06
A1655/1630	8 hrs	0.006	0.009	0.005	1.17E-05
	24 hrs	2.29E-06	2.45E-05	0.032	3.72E-13
	1 hr	7.40E-05	8.58E-04	1.88E-05	0.787

In the PCA score plots of the assay with hydrochloric acid (figure 4.17), it was observed that it is possible to detect the effect of acidic environments of the *E. coli* metabolism independently of the incubation period. This result is corroborated by the diverse spectral ratios (table 4.14) that enable to discriminate the effect of this stress agent, as A2960/2920, A1550/1240 and A1655/1630.

a)

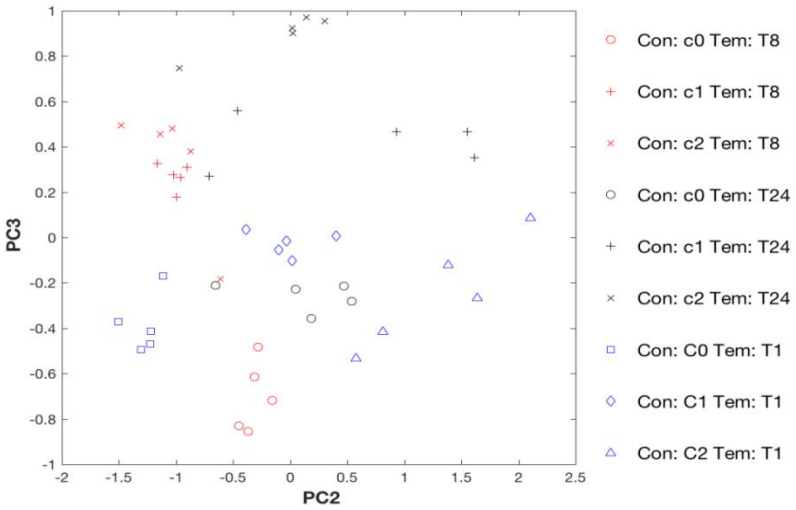

b)

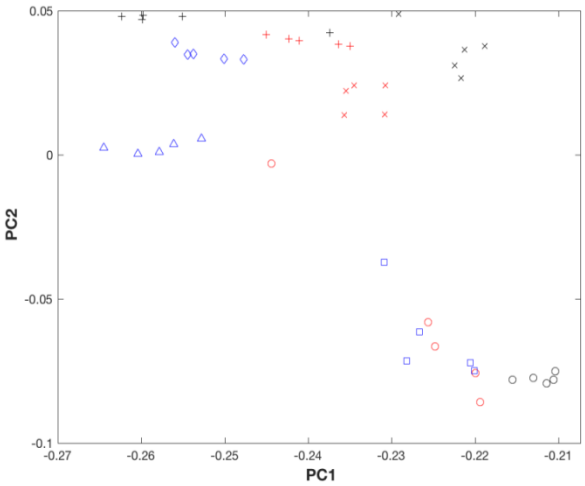

Figure 4.17 - PCA score plot of FTIR spectra of *E. coli* submitted to different hydrochloric acid concentrations (C0 = 0; C1 = 250; C2 = 500 µL) and with different incubation times (1, 8 and 24 hrs) a) without preprocessing b) preprocessed by second derivative. PC1, PC2 and PC3 represent 95%, 4% and 1% of data variance, respectively

Table 4.14 - p-values of the spectral ratios obtained from the quintuplicates of the assay with *E. coli* with different acid hydrochloric concentrations (C0 = 0; C1 = 250; C2 = 500 µL) and with different incubation times (1, 8 and 24 hrs). The statistically significant p-values ($p<0.05$) are highlighted in green

Spectral ratio	**Incubation time**	**C0 *versus* C1**	**C0 *versus* C2**	**C1 *versus* C2**	**C0 *versus* C1 and C2**
A2960/2920	8 hrs	0.003	6.54E-04	8.25E-04	5.81E-05
	24 hrs	0.005	6.77E-06	3.56E-06	0.009
	1 hr	0.032	7.05E-04	0.096	9.55E-04
A1550/1240	8 hrs	0.123	0.002	0.013	0.006
	24 hrs	4.36E-04	8.88E-04	0.013	1.84E-04
	1 hr	0.002	0.002	0.694	2.39E-06
A1655/1630	8 hrs	0.006	0.009	0.005	1.17E-05
	24 hrs	2.00E-06	2.44E-05	0.032	3.72E-13
	1 hr	7.40E-05	8.58E-04	1.88	0.788

In the case of exposure of *E. coli* to basic conditions, it was possible to observe in the PCA score plot (figure 4.18) that it was also possible to discriminate the effect of basic conditions independently of the incubation period. This was according to statistic significant spectral ratios that enable to discriminate this stress agent, especially A2960/2920, A1450/1470 and A1170/1655 (table 4.15).

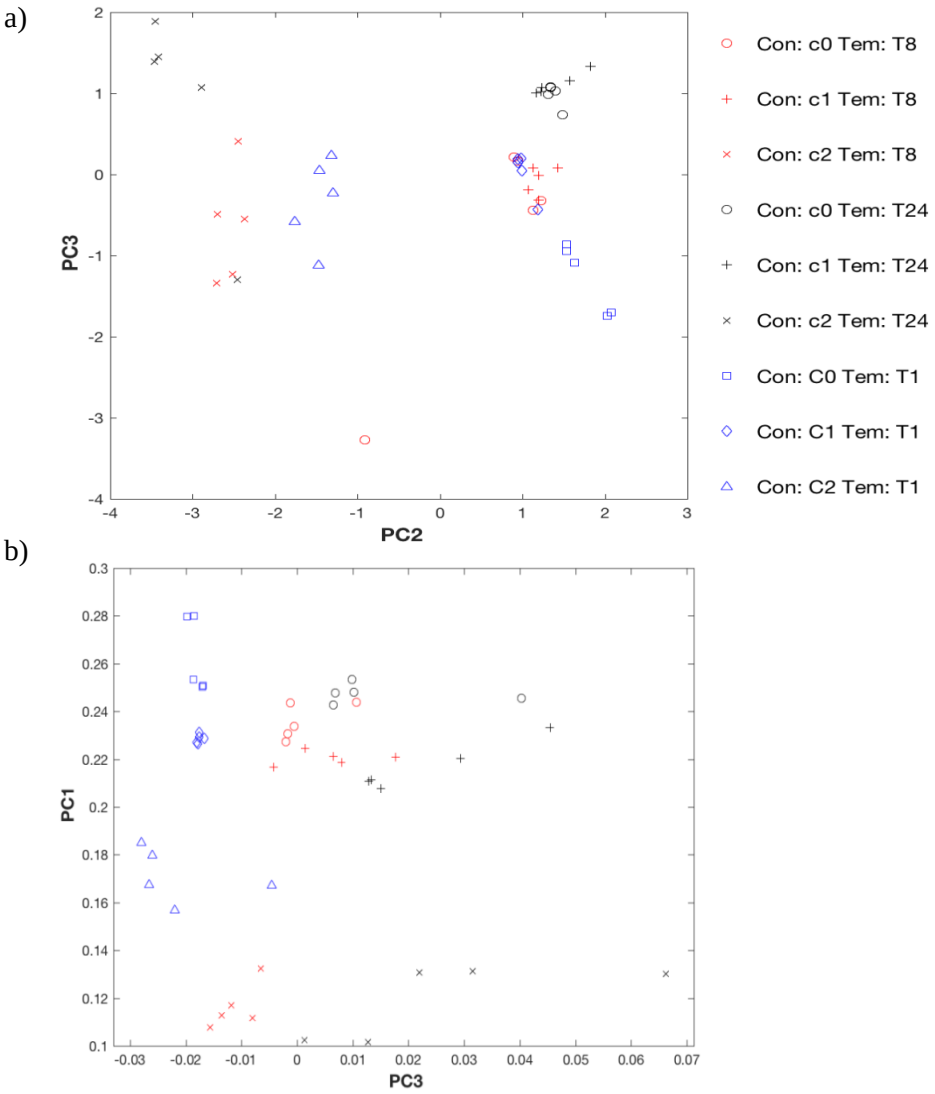

Figure 4.18 - PCA score plot of FTIR spectra of *E. coli* submitted to different sodium hydroxide concentrations (C0 = 0; C1 = 250; C2 = 500 µL) and with different incubation times (1, 8 and 24 hrs) a) preprocessed by base line correction, Min Amide I normalization and MSC b) preprocessed by second derivative. PC1, PC2 and PC3 represent 88%, 8% and 4% of data variance, respectively

Table 4.15 - p-values of the spectral ratios obtained from the quintuplicates of the assay with *E. coli* with different sodium hydroxide concentrations (C0 = 0; C1 = 250; C2 = 500 µL) and with different incubation times (1, 8 and 24 hrs). The statistically significant p-values ($p<0.05$) are highlighted in green

Spectral ratio	**Incubation time**	**C0 *versus* C1**	**C0 *versus* C2**	**C1 *versus* C2**	**C0 *versus* C1 and C2**
A2960/2920	8 hrs	7.77E-04	0.175	0.002	0.205
	24 hrs	2.90E-04	0.025	1.94E-04	0.379
	1 hr	0.001	0.011	0.001	0.547
A1450/1470	8 hrs	0.001	0.003	7.01E-05	0.938
	24 hrs	0.011	4.65E-05	0.001	0.849
	1 hr	0.009	0.003	0.003	0.927
A1170/1655	8 hrs	0.472	2.67E-06	3.34E-05	0.075
	24 hrs	0.071	1.12E-04	0.003	0.016
	1 hr	2.76E-04	6.25E-04	0.004	0.005

In addition to having analysed the effect of each stress agent over the exposure time, PCA of all stress run together for the three different incubation time (figure 4.19), highlighted that the optimum period of incubation to discriminate the effect of stress agents was 24 hrs. Only with 24 hrs of incubation it was possible for example to observe the effect of the ethanol and bleach (at its higher concentrations), were with a lower incubation period was not possible to discriminate the effect of these stress agents in relation to the control experiment. While it was always possible to detect the effect of high concentration of salt, acidic and basic environment on the *E. coli*, independently of the incubation period.

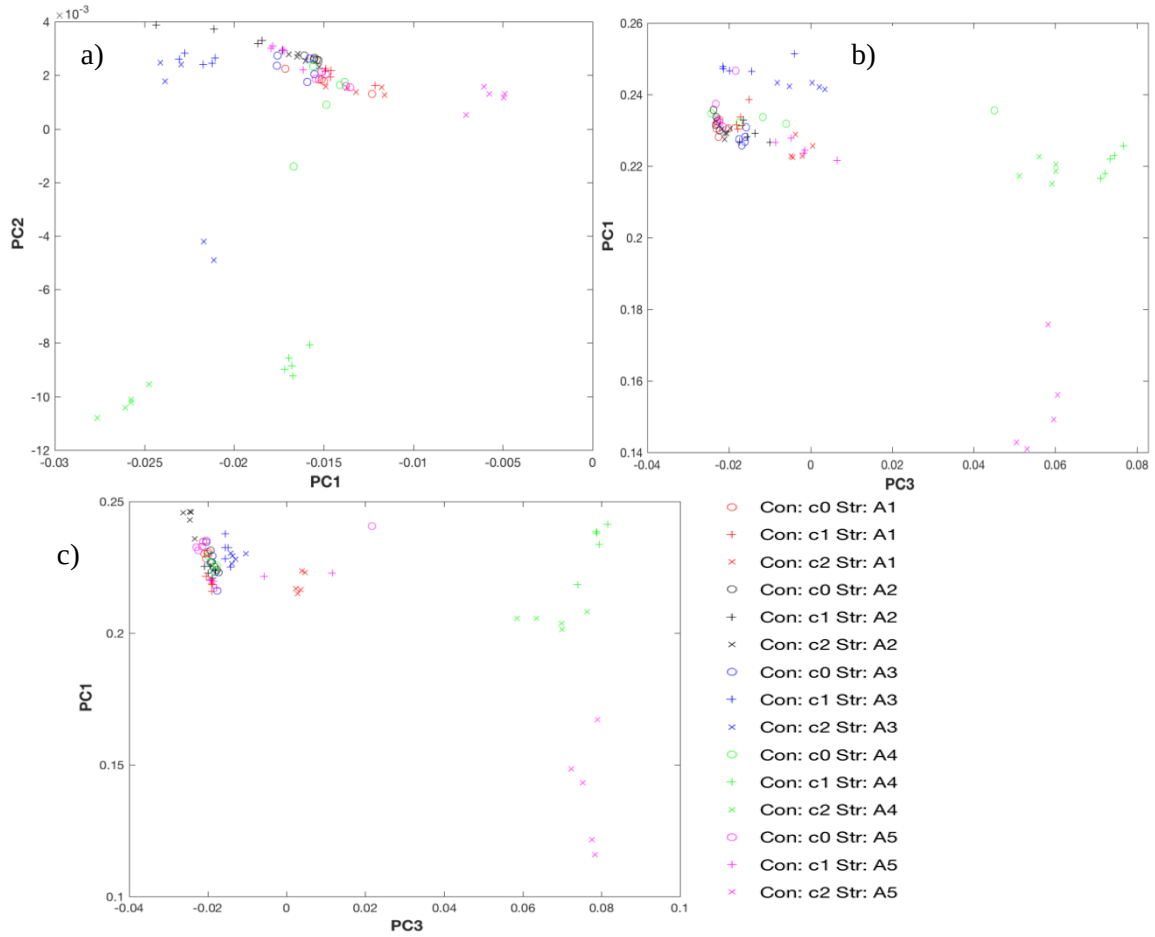

Figure 4.19 - PCA score plot of FTIR spectra of *E. coli* submitted to different concentrations (C) of the stress agents ethanol (A1), bleach (A2), sodium chloride (A3), hydrochloric acid (A4) and sodium hydroxide (A5) and with different incubation times (1, 8 and 24 hrs) a) after one hr of incubation, preprocessed by second derivative b) after eight hrs of incubation, preprocessed by second derivative c) after twenty four hrs of incubation, preprocessed by second derivative. PC1, PC2 and PC3 represent 94%, 4% and 2% of data variance, respectively

4.1.4 Global analysis of the bioassay

The optimization of this bioassay had as main goals to determine the best conditions to distinguish the controls from the samples exposed to the stress agents and in addition to distinguish the agents tested. As expected the conditions tested (nutrient concentrations, growth phase and incubation time) affects the cell metabolism and consequently the cell sensitivity towards the stress agents. Due to the fact that each stress agent has different modes of action on the metabolism of *E. coli*, slight differences were observed in the optimal conditions (table 4.16).

In the assay to optimize the nutrient medium concentration, the reproducibility of the assays with sodium chloride and hydrochloric acid was independent of the nutrient concentration. The nutrient concentration of the medium seems to only interfere with the stress agents alcohol, bleach and sodium hydroxide. In the assay with ethanol the medium with double nutrient concentration (M5x) presents the highest reproducibility and sensitivity. In the case of bleach, a consensus was not reached between the nutrient medium 2.5x and 5x. With sodium hydroxide the 2.5x nutrient concentration presents the highest reproducibility.

Cells that have grown for 24 hrs were best suited for detecting the action of ethanol, bleach and hydrochloric acid. In case of the assay with hydrochloric acid the cells that have grown for 16 hrs makes all possible to obtain a high reproducibility of the assay. The reproducibility of the assays with sodium chloride and sodium hydroxide showed to be independent from the growth phase of the cells used.

In the case of the assay incubation time, it was observed that for all stress agents tested the reproducibility of the assay was independent of the exposure time.

Table 4.16 - Optimal conditions for the bioassay for each stress agent taking into account nutrient concentration, *E. coli* growth phase and incubation time

	Nutrient medium concentration	**Growth phase**	**Incubation time**
Ethanol	M5x	24 hrs	Any incubation time tested
Bleach	M2.5x or M5x	24 hrs	Any incubation time tested
Sodium chloride	Any nutrient medium tested	Any growth phase tested	Any incubation time tested
Hydrochloric acid	Any nutrient medium tested	16 or 24 hrs	Any incubation time tested
Sodium hydroxide	M2.5x	Anygrowth phase tested	Any incubation time tested

With the analysis per stress agent, it was not possible to conclude the optimal conditions to evaluate alterations in the metabolism of *E. coli* cells when exposed to different types of stress. Only after the analysis of the PCA of the assays with all the agents together it was possible to conclude that for stress conditions with a high impact on cellular metabolism the use of an optimized bioassay is not as relevant. On the contrary, for conditions with a reduced impact on cell metabolism, optimization of the assay proved to be critical. For example, the effect of high concentrations of salt and acidic or basic media can be observed even in sub-optimized assays. However, for stress conditions evaluated with ethanol and beach, it was only possible to evidence the effect of these conditions on cell metabolism after optimization of the assay, that is, only if using reduced nutrient concentrations, *E. coli* in the stationary growth phase and an incubation time with the stress agent of 24 hrs.

Another goal of this work was to find spectral biomarkers to detect the action of stress agents on the metabolism of bacteria. For this purpose, the t-student test was used to analyse if the spectral ratios were statistically significant (p-values less than 0.05). All spectral ratios, chosen according to the peaks of the second derivative, were tested for all stress agents but different results were observed (table 4.17). Since each wavelength represents different molecules, this observation can be explained by the fact that each stress agent has different effects on *E. coli* cells, as was seen in the introduction.

In case of the ethanol, the spectral ratios more significant were in general: A2960/2920, A2960/2850, and A1550/1240. As previously mentioned the spectral ratios A2960/2920 and A2960/2850 allow to evaluate the state of cellular membranes of cells, which means that ethanol alters the cell membranes of *E. coli* cells, as was seen in the literature. We also saw that ROS produced due to stress caused by ethanol damages cell's DNA and ethanol can altering the function of proteins, A1550/1240 spectral ratio allows us to see these effects of ethanol on the cells.

Bleach attacks essential cell components including lipids, proteins and DNA. The component of the cell richest in lipids is the cellular membrane. The spectral ratios A2960/2920, A2960/2850 and A1655/1240 (evaluates the effect on DNA and proteins) proves that this stressing agent interferes with the cellular components mentioned.

The stress agents sodium chloride, hydrochloric acid and sodium hydroxide interfere with the osmotic balance of the cells which can destroy cell membranes and causes leakage of the internal cell content. Therefore, it was not surprising that in the assays with these agents the following spectral ratios were found to be significant statistically: A2960/2920 and A2960/2850 (evaluate the effect on cellular membranes), A1550/1240, A1080/1240, A1655/1550 and A1170/1655 (evaluate the effect on proteins and genetic material of cells).

Spectral ratio A2960/2920 and/or A2960/2850 showed to be significant statistically in all the stress agents tested. This leads to the conclusion that all stress agents have some effect on the cytoplasmic membrane of *E. coli* cells, being good spectral biomarkers to evaluate the effect of stress agents on the *E. coli* metabolism.

Table 4.17 - Main spectral ratios that reflected the effect of each stress agents on the cell metabolism

Stress agent	Spectral ratios
Ethanol	A2960/2920
	A2960/2850
	A1550/1240
Bleach	A2960/2920
	A2960/2850
	A1655/1240
Sodium chloride	A2960/2920
	A2960/2850
	A1550/1240
Hydrochloric acid	A2960/2920
	A1080/1240
	A1655/1550
Sodium hydroxide	A2960/2850
	A1080/1240
	A1170/1655

4.2 Application of the bioassay

For the application of the bioassay, it was chose to expose the *E. coli* bacteria to six antibiotics with three different types of mechanism of action because the need for novel, safe and more efficient antibiotics is a key challenge to the pharmaceutical industry today, moreover, increase in opportunistic infections in the immune compromised host has influenced this demand. Nowadays, evaluating, in a short time, the metabolic changes of the bacteria cells when exposed to these substances and knowing which one is most effective is very important. The use of the FTIR spectrometry technique seems to be a good alternative to achieve these objectives in the near future. As results of the bioassay optimization conclusions, for this antibiotic assay it was chose to use 1.25x nutrient medium culture, cells that grew to stationary growth phase and expose the samples to antibiotics for 24 hrs. In this assay the same procedures were used for preparing the samples and analysing the results (PCA score plots and p-values of the spectral ratios).

In the PCA score plots of the first antibiotic tested, amoxicillin (figure 4.20), it was possible to observe that the controls were separated from the samples exposed to this antibiotic and in general the samples exposed to different concentrations were separated from one another. The high sensitivity of the method even enables to detect the effect of the bacteria metabolism with the lowest amoxicillin concentration. The following spectral ratios enable to discriminate the antibiotics effect: A2960/2920, A2960/2850, A1655/1630 (table 4.18).

a)

b)

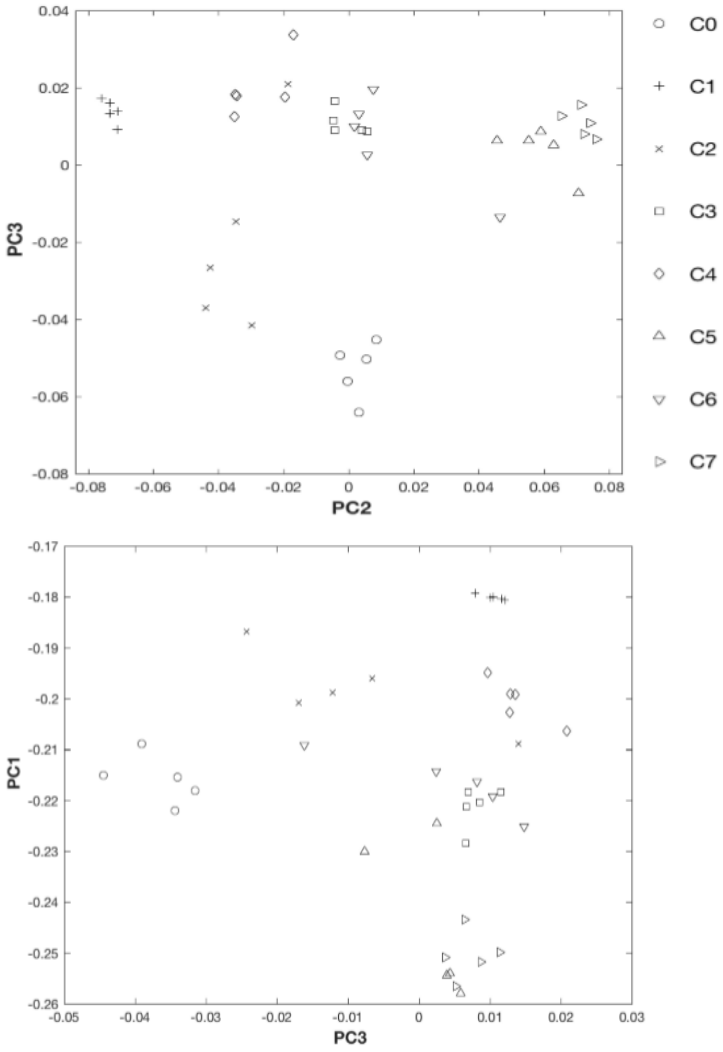

Figure 4.20 - PCA score plot of FTIR spectra of *E. coli* submitted to different concentrations of the antibiotic amoxicillin (C0 = 0; C1 = 0.01; C2 = 0.04; C3 = 0.2; C4 = 5; C5 = 25; C6 = 62.5; C7 = 125 mg/µL) a) preprocessed by second derivative b) preprocessed by second derivative. PC1, PC2 and PC3 represent 98%, 1% and 1% of data variance, respectively

Table 4.18 - p-values of the spectral ratios obtained from the quintuplicates of the assay with *E. coli* with different amoxicillin concentrations (C0 = 0; C1 = 0.01; C2 = 0.04; C3 = 0.2; C4 = 5; C5 = 25; C6 = 62.5; C7 = 125 mg/µL). The statistically significant p-values (p<0.05) are highlighted in green

Spectral ratio	**C0 *vs* C1**	**C0 *vs* C2**	**C0 *vs* C3**	**C0 *vs* C4**	**C0 *vs* C5**	**C0 *vs* C6**	**C0 *vs* C7**
A2960/2920	0.018	0.006	0.022	1.133E-04	0.272	0.004	0.046
A2960/2850	0.017	0.031	0.019	0.004	0.154	0.015	0.189
A1655/1630	0.015	0.129	1.6E-04	0.032	0.028	0.004	3.92E-05

In the PCA score plots resulting from the exposure to ampicillin (figure 4.21), it was observed that 0.01 mg/µL of this antibiotic was also enough to detect its effect on *E.coli* cells. Since the mechanism of action of ampicillin is due to its interference with cell membrane synthesis, it was expected that the spectral ratios more statistically significant were A2960/2920 and A2960/2850. However, the most statistic significant spectral ratios were A1550/1240 and A1170/1550, that result in discrimination low antibiotic concentration as low as C2 (table 2.19).

a)

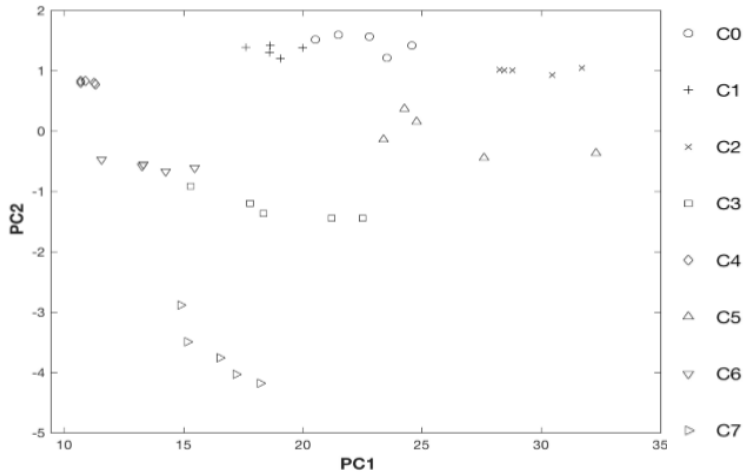

b)

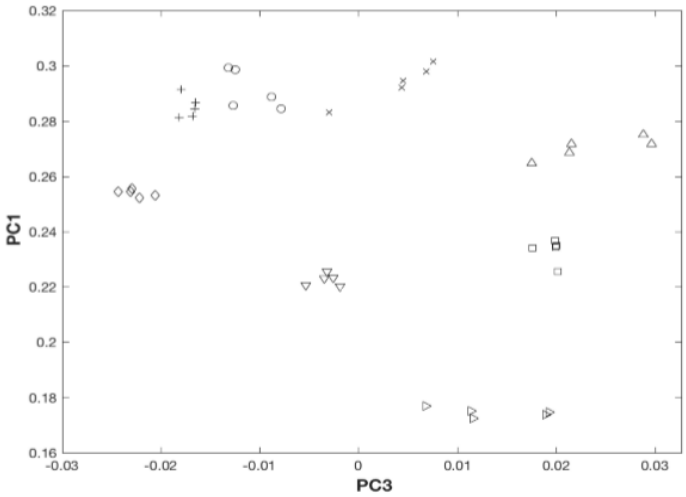

Figure 4.21 - PCA score plot of FTIR spectra of *E. coli* submitted to different concentrations of the antibiotic ampicillin (C0 = 0; C1 = 0.01; C2 = 0.04; C3 = 0.2; C4 = 5; C5 = 25; C6 = 62.5; C7 = 125 mg/µL) a) without preprocessing b) preprocessed by second derivative. PC1, PC2 and PC3 represent 98%, 1% and 1% of data variance, respectively

Table 4.19 - p-values of the spectral ratios obtained from the quintuplicates of the assay with *E. coli* with different ampicillin concentrations (C0 = 0; C1 = 0.01; C2 = 0.04; C3 = 0.2; C4 = 5; C5 = 25; C6 = 62.5; C7 = 125 mg/µL). The statistically significant p-values (p<0.05) are highlighted in green

Spectral ratio	**C0 *vs* C1**	**C0 *vs* C2**	**C0 *vs* C3**	**C0 *vs* C4**	**C0 *vs* C5**	**C0 *vs* C6**	**C0 *vs* C7**
A2960/2920	0.053	0.499	0.960	0.001	0.032	0.043	0.307
A1550/1240	0.619	9.44E-04	5.48E-04	0.049	7.26E-04	0.025	3.07E-05
A1170/1550	0.196	2.91E-04	3.69E-05	0.017	3.27E-04	6.21E-04	1.69E-04

Like previous antibiotics, the score plots of the assay with ciprofloxacin (figure 4.22), enable to discriminate this antibiotic concentration. The spectral ratios more statistically significant were: 2960/2920, 1655/1690 and 1655/1550 (table 4.20). It was possible to discriminate the effect of ciprofloxacin on cell lipids from C6 concentration (62.5 mg/µL) and at proteins levels already at the lowest antibiotic concentration (0.01 mg/µL).

a)

b)

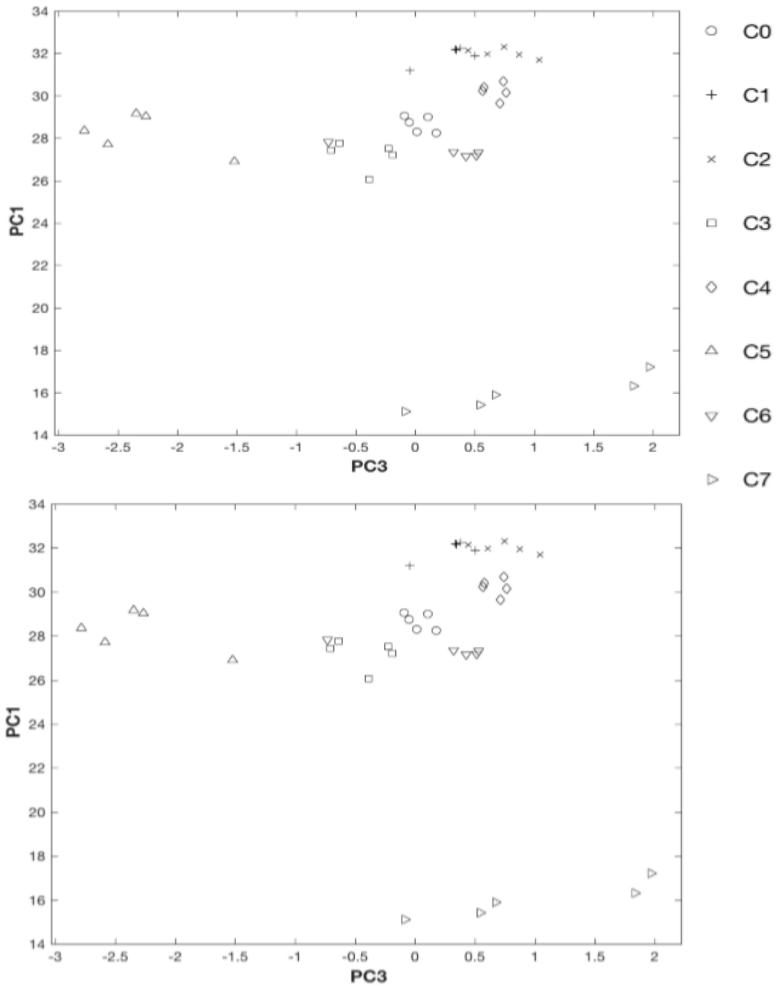

Figure 4.22 - PCA sore plot of FTIR spectra of *E. coli* submitted to different concentrations of the antibiotic ciprofloxacin (C0 = 0; C1 = 0.01; C2 = 0.04; C3 = 0.2; C4 = 5; C5 = 25; C6 = 62.5; C7 = 125 mg/µL) a) preprocessed by base line correction and Min Amide I normalization b) preprocessed by Min Amide I normalization. PC1, PC2 and PC3 represent 98%, 1% and 1% of data variance, respectively

Table 4.20 - p-values of the spectral ratios obtained from the quintuplicates of the assay with *E. coli* with different ciprofloxacin concentrations (C0 = 0; C1 = 0.01; C2 = 0.04; C3 = 0.2; C4 = 5; C5 = 25; C6 = 62.5; C7 = 125 mg/µL). The statistically significant p-values (p<0.05) are highlighted in green

Spectral ratio	C0 *vs* C1	C0 *vs* C2	C0 *vs* C3	C0 *vs* C4	C0 *vs* C5	C0 *vs* C6	C0 vs C7
A2960/2920	0.212	0.161	0.198	0.492	0.108	7.65E-04	0.028
A1655/1690	0.008	0.002	0.029	6.2E-04	0.004	4.62E-04	0.133
A1655/1550	2.66E-04	1.54E-05	0.932	0.004	0.006	3.83E-04	0.004

Analysis of the score plots from the erythromycin assay (figure 2.23), shows that all samples that were exposed to this antibiotic were separated from those were not exposed. Therefore, 0.01 mg/µL of erythromycin was sufficient for observing changes in the *E. coli* metabolism. From concentration C1, the following statistically significant spectral ratios were observed: A2960/2850, A1655/1550 and A1550/1240 (table 4.21). This observation reflects the mechanism of action of this antibiotic which is inhibits protein synthesis.

a)

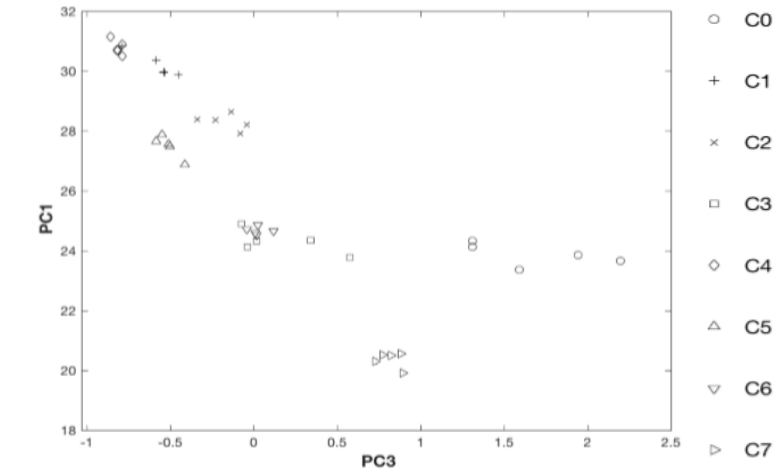

b)

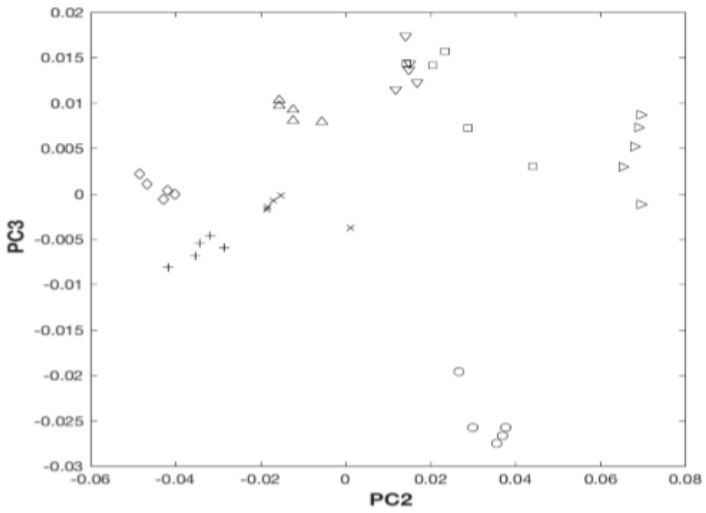

Figure 4.23 - PCA sore plot of FTIR spectra of *E. coli* submitted to different concentrations of the antibiotic erythromycin (C0 = 0; C1 = 0.01; C2 = 0.04; C3 = 0.2; C4 = 5; C5 = 25; C6 = 62.5; C7 = 125 mg/µL) a) preprocessed by base line correction and Min Amide I normalization b) preprocessed by second derivative. PC1, PC2 and PC3 represent 98%, 1% and 1% of data variance, respectively

Table 4.21 - p-values of the spectral ratios obtained from the quintuplicates of the assay with *E. coli* with different erythromycin concentrations (C0 = 0; C1 = 0.01; C2 = 0.04; C3 = 0.2; C4 = 5; C5 = 25; C6 = 62.5; C7 = 125 mg/µL). The statistically significant p-values (p<0.05) are highlighted in green

Spectral ratio	**C0 *vs* C1**	**C0 *vs* C2**	**C0 *vs* C3**	**C0 *vs* C4**	**C0 *vs* C5**	**C0 *vs* C6**	**C0 *vs* C7**
A2960/2850	0.007	0.016	0.242	0.002	0.004	0.011	9.81E-05
A1655/1550	9.45E-04	0.002	0.041	7.9E-05	0.002	0.007	0.001
A1550/1240	1.42E-04	3.65E-06	6.48E-07	3.18E-07	1.04E-04	4.54E-05	3.9E-05

In the case of the score plots of the metronidazole assay (figure 4.24), all the samples exposed to this antibiotic were separate from the controls. From the first concentration tested, the statistically significant spectral ratios were observed: A2960/2920 and A2960/2850. The A1655/1550 was statistic significant only for some antibiotic concentrations (table 4.22).

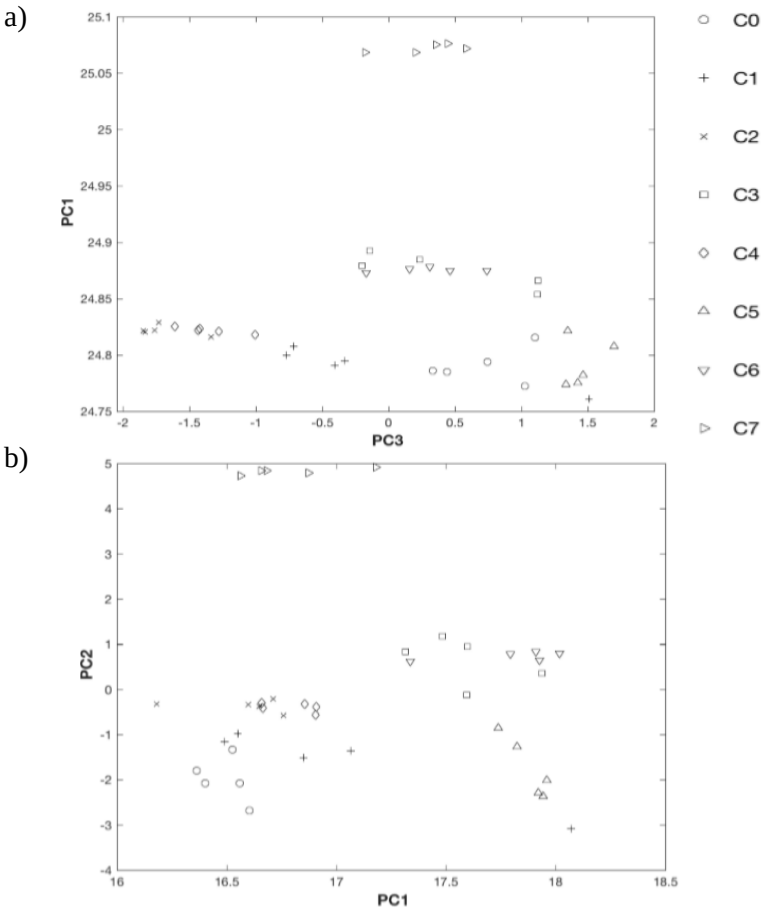

Figure 4.24 - PCA sore plot FTIR spectra of *E. coli* submitted to different concentrations of the antibiotic metronidazole (C0 = 0; C1 = 0.01; C2 = 0.04; C3 = 0.2; C4 = 5; C5 = 25; C6 = 62.5; C7 = 125 mg/µL) a) preprocessed by base line correction, Min Amide I normalization and MSC b) preprocessed by Min Max normalization. PC1, PC2 and PC3 represent 98%, 1% and 1% of data variance, respectively

Table 4.22 - p-values of the spectral ratios obtained from the quintuplicates of the assay with *E. coli* with different metronidazole concentrations (C0 = 0; C1 = 0.01; C2 = 0.04; C3 = 0.2; C4 = 5; C5 = 25; C6 = 62.5; C7 = 125 mg/µL). The statistically significant p-values (p<0.05) are highlighted in green

Spectral ratio	**C0 *vs* C1**	**C0 *vs* C2**	**C0 *vs* C3**	**C0 *vs* C4**	**C0 *vs* C5**	**C0 *vs* C6**	**C0 *vs* C7**
A2960/2920	0.013	2.48E-04	0.004	0.008	0.882	0.018	0.195
A2960/2850	2.85E-05	2.84E-04	1.1E-04	5.18E-04	0.001	5.91E-05	2.23E-05
A1655/1550	0.052	4.77E-04	0.156	3.48E-04	0.089	0.034	0.002

Finally, in the score plots of the neomycin assay (figure 4.25), it was observed that it was possible to discriminate all the antibiotic concentrations tested. The following statistically significant spectral ratios were observed: A2960/2920, A1550/1240 and A1170/1550 (table 4.23). This observation agrees with the fact that this antibiotic is an inhibitor of protein synthesis.

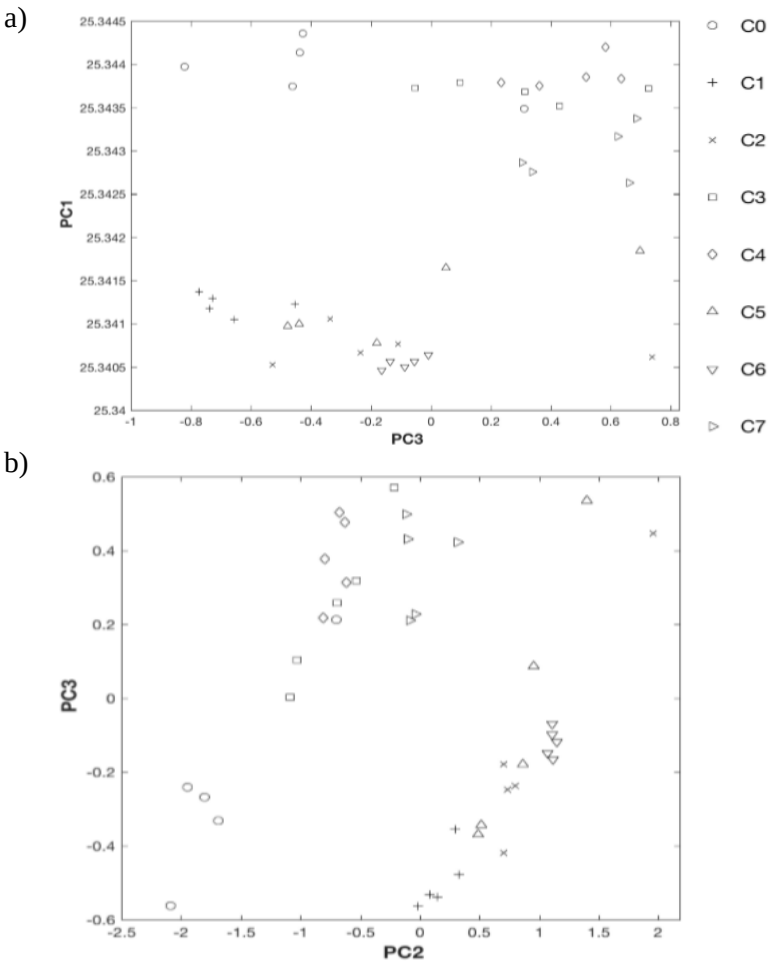

Figure 4.25 - PCA sore plot FTIR spectra of *E. coli* submitted to different concentrations of the antibiotic neomycin (C0 = 0; C1 = 0.01; C2 = 0.04; C3 = 0.2; C4 = 5; C5 = 25; C6 = 62.5; C7 = 125 mg/µL) a) pre-processed by base line correction, Min Amide I normalization and MSC b) pre-processed by Min Max normalization. PC1, PC2 and PC3 represent 98%, 1% and 1% of data variance, respectively

Table 4.23 - p-values of the spectral ratios obtained from the quintuplicates of the assay with *E. coli* with different neomycin concentrations (C0 = 0; C1 = 0.01; C2 = 0.04; C3 = 0.2; C4 = 5; C5 = 25; C6 = 62.5; C7 = 125 mg/μL). The statistically significant p-values (p<0.05) are highlighted in green

Spectral ratio	**C0 *vs* C1**	**C0 *vs* C2**	**C0 *vs* C3**	**C0 *vs* C4**	**C0 *vs* C5**	**C0 *vs* C6**	**C0 *vs* C7**
A2960/2920	0.028	0.072	0.013	0.451	0.022	0.003	0.019
A1550/1240	0.027	0.025	0.417	0.081	0.009	0.012	0.163
A1170/1550	0.048	0.039	9.49E-04	0.002	0.017	0.046	0.007

As it was made for stress agents, in addition to analysing the PCA of each separate antibiotic, it were also analysed the PCA of all antibiotics together to observe if it would be possible to separate the action of each antibiotic on *E.coli* metabolism.

In the score plot (figure 4.26), it was observed that the samples that were exposed to higher concentrations of the antibiotics metronidazole, ciprofloxacin, erythromycin and ampicillin were in groups separated from each other. However, despite the optimization of the test conditions, it was not possible to distinguish the action of amoxicillin and neomycin.

The spectral ratio A2960/2920 and/or A2960/2850 were statistically significant for all antibiotic tested, confirming the importance of this spectral region as a biomarker of response to stress conditions. In general, the spectral ratio more statistically significant corresponded to the known antibiotics mechanism of action. For example, in case of neomycin it was observed an effect on the protein synthesis. However, in the case of the antibiotics inhibitors of DNA synthesis, ciprofloxacin and metronidazole, no direct action was observed in the genetic material of the cells but instead changes in the cell membrane and in the proteins. This can be explained by the fact that stress conditions are affecting the overall metabolism of *E. coli* cells, being that independently of its mechanism of action, all the antibiotics tested provoked alterations in the cellular membrane and in the proteins.

a)

b)

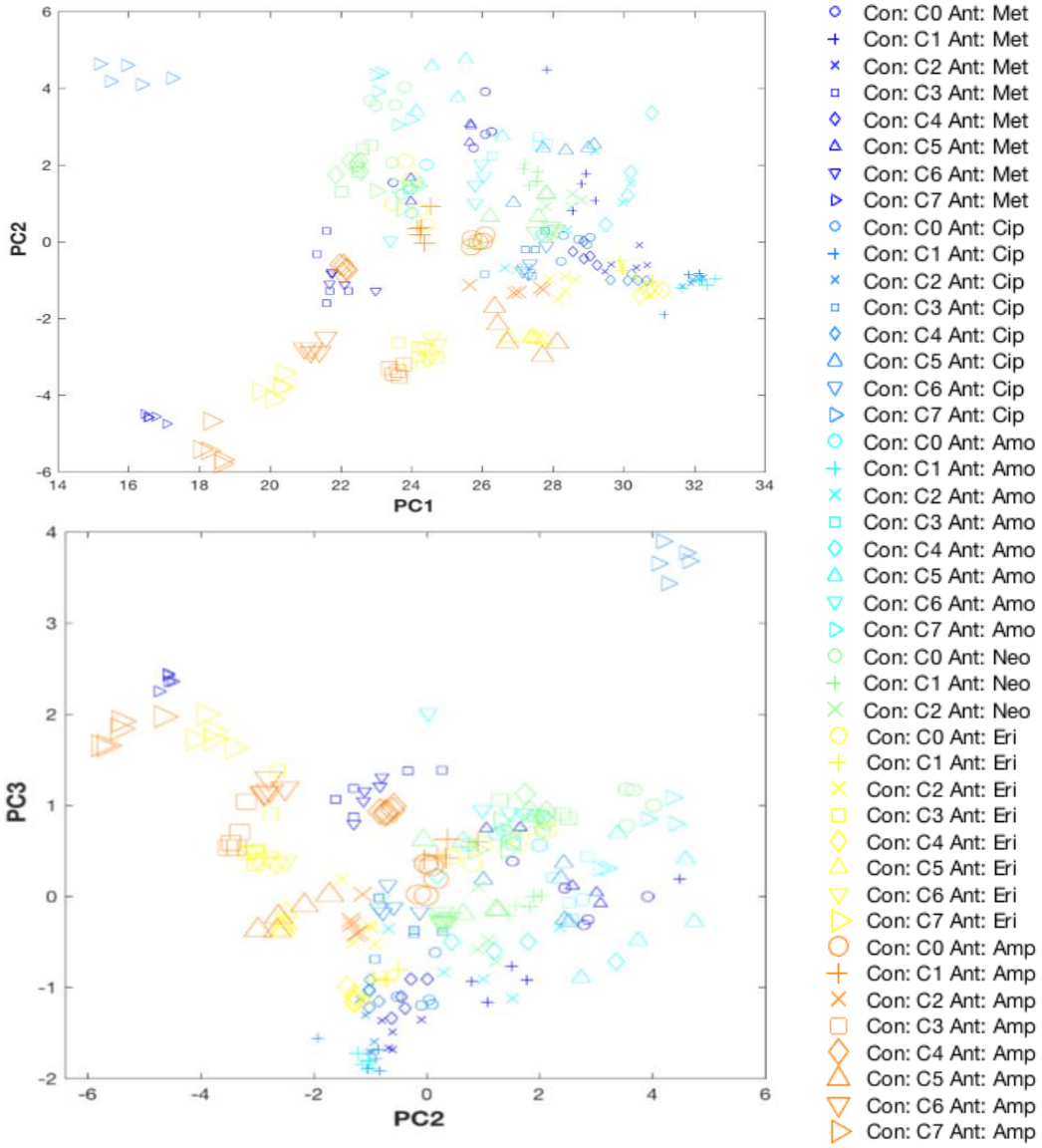

Figure 4.26 - PCA sore plot FTIR spectra of *E. coli* submitted to different concentrations of the all antibiotics tested (amoxicillin, ampicillin, ciprofloxacin, erythromycin, metronidazole and neomycin) a) preprocessed by base line correction and Min Amide I normalization b) preprocessed by base line correction and Min Amide I normalization. PC1, PC2 and PC3 represent 98%, 1% and 1% of data variance, respectively

5. Conclusions and prospects

Along the present work, it was possible to observe that the bioassay enables to discriminate in a simple, economic and high-throughput mode the metabolic impact of different stress agents on *E. coli* metabolism. To optimise the bioassay, in order to increase the discrimination capacity of the assay, not only to discriminate the effect of different agents but also the impact of the concentration of each agent on the *E. coli* metabolism the following parameters were optimised: the nutrient content of the incubation mixture, the growth phase of the *E. coli* cells used and the stress agent exposure time. Ultimately it was possible to determine the optimal conditions that ensure the bioassay has enough sensitivity to distinguish between the different metabolic impacts of the stress agents used, while being sufficiently reproducible to ensure a coherent bioassay. Interestingly the results indicate that different parameters are better suited for different stressing agents, however a good compromise was achieved with the described optimization, since the bioassays' ability to distinguish the impact of different stress agents was generally suitable.

The optimization of the bioassay was proved to be more important for stress agents with reduced impact on cellular metabolism than for stress agents with a high impact on cellular metabolism, where the use of a bioassay is not as essential.

This work highlights the applicability of FTIR spectroscopy to categorize microbial stress responses, and therefore reinforces FTIR spectroscopy has a powerful tool for metabolic fingerprinting with the advantage of being a rapid and economic technology capable of high-throughput.

In a future work, it will be interesting to continue the optimization of the bioassay taking into account other parameters as well to test other stress agents and different concentrations. In sum, FTIR spectroscopy was presented as a highly promising tool to evaluate the metabolic stress response of microorganism.

6. References

Ahmed, S.S.S.J., Santosh, W., Kumar, S., Christlet, T.H.T. (2010). Neural network algorithm for the early detection of Parkinsons disease from blood plasma by FTIR micro-spectroscopy. *Vibrational Spectroscopy* 53: 181–188

Aksoy, C., Severcan, F. (2012). Role of vibrational spectroscopy in stem cell research. *Spectroscopy: An International Journal* 27:167–184

Amiali, N.M., Mulvey, M.R., Sedman, J., Simor, A.E., Ismail, A.A. (2007). Epidemiological typing of methicillin-resistant Staphylococcus aureus strains by Fourier transform infrared spectroscopy. *Journal of Microbiological Methods* 69:146–153

Arnold, S.A., Crowley, J., Woods, N., Harvey L.M., McNeil, B. (2003). In situ near infrared spectroscopy to monitor key analytes in mammalian cell cultivation. *Biotechnology and Bioengineering* 84:13–19

Babrah, J. (2009). A study of FT-IR spectroscopy for the identification and classification of hematological malignancies. PhD Thesis, Cranfield University, United Kingdom

Bellisola, G. and Sorio, C. (2012). Infrared spectroscopy and microscopy in cancer research and diagnosis. *American Journal of Cancer Research* 2(1): 1-21

Bogomolny, E., Huleihel, M., Suproun, Y., Sahu, R.K., Mordechai, S. (2007). Early spectral changes of cellular malignant transformation using Fourier transform infrared microspectroscopy. *Journal of Biomedical Optics* 12:024003

Canetta, E., Adya, A.K., Walker, G.M. (2006). Atomic force microscopic study of the effects of ethanol on yeast cell surface morphology. *FEMS Microbiology Letters* 255 (2): 308-315

Cao, H. , Wei, D., Yang Y., Shang, Y., Li G., Zhou Y., Ma, Q., Xu, Y. (2017). Systems-level understanding of ethanol-induced stresses and adaptation in *E. coli*. *Scientific Reports* 7: 44150

Chan, K.L.A. and Kazarian, S.G. (2013). Correcting the effect of refraction and dispersion of light in FT-IR spectroscopic imaging in transmission through thick infrared windows. *Analytical chemistry* 85: 1029–1036

Christian, G.D. (1994). *Analytical Chemistry*. WILEY: United States

Chung, H.J., Bang, W., Drake, M.A. (2006). Stress Response of *Escherichia coli*. Comprehensive Reviews in Food Science and Food Safety

Corte, L., Rellini, P., Roscini, L., Fatichenti, F., Cardinali, G. (2010). Development of a novel, FTIR (Fourier transform infrared spectroscopy) based, yeast bioassay for toxicity testing and stress response study. *Analytica Chimica Acta* 659: 258–265

Corte, L., Antonielli, L., Roscini, L., Fatichenti, F., Cardinali, G. (2011). Influence of cell parameters in Fourier transform infrared spectroscopy analysis of whole yeast cells. *Analyst* 136: 2339–2349

Davis, R. and Mauer, L.J. (2010). Fourier tansform infrared (FT-IR) spectroscopy: A rapid tool for detection and analysis of foodborne pathogenic bacteria. *Formatex* 1582-1594

Davis, R., Paoli, G., Mauer, L.J. (2012). Evaluation of Fourier transform infrared (FT-IR) spectroscopy and chemometrics as a rapid approach for sub-typing Escherichia coli O157:H7 isolates. *Food Microbiology* 31:181–190

Douthwaite, S., Aagaard, C. (1993). Erythromycin binding is reduced in ribosomes with conformational alterations in the 23 S rRNA peptidyl transferase loop. *Journal of molecular biology* 232(3):725-31

Duygu, D., Baykal, T., Açikgöz, I., Yildiz, K. (2009). Fourier Transform Infrared (FT-IR) Spectroscopy for Biological Studies. *Journal of Science* 22:117-121

Estrela, C., Ribeiro, R.G., Estrela, C.R.A., Pécora, J.D., Sousa-Neto, M.D. (2003). Antimicrobial effect of 2% sodium hypochlorite and 2% chlorhexidine tested by different methods. *Brazilian Dental Journal* 14 (1): 58-62

Fearn, T., Riccioli, C., Garrido-Varo, A., Guerrero-Ginel, J.E. (2009). On the geometry of SNV and MSC. *Chemometrics and Intelligent Laboratory Systems* 96:22-26

Gill, A.E., Amyes, S.G. (2004). The contribution of a novel ribosomal S12 mutation to aminoglycoside resistance of Escherichia coli mutants. *Journal of chemotherapy* 16(4):347-9

Graça, G., Moreira, A.S., Correia, A.J.V., Goodfellow, B.J., Barros, A.S., Duarte, I.F., Carreira, I.M., Galhano, E., Pita, C., Almeida, M.C., Gil, A.M. (2013). Mid-infrared (MIR) metabolic fingerprinting of amniotic fluid: a possible avenue for early diagnosis of prenatal disorders? *Analytica Chimica Acta* 764:24–31

Greenler, R. (1966). Infrared study of adsorbed molecules on metal surfaces by reflection techniques. *The Journal of Chemical Physics* 44: 310–315.

Griffiths, P.R. (2002). Introduction to Vibrational Spectroscopy, in Chalmers J.M. and Griffiths P. (Eds.). *Handbook of Vibrational Spectroscopy*. Wiley: United States

Hammiche, A., German, M.J., Hewitt, R., Pollock, H.M., Martin, F.L. (2005). Monitoring cell cycle distributions in MCF-7 cells using near-field photothermal microspectroscopy. *Biophysical Journal* 88:3699–3706

Helm, D., Labischinski, H., Schallehn, G., Naumann, D. (1991). Classification and identification of bacteria by Fourier-transform infrared spectroscopy. *Journal of General Microbiology* 137(1): 69-79

Hengge-Aronis, R. (2002). Recent Insights into the General Stress Response Regulatory Network in Escherichia coli. *Journal of Molecular Microbiology and Biotechnology* 4(3): 341–346

Ho-Hyuk, J., Sung-Ho, A., Myung-Deok, K., Chan-Wha, K. (2008). Use of hydrogen peroxide as an effective disinfectant to Actinobacillus ureae. *Process Biochemistry* 43: 225-228

Hosein, A., Breidt, F., Smith, C. (2011). Modeling the Effects of Sodium Chloride, Acetic Acid, and Intracellular pH on Survival of *Escherichia coli* O157:H7. *American Society for Microbiology* 77: 889–895

Jamin, N., Miller, L., Moncuit, J., Fridman, W.H., Dumas, P., Teillaud, J.L. (2003). Chemical heterogeneity in cell death: combined synchrotron IR and fluorescence microscopy studies of single apoptotic and necrotic cells. *Biopolymers* 72:366–373

Jolliffe, I.T. (2002). *Principal Component Analysis*. Springer: New York, USA

Khanmohammadi, M., Garmarudi, A.B., Ramin, M., Keyvan, G. K. (2013). Diagnosis of renal failure by infrared spectrometric analysis of human serum samples and soft independent modeling of class analogy. *Microchemical Journal* 106:67–72

Kyriakides, B. C. (1998). *E. coli* – A practical approach to the organism and its control in foods. Pratical Food Microbiology Series. London: Blackie Academic & Professional.

Landgrebe, D., Haake, C., Höpfner, T., Beutel, S., Hitzmann, B., Beutel, S., Hitzmann, B., Scheper, T., Rhiel, M., Reardon, K.F. (2010). On-line infrared spectroscopy for bioprocess monitoring. *Applied Microbiology and Biotechnology* 88:11-22

Lavine, B. K. 1998. Chemometrics. *Analytical Chemistry* 70:209R-228R.

Leavis, H.L., Willems, R.J., Top, J., Bonten, M.J. (2006). High-level ciprofloxacin resistance from point mutations in gyrA and parC confined to global hospital-adapted clonal lineage CC17 of *Enterococcus faecium*. *Journal of clinical microbiology* 44(3):1059-64

Li, A.Q., Dai, N., Yan, J., Zhu, Y.L. (2007). Screening for metronidazole-resistance associated gene fragments of Helicobacter pylori by suppression subtractive hybridization. *Journal of Zhejiang University. Medical Science* 36(5):465-9

Liang, P., Labedan, B., Riley, M. (2002). Physiological genomics of *Escherichia coli* protein families. *Physiologycal Genomics* 9: 15–26

Lima, C., Goulart, V., Côrrea, L., Pereira, T., Zezell, D. (2015). ATR-FTIR Spectroscopy for the Assessment of Biochemical Changes in Skin Due to Cutaneous Squamous Cell Carcinoma. *International Journal of Molecular Sciences* 16: 6621-6630

Lourenço, N.D., Lopes, J.A., Alemida, C.F., Sarraguça, M.C., Pinheiro, H.M. (2012). Bioreactor monitoring with spectroscopy and chemometrics: a review. *Analytical and Bioanalytical Chemistry* 404:1211-1237

Maquelin, K., L.-P. Choo-Smith, C. Kirschner, N. A. Ngo-Thi, D. Naumann, G. J. Puppels. (2002). Vibrational spectroscopic studies of microorganisms, p. 3308-3334. In J. M. e. P. R. G. Chalmers (ed.), Handbook of Vibrational Spectroscopy, 1ª ed, vol. 5. John Wiley & Sons, Chichester.

Martin, D.H. and Puplett, E. (2002). Polarised interferometric spectrometry for the millimetre and submillimetre spectrum. *Infrared Physics* 10:105-109

Moen, B., Janbu, A. O., Langsrud, S., Langsrud, O., Hobman, J. L., Constantinidou, C., Kohler, A., Rudi, K. (2009). Global responses of Escherichia coli to adverse conditions determined by microarrays and FT-IR spectroscopy. *Canadian Journal of Microbiology* 55: 714–728

Naes, T., Isaksson, T., Fearn, T., Davies, T. (2002). *Multivariate Calibration and Classification*. NIR Publications: Chichester, United Kingdom

Naumann, D. (2001). FT-Infrared and FT-Raman spectroscopy in biomedical research. *Applied Spectroscopy Reviews* 36:239-298.

Norris, K. P. (1959). Infra-red spectroscopy and its application to microbiology. Microbiological Research Establishment, Ministry of Supply, Porton, Wilts

Okamoto, T., Yoshiyama, H., Nakazawa, T., Park, I.D., Chang, M.W., Yanai, H., Okita, K., Shirai, M. (2002). A change in PBP1 is involved in amoxicillin resistance of clinical isolates of Helicobacter pylori. *The Journal of antimicrobial chemotherapy* 50(6):849-56

Oliveira, R. and Silva, A. (2014). William Herschel, the invisible rays and the first ideas about infrared radiation. *Revista Brasileira de Ensino de Física* 36: 2-6

Otto, M. (1999). *Chemometrics: Statistics and Computer Application in Analytical Chemistry*. WILEY-VCH: Freiberg, Germany

Randolph, T.W. (2006). Scaled-based normalization of spectral data. *Cancer Biomarkers* 2:135-144

Reich, G. (2005). Near-Infrared spectroscopy and imaging: Basic principles and pharmaceutical applications. *Advanced Drug Delivery Reviews* 57:1109-1143

Salmond, C. V., Kroll, R. G., Booth, I. R. (1984). The Effect of Food Preservatives on pH Homeostasis in *Escherichia coIi*. *Journal of General Microbiology* 130: 2845-2850

Scholz, T., Lopes, V.V., Calado, C.R.C. (2012). High-throughput analysis of the plasmid bioproduction process in Escherichia coli by FTIR spectroscopy. *Biotechnology and Bioengineering* 109:2279-2285

Sellick, C.A., Hansen, R., Jarvis, R.M., Maqsood, A.R., Stephens, G.M., Dickson, A.J., Goodacre, R. (2010). Rapid monitoring of recombinant antibody production by mammalian cell cultures using Fourier Transform infrared spectroscopy and chemometrics. *Biotechnology and Bioengineering* 106:432–442

Sharma, M. and Beuchat, L. (2004). Sensitivity of Escherichia coli O157:H7 to Commercially Available Alkaline Cleaners and Subsequent Resistance to Heat and Sanitizers. *American Society for Microbiology* 70: 1795 – 1803

Smith, B.C. (2011). *Fourier Transform Infrared Spectroscopy*. New York: CRC Press

Stuart, B. (2004). Infrared Spectroscopy: Fundamentals and Applications. WILEY: United States

Thomas, N. (1991). The early history of spectroscopy. *Journal of Chemical Education* 68 (8): 631

Williamson, R., Hakenbeck, R., Tomasz, A. (1980). In vivo interaction of beta-lactam antibiotics with the penicillin-binding proteins of Streptococcus pneumoniae. *Antimicrobial Agents and Chemotherapy* 18(4):629-37

References on the web

ASD$_{inc}$. What is a Derivative Spectrum? Retrieved on August 22, 2017 on the website: https://www.asdi.com/learn/faqs/what-is-a-derivative-spectrum

CAMO Software Inc. Bridging the Gap between the State and Measurement of a Chemical System. Retrieved on August 27, 2017 on the website: http://www.camo.com/downloads/resources/application_notes/Chemometric%20Analysis%20for%20Spectroscopy.pdf

Centers for Disease Control and Prevention. *E. coli* (*Escherichia coli)* - General Information. Retrieved on August 5, 2017 on the website: https://www.cdc.gov/ecoli/index.html

Edmund Scientific. The Correct Material for Infrared (IR) Applications. Retrieved on August 10, 2017 on the website: https://www.edmundoptics.com/resources/application-notes/optics/the-correct-material-for-infrared-applications/

KHANACADEMY. Light: Electromagnetic waves, the electromagnetic spectrum and photons. Retrieved on August 9, 2017 on the website: https://www.khanacademy.org/science/physics/light-waves/introduction-to-light-waves/a/light-and-the-electromagnetic-spectrum

Thermo Scientific. Advantages of a Fourier Transform Infrared Spectrometer. Retrieved on August 15, 2017 on the website: https://tools.thermofisher.com/content/sfs/brochures/TN50674-E-0215M-FT-IR-Advantages.pdf

Instituto nacional de saúde Dr. Ricardo Jorge. Resistência aos Antimicrobianos. Retrieved on August 26, 2017 on the website: http://www2.insa.pt/sites/INSA/Portugues/Paginas/AntibioticosResi.aspx